INFUSER: Influence-Guided Self-Evolution Improves Reasoning

Siyu Chen[1] Miao Lu[2] Beining Wu[3] Heejune Sheen[1] Fengzhuo Zhang[1]
Shuangning Li[3] Zhiyuan Li[4] Jose Blanchet[2] Tianhao Wang[5] Zhuoran Yang[1]

[1]Yale University [2]Stanford University [3]University of Chicago
[4]Toyota Technological Institute at Chicago [5]University of California, San Diego

Abstract

Self-evolution offers a scalable path to stronger reasoning: a pretrained language model improves itself with only minimal external supervision. Yet existing methods either depend on extensively curated or teacher-generated training data, or, when the generator runs unsupervised, reward it by a difficulty heuristic that need not improve the solver. We introduce **INFUSER**, an iterative co-training framework with two co-evolving roles: a *Generator* that drafts questions and reference golden answers from a pool of unstructured, automatically collected documents, and a *Solver* that improves by training on them. The solver is trained with standard correctness rewards against the generator-provided answers, while the generator is rewarded by an *optimizer-aware influence score* that measures whether each proposed question would actually improve the solver on the target distribution. Because this continuous, noisy influence score is poorly served by standard GRPO, we propose **DuGRPO**, a dual-normalized variant of GRPO, for generator training. Together, these turn the document pool into an *adaptive curriculum* that favors questions useful to the current solver, not just hard ones. On Qwen3-8B-Base, INFUSER outperforms strong self-evolution baselines with over 20% relative improvement on Olympiad and SuperGPQA benchmarks, and an 8B INFUSER co-evolving generator outperforms a frozen 32B thinking generator on math and coding. Ablations confirm each design choice is necessary, and two extensions, applying INFUSER to an instruction-finetuned anchor and augmenting it with rule-verifiable RLVR data, further demonstrate the flexibility and generalizability of the framework. Code is available at https://github.com/FFishy-git/INFUSER.

Figure 1: **INFUSER** on Qwen3 base anchors. *Left:* relative accuracy gain over Qwen3-8B-Base on four headline benchmarks for each self-evolution method. *Right:* validation-set accuracy curves over training iterations for INFUSER versus a fixed-generator baseline with matching hyperparameters on Qwen3-4B-Base (left subpanel) and Qwen3-8B-Base (right subpanel); curves are averaged over 3 random seeds.

Author emails: siyu.chen.sc3226@yale.edu, miaolu@stanford.edu, beiningw@uchicago.edu, heejune.sheen@yale.edu, fengzhuo.zhang@yale.edu, shuangning.li@chicagobooth.edu, zhiyuanli@ttic.edu, jblanche@stanford.edu, tianhaowang@ucsd.edu, zhuoran.yang@yale.edu.

1 Introduction

Reinforcement learning with verifiable rewards (RLVR) underlies much of the recent progress in reasoning for large language models (Guo et al., 2025; Kimi Team et al., 2025; Shao et al., 2024; Yu et al., 2025a; Zhang et al., 2025), but its scalability is bottlenecked by the supply of high-quality, verifiable training data, which is costly to produce in both research and industry settings. *Self-evolution* offers a path beyond this bottleneck: a generator proposes high-quality training data with itself or from unstructured documents, and a solver trains on that data. The whole improvement loop runs without an externally curated training corpus or teacher model (Huang et al., 2025; Liu et al., 2025b; Yu et al., 2025b). In principle, this either creates training signal from the model itself or converts abundant unstructured corpora into the structured signals that RLVR consumes.

Existing self-evolution methods, however, share two limitations that constrain their effectiveness. The first concerns *grounding*: the anchoring of generated training data in external sources rather than only the model's own outputs. Pure self-play methods such as R-Zero (Huang et al., 2025) forgo such an anchor and draw supervision entirely from the model's own outputs, which bounds learning by the model's prior knowledge and exposes the solver to hallucinated reference answers; executor-based methods such as AZR (Zhao et al., 2025) substitute a code or symbolic executor for documents, restoring formal verifiability but restricting the framework to domains in which such an executor exists, e.g., code and mathematics. The second concerns the *generator's training objective*. Document-grounded approaches such as SPICE (Liu et al., 2025b) draw training questions from an external corpus, yet reward the generator by a difficulty heuristic that is maximized when the solver succeeds on approximately half of its rollouts. Difficulty is a coarse surrogate for utility: a question may register as difficult because it is ambiguously phrased, misaligned with its source document, or paired with an incorrect generated reference answer, and training on such a question carries no guarantee of improving the solver. These two limitations together leave the following question open:

Can we train a generator to produce document-grounded training data that genuinely improves the current solver, while co-evolving with it?

We address this question by formulating self-evolution as a bilevel game between a generator π_ϕ and a solver π_θ, both initialized from the same pretrained model. As illustrated in Figure 2, for each iteration, the generator proposes self-generated question–answer (QA) pairs conditioned on an unstructured corpus (textbook chunks in our experiments), which form the *curriculum*, and the solver is trained via a standard RLVR pipeline on this curriculum. To make these QA pairs more helpful for improving the solver's capability on the distribution of reasoning tasks we ultimately care about (our *target distribution*), we leverage a small QA dataset sampled from that target, referred to as a development dataset (*dev set*), to anchor the generator's optimization objective. The document pool supplies candidate curricula; it is not itself the target distribution. Rather than scoring a question by how difficult it is for the solver, we equip the generator with an *optimizer-aware influence score*, a per-question scalar that quantifies whether training the solver on the candidate question would actually improve its expected reward on the dev set. This score reduces to the cosine alignment between the dev-set gradient and the question's AdamW-induced update direction, and can be efficiently computed from minibatch data.

Leveraging this bilevel game framework with the influence score serving as the generator's reward, we propose **INFUSER** (**INF**luence-g**U**ided **S**elf-**E**volution Improves **R**easoning), a flexible self-evolution framework where both the generator and solver are trained using policy gradient methods, e.g., variants of GRPO (Shao et al., 2024). We instantiate INFUSER by optimizing the solving using Dr.GRPO (Liu et al., 2025e) and propose to train the generator using **DuGRPO**, a

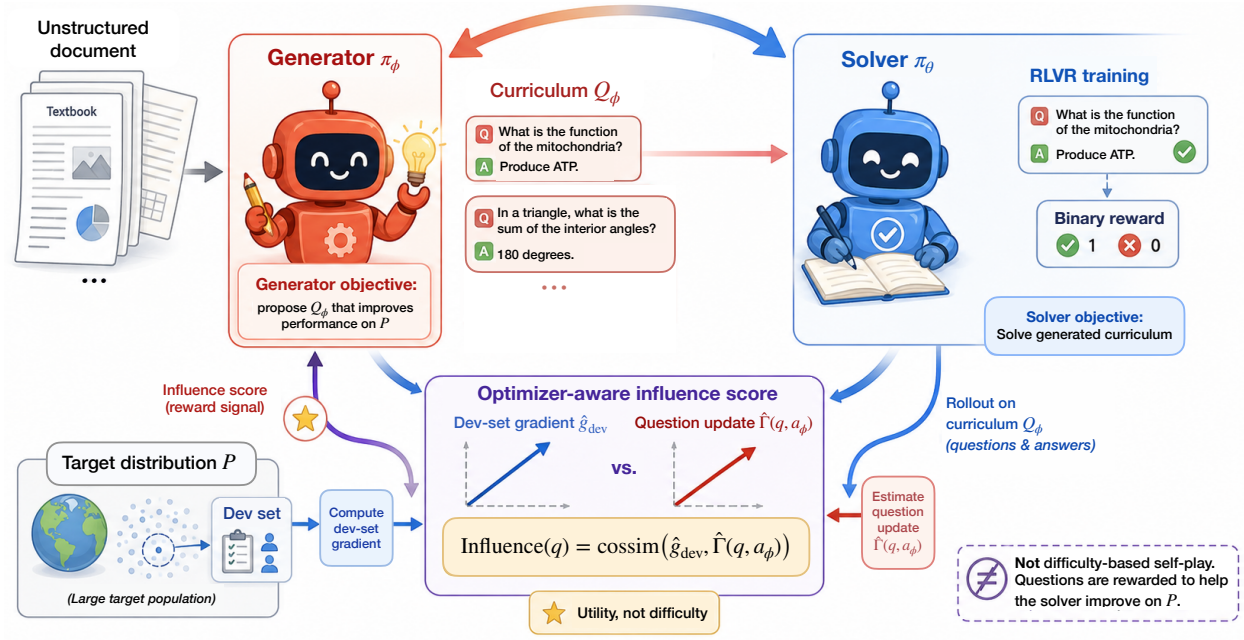

Figure 2: **INFUSER** casts document-grounded self-evolution as bilevel co-evolution between a generator and a solver. The generator proposes a curriculum from unstructured documents, the solver improves on this curriculum through RLVR training, and the generator is rewarded by an optimizer-aware influence score that measures whether each generated question induces a solver update aligned with target-distribution improvement.

variant of GRPO whose advantage estimator combines group-level and batch-level normalization to accommodate the continuous, noisy nature of the influence reward. Figure 2 illustrates the resulting data flow.

INFUSER delivers strong empirical gains under this design. On Qwen3-8B-Base it attains the top score on every category average (math, general reasoning, medical, and coding) and on 8 of 14 individual benchmarks, with relative gains over the base model exceeding 20% on GPQA-Diamond, SuperGPQA, BBEH, AIME, HMMT, and OlympiadBench (Math). When comparing Qwen3-4B-Base and Qwen3-8B-Base anchors, we find that INFUSER's gains are much more consistent in model size than other baselines, highlighting the ability to scale self-evolution to larger models. Notably, an 8B INFUSER *co-evolving* generator already outperforms a *frozen* 32B thinking generator significantly on math and coding. A generator-quality analysis further shows that the co-evolving generator produces increasingly well-posed and challenging questions across training, and the solver tracks this rising curriculum, so both players improve under the coupled training loop.

Finally, INFUSER generalizes along two further axes. It continues to improve an already *instruction-finetuned* anchor (OLMo-3-7B-Instruct-SFT), leading on 10 of 13 benchmarks versus the fixed generator baseline (§4); and a single INFUSER loop can augment document-grounded self-evolution with rule-verifiable RLVR, eliciting enhanced reasoning depth for better performance on challenging math benchmarks (§5).

Related Work. INFUSER builds on recent progress in reinforcement learning with verifiable rewards (RLVR) for language-model reasoning. DeepSeekMath introduced GRPO as an efficient RL objective for mathematical reasoning (Shao et al., 2024), and DeepSeek-R1-Zero showed that rule-based RL can elicit long-chain reasoning from a pretrained base model without an SFT cold start (Guo et al., 2025). Follow-up studies show that this "zero-style" RLVR recipe is sensitive to base-model capability, reward design, query difficulty, and training dynamics (Zeng et al., 2025), while broad-domain systems such as General-Reasoner extend verifiable RL beyond math with

large curated problem collections (Ma et al., 2025). This line establishes RLVR as a powerful post-training paradigm, but it still leaves open how to obtain training questions that are both verifiable and useful for the current model.

Self-improvement and self-play methods address this data bottleneck by letting the model generate or select its own training signal. STaR bootstraps reasoning traces through iterative generation and filtering (Zelikman et al., 2022), while recent self-evolution methods train generators, challengers, or conjecturers to produce tasks near the solver's current capability boundary (Dong and Ma, 2025; Huang et al., 2025; Zhao et al., 2025). Document-grounded variants such as SPICE further mine corpus environments to produce reasoning tasks from unlabeled text (Liu et al., 2025b). These approaches make the curriculum adaptive, but the generator is often rewarded by pass-rate, difficulty, or heuristic filtering signals. INFUSER instead asks a more direct question: would training on this generated question improve the solver on the target distribution?

Our answer connects self-evolution with influence-guided data optimization and meta-learning. Classical influence functions measure how training examples affect downstream predictions (Koh and Liang, 2017), and scalable gradient-alignment methods such as LESS use related signals to select useful instruction-tuning data from an existing pool (Xia et al., 2024). Recent synthesis methods train teachers or generators to produce influential data for a target student (Fan et al., 2026; Li et al., 2024). INFUSER differs by jointly co-evolving the generator and solver from the same pretrained model: the solver learns from document-grounded generated QA pairs, while the generator is trained through a bilevel objective approximated by an optimizer-aware influence reward tied to held-out solver performance. This places INFUSER within data-centric meta-learning (Hospedales et al., 2021; Vanschoren, 2018; Vilalta and Drissi, 2002), but with an evolving curriculum rather than a fixed synthetic dataset. A detailed discussion is deferred to §B.

2 Method

Notation. Throughout this paper, we write θ and ϕ for the solver and generator parameters. Both solver and generator models are initialized from the same pretrained checkpoint, but maintain separate parameters and optimizer states throughout training. We let q denote a question, and let $\{a, a_\phi, a^*\}$ denote various answers to the question q. We write $\mathcal{P}$ for the target distribution over verified QA pairs (q, a^*) that the solver is intended to improve on. In the main experiments, this target is instantiated by a science-reasoning dev set sampled from SuperGPQA Science; broader benchmark suites are used to measure aligned performance and transfer rather than to define the training target. For nonzero vectors u and v, we define $\mathrm{cossim}(u, v) := \langle u, v\rangle/(\|u\|\,\|v\|)$. See complete notation table in §A.

2.1 Game-theoretic Formulation for Self-Evolution

We formulate self-evolution as a bilevel game in which the solver trains on a curriculum of QA pairs proposed by the generator, and the generator is in turn optimized so that the induced solver update improves performance on the target distribution. The generator and the solver play the roles of *leader* and *follower*, respectively. We let π_ϕ and π_θ denote generator and solver language models, respectively, where ϕ and θ are parameters. Given any question q, the solver model π_θ outputs an answer $a \sim \pi_\theta(\cdot \mid q)$ through the conditional generation of the language model. In contrast, the generator π_ϕ takes an unstructured document d as input, and generates a QA pair (q, a_ϕ) based on d, i.e., $(q, a_\phi) \sim \pi_\phi(\cdot \mid d)$. Here q is the *generated question* and a_ϕ is the generator's *proposed reference answer*, which may be noisy or even wrong. To obtain a curriculum of QA pairs, denoted by $\mathcal{Q}_\phi$, we sample (q, a_ϕ) from π_ϕ, with the document d chosen from a document pool, denoted by $\mathcal{D}_{\mathrm{doc}}$. Here

$\mathcal{D}_{\text{doc}}$ contains unstructured texts relevant to the target distribution $\mathcal{P}$, ensuring that the generator is *grounded*.

In a nutshell, in the bilevel game of self-evolution, the objectives of the solver π_θ and generator π_ϕ are as follows:

(i) The solver π_θ aims to solve the curriculum of QA data $\mathcal{Q}_\phi$ generated by the generator π_ϕ;

(ii) The generator π_ϕ aims to generate $\mathcal{Q}_\phi$ that is beneficial for learning $\mathcal{P}$, in the sense that, after training on $\mathcal{Q}_\phi$, the solver π_θ achieves a higher accuracy for solving questions from $\mathcal{P}$.

Moreover, the solver π_θ and generator π_ϕ are initialized from the same language model, trained iteratively at the same time, while interacting with each other. In its idealized population form, illustrated in Figure 3, this bilevel game is mathematically formulated as

$$\begin{aligned} \max_{\phi} \quad & J(\theta^*(\phi)) \coloneqq \mathbb{E}_{(q,a^*)\sim\mathcal{P},\, a\sim\pi_{\theta^*(\phi)}(\cdot|q)}\left[r(a,a^*;q)\right] \\ \text{s.t.} \quad & \theta^*(\phi) = \operatorname*{argmax}_{\theta}\ J(\theta;\mathcal{Q}_\phi), \qquad J(\theta;\mathcal{Q}_\phi) \coloneqq \mathbb{E}_{(q,a_\phi)\sim\mathcal{Q}_\phi,\, a\sim\pi_\theta(\cdot|q)}\left[r(a,a_\phi;q)\right]. \end{aligned} \tag{2.1}$$

Here, $r(a,b;q)\in\{0,1\}$ denotes a binary *verifiable reward* function, which quantifies whether answer a is correct for question q, using b as the *reference*. We omit the dependency of unstructured document d in (2.1) to simplify the notation, which is used to generate $\mathcal{Q}_\phi$.

Interpretation of (2.1). In the **lower level** problem of (2.1), we generate a QA dataset $\mathcal{Q}_\phi$ using generator π_ϕ, and train the solver π_θ by assuming a_ϕ is the ground truth answer. With the binary reward r, $J(\theta;\mathcal{Q}_\phi)$ corresponds to the accuracy of the solver π_θ on the curriculum $\mathcal{Q}_\phi$. For a fixed generator, the best solver (best-response) is denoted by $\theta^*(\phi)=\operatorname{argmax}_\theta J(\theta;\mathcal{Q}_\phi)$, which corresponds to the ideal solver fully trained on data generated from π_ϕ. Fixing the generator, the solver's problem is the same as the standard RLVR problem with data $\mathcal{Q}_\phi$, and thus can be solved using policy-gradient type algorithms (Guo et al., 2025; Shao et al., 2024). Furthermore, in the **upper level** problem of (2.1), the objective $J(\theta^*(\phi))$ corresponds to the accuracy of the *best-response* solver model on the *target distribution* $\mathcal{P}$. The generator aims to maximize this objective indirectly by designing better $\mathcal{Q}_\phi$. Ideally, if $\mathcal{Q}_\phi$ is close to the $\mathcal{P}$, then $\theta^*(\phi)$ is close to the best model for $\mathcal{P}$.

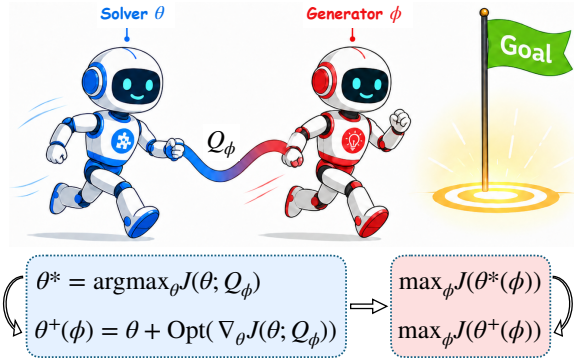

Figure 3: Bilevel view of the problem: the generator proposes a curriculum, the solver optimizes on it. The generator's goal is to induce a solver optimization that best generalizes to the target distribution. The formula at the bottom illustrates approximations made to (2.1)

Cooperative by design: rewarding the generator for helping, not hindering. In (2.1), the generator π_ϕ is optimized not merely to produce answerable questions, but more importantly, to induce a solver response that improves target-distribution performance. The game is "cooperative" only in the operational sense that the generator is rewarded for improving the solver rather than defeating it. We note that the bilevel game in (2.1) is not a cooperative game in the strict sense of game theory, because the generator and solver do not share the same optimization objective — it is a non-cooperative game where each player has its own objective (Başar and Olsder, 1998). In particular, the solver only optimizes the generated-reference objective $J(\theta;\mathcal{Q}_\phi)$, which is a *proxy* for

the true target $J(\theta)$, while the generator's job is precisely to keep that proxy faithful, shaping $\mathcal{Q}_\phi$ so that progress on $J(\theta; \mathcal{Q}_\phi)$ translates into progress on $J(\theta)$. The cooperative nature is achieved by reward design — the generator is rewarded by improving the solver's performance on the target distribution. To achieve such a goal, intuitively, we want to ensure (i) the solver learns to solve the curriculum $\mathcal{Q}_\phi$ and (ii) the curriculum $\mathcal{Q}_\phi$ is close to the target distribution $\mathcal{P}$. For a perfect generator such that $\mathcal{Q}_\phi$ has the same distribution as $\mathcal{P}$, the two optimization objectives in (2.1) coincide, hence improving the solver also benefits the generator.

Benefits of (2.1) compared with RLVR. When we have access to the target distribution $\mathcal{P}$, a direct approach is to train the solver using samples from $\mathcal{P}$ via RLVR. It seems that self-evolution in (2.1) is a detour. We argue that this approach offers two advantages:

(i) The solver is never directly trained on $\mathcal{P}$. Rather, $\mathcal{P}$ is used as a reference for the generator and the solver is trained on synthetic data based on unstructured texts. Thus, the self-evolution approach requires less golden data than RLVR, which is more appealing when the golden data is costly to obtain.

(ii) More importantly, when $\mathcal{P}$ is too challenging for the language model, direct RLVR is challenging. This is because the training signals of policy gradient algorithms such as GRPO (Shao et al., 2024) are computed by the *relative advantage* of repeated rollouts. When $\mathcal{P}$ is challenging, most of the generated answers are incorrect, and thus the training signals are weak, which makes GRPO struggle. In contrast, by bringing a generator into the scope and training the solver using generator's synthetic data, we are able to obtain more meaningful training signals for the solver. This is because the generator can generate easier QA pairs to guide the solver, and gradually increase the difficulty level during self-evolution.

From bilevel formulation to practical training. This ideal formulation clarifies the target, but it is not yet a practical training objective. It overlooks two key aspects of online self-evolution. First, every generator update would require recomputing the lower-level best response $\theta^*(\phi)$ by training the solver to convergence on the current curriculum $\mathcal{Q}_\phi$, which is prohibitively expensive at LLM scale. Second, the best-response view is static: it evaluates a curriculum only after full solver adaptation, overlooking the fact that solver at different stages of training may have different needs, and a curriculum that is good for the final adapted solver may not be good for the solver during the course of optimization. This means the generator also needs to *co-evolve* with the solver. We therefore replace the ideal population game with a turn-based, myopic one-step objective that encompasses the above-mentioned considerations.

▷ ***Per-iteration lower level (solver).*** We consider the question generation process to be document-conditioned. At each iteration, the generator samples documents $d \sim \mathcal{D}_{\text{doc}}$ and produces self-generated QA pairs $(q, a_\phi) \sim \pi_\phi(\cdot \mid d)$, forming a minibatch from $\mathcal{Q}_\phi$ (see §I for the construction of $\mathcal{D}_{\text{doc}}$). The generated pair is checked for parseable QA format, but the document is not a formal verifier for the factual correctness of a_ϕ. The solver then takes a single RL update on this batch, defining the *solver-update map* $\theta^+(\phi)$:

$$\theta^+(\phi) = \theta + \Delta\theta(\phi), \qquad \Delta\theta(\phi) = \text{Opt}\big(\nabla_\theta J(\theta;\, \mathcal{Q}_\phi)\big), \tag{2.2}$$

where $\text{Opt}(\cdot)$ is the optimizer update rule (e.g., AdamW) and $\nabla_\theta J(\theta;\, \mathcal{Q}_\phi)$ is the solver's policy gradient computed using minibatch $\mathcal{Q}_\phi$. Under (2.2), the generator's curriculum $\mathcal{Q}_\phi$ induces a *solver step* $\theta^+(\phi)$. This approximation avoids the cost of full convergence to $\theta^*(\phi)$, while maintaining a useful coupling between the generator's curriculum and the solver's optimization trajectory. In

the next part we will see how $\theta^+(\phi)$ can be used to derive a practical training objective for the generator.

▷ ***Per-iteration upper level (generator).*** The ideal upper level depends on the exact best response $\theta^*(\phi)$, but INFUSER only has the one-step adapted solver $\theta^+(\phi)$ from (2.2). Replacing $\theta^*(\phi)$ with this practical update map gives the generator objective:

$$\max_{\phi} \; J(\theta^+(\phi)) \quad \text{s.t.} \quad \theta^+(\phi) \text{ is given by (2.2).} \tag{2.3}$$

In this reduced problem, the solver updates its parameters θ using the generator's curriculum to obtain $\theta^+(\phi)$, while the generator updates ϕ to shape a curriculum whose induced solver step best improves target-distribution performance, as measured by $J(\theta^+(\phi))$. This formulation precisely captures the nested learning nature for the generator, where the influence of the generator's curriculum on the performance is mediated through the solver-update map $\theta^+(\phi)$. Since the population objective $J(\theta^+(\phi))$ is not directly computable, §2.3 instantiates it with a held-out development-set surrogate. That is, we replace the expectation with respect to $\mathcal{P}$ in (2.1) by the empirical mean over a fixed dev set sampled from $\mathcal{P}$. See §2.3 for details.

Challenges in solving (2.3). Even if we simplify the inner optimization to a single RL step, directly solving (2.3) via first-order methods is still challenging. The main challenge lies in the fact that $\nabla_\phi J(\theta^+(\phi))$ requires $\nabla_\phi \theta^+(\phi)$, which is hard to compute. Two typical ways to solve (2.3) are black-box outer-loop search and exact meta-gradient optimization. Both are impractical for LLM-scale online curriculum learning: the former reruns the full inner update for each generator proposal, while the latter backpropagates through the solver update as in MAML-style bilevel optimization (Finn et al., 2017). We defer details on these algorithms to §E. In the next subsection, we adopt a first-order approximation that turns the outer objective (2.3) into an influence-guided learning signal for the generator.

2.2 Self-evolution through Influence-Guided Optimization

To avoid the cost of exact bilevel differentiation in solving (2.3), we adopt a first-order approximation inspired by influence functions (Hampel, 1974; Koh and Liang, 2017; v. Mises, 1947). Consider the first-order Taylor expansion of the outer objective $J(\theta^+(\phi))$ around the current solver parameters θ:

$$J(\theta^+(\phi)) \approx J(\theta) + \big\langle \nabla_\theta J(\theta),\ \Delta\theta(\phi) \big\rangle. \tag{2.4}$$

We use this as a local first-order approximation: RL fine-tuning typically uses very small learning rates (order of 10^{-6}), making the single-step update $\|\Delta\theta(\phi)\|$ small, while the neglected term is second order in the update norm. See the bound in §D. Since $J(\theta)$ does not depend on ϕ, the generator can optimize the inner product term as a proxy for improving $J(\theta^+(\phi))$.

SGD example: influence scores as reward. Temporarily supposing $\mathrm{Opt}(\cdot)$ is the vanilla SGD update, we can decompose $\langle \nabla_\theta J(\theta), \Delta\theta(\phi) \rangle$ over the individual questions in the curriculum $\mathcal{Q}_\phi$ to obtain a per-question score that the generator can optimize via policy gradients. With a little abuse of notation, writing $g(q, a_\phi) = \nabla_\theta J(\theta;\, q, a_\phi)$ as the policy gradient induced by question $(q, a_\phi) \in \mathcal{Q}_\phi$, SGD with learning rate η_s on the mean batch loss gives

$$\big\langle \nabla_\theta J(\theta),\ \Delta\theta(\phi) \big\rangle = \frac{\eta_s}{|\mathcal{Q}_\phi|} \sum_{(q,a_\phi)\in\mathcal{Q}_\phi} \big\langle \nabla_\theta J(\theta),\ g(q, a_\phi) \big\rangle. \tag{2.5}$$

Each question's contribution is captured by the per-sample inner product $\langle \nabla_\theta J(\theta),\, g(q, a_\phi)\rangle$, the classical influence function, which gives a clean per-question score. Crucially, this score depends only on the static gradient $\nabla_\theta J(\theta)$ and the generated question–answer pair (q, a_ϕ), so it can be treated as standard **per-sample reward** for the generator and optimized with policy gradients, sidestepping the need to differentiate through the solver update map $\Delta\theta(\phi)$.

Optimizer-aware influence score. For the AdamW solver optimizer, we summarize the update induced by each generated pair with an optimizer-preconditioned per-question direction $\Gamma(q, a_\phi)$. This gives the following score.

Definition 2.1 (Optimizer-aware influence score)**.** *For solver parameter θ, let $J(\theta)$ denote the target performance. For a generated pair (q, a_ϕ), define the population single-question solver objective and its gradient as*

$$J(\theta; q, a_\phi) \coloneqq \mathbb{E}_{a\sim\pi_\theta(\cdot|q)}[r(a, a_\phi; q)], \qquad g(q, a_\phi) \coloneqq \nabla_\theta J(\theta; q, a_\phi). \tag{2.6}$$

Let $\Gamma(q, a_\phi)$ denote the AdamW-preconditioned per-question solver update direction induced by $g(q, a_\phi)$, holding the current solver optimizer state fixed. The exact preconditioning rule and its connection to AdamW are given in §D.2. The optimizer-aware influence score for generated (q, a_ϕ) at solver state θ is then

$$s(q, a_\phi) \;\coloneqq\; \operatorname{cossim}\big(\nabla_\theta J(\theta),\; \Gamma(q, a_\phi)\big). \tag{2.7}$$

Here, $\Gamma(q, a_\phi)$ plays the role of $g(q, a_\phi)$ in the SGD decomposition (2.5), so a positive cosine in (2.7) means training on q is expected to improve $J(\theta)$ (see §D for the derivation of Γ). We use cosine similarity rather than a raw inner product to avoid a spurious correlation between sequence length and gradient norm (Xia et al., 2024).

Influence score as generator's RL reward. As in the SGD case, $s(q, a_\phi)$ then serves directly as the generator's RL reward, with the generator facing the following optimization problem:

$$\max_{\pi_\phi} \mathbb{E}_{d\sim\mathcal{D}_{\mathrm{doc}},\,(q,a_\phi)\sim\pi_\phi(\cdot|d)}[s(q, a_\phi)]. \tag{2.8}$$

This optimizer-aware influence score therefore serves as a dense signal that judges whether the generated questions are useful for the solver at its current state, without requiring explicit optimizer differentiation or expensive black-box search. In the main algorithm, we only use $s(q, a_\phi)$ as the generator's scalar reward: each generated question is rated by its usefulness to the current solver, and the generator is updated to produce questions with higher influence scores. For completeness, §C.2 gives the corresponding REINFORCE estimator for (2.8); the actual generator update used by INFUSER is the DuGRPO update in §2.3, which normalizes these continuous influence rewards.

2.3 INFUSER: Co-evolving Generator and Solver with Influence-Guided RL

We now propose INFUSER (see Algorithm 1), a practical online algorithm that co-evolves the generator and solver using the one-step influence approximation above. At each iteration, INFUSER estimates a dev-set target direction, scores generated questions by their alignment with that direction, and alternates generator and solver RL updates on the resulting curriculum. The main components are therefore a dev-set-based empirical influence estimate, alternating solver–generator optimization, and a Dual-normalized Group Relative Policy Optimization (DuGRPO) update that stabilizes generator learning from continuous influence rewards. We detail these ingredients below.

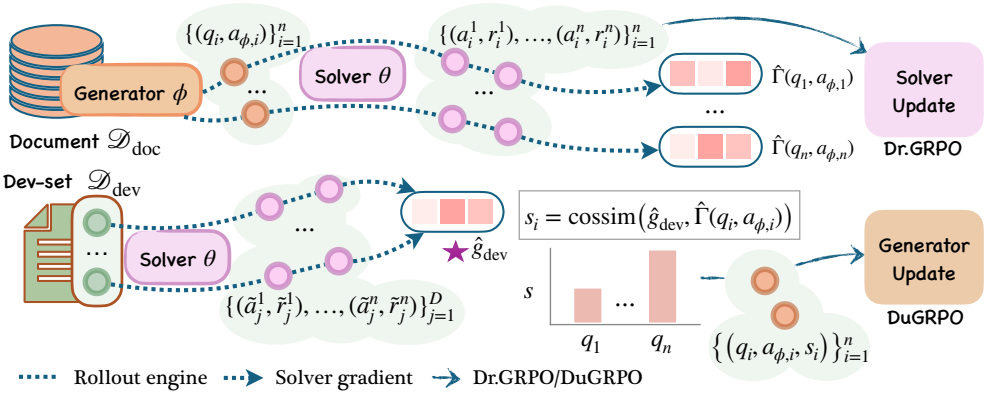

Figure 4: Detailed data flow for INFUSER. **Top:** In Phase 2, the generator produces self-generated QA pairs from documents, and in phase 3, the solver produces answers to these questions and receives binary rewards. Each question also receives an AdamW gradient direction $\hat{\Gamma}(q_i, a_{\phi,i})$. **Bottom Left:** In Phase 1, the solver produces answers to dev set questions, which are used to compute the reference gradient $\hat{g}_{\text{dev}}$. **Bottom Right:** In Phase 4, the influence scores are computed as the cosine similarity $\text{cossim}(\hat{g}_{\text{dev}}, \hat{\Gamma}(q_i, a_{\phi,i}))$ and used as rewards for the generator update. The solver's answers and rewards from Phase 3 are used for the solver update.

Algorithm 1: INFUSER (Detailed version in Algorithm 2)

Input: Pretrained LLM (for initializing both π_θ and π_ϕ), a document pool $\mathcal{D}_{\text{doc}}$, a small fixed dev set $\mathcal{D}_{\text{dev}}$, batch size B, group size n, maximum training iterations T, and invalid question penalty ρ_{inv}.

Output: A solver improved by training on a generator-adapted curriculum.

for *training loop* $1, \ldots, T$ **do**

- **Phase 1: Ask what is the improvement direction.** Run the current solver on $\mathcal{D}_{\text{dev}}$ with n rollouts and compute a dev reference gradient $\hat{g}_{\text{dev}}$ by (2.11).
- **Phase 2: Ask the generator for candidate question-answer pairs.** Sample B documents from $\mathcal{D}_{\text{doc}}$. For each sampled document d, have the generator write n question-answer pairs $(q, a_\phi) \sim \pi_\phi(\cdot \mid d)$. Filter out invalid questions with format issue to obtain curriculum $\mathcal{Q}_\phi$.
- **Phase 3: Test how each candidate would train the solver.** For each $(q, a_\phi) \in \mathcal{Q}_\phi$, run the solver on each generated question q for n times, score its answers against the reference answer a_ϕ, and compute the per-question solver update direction $\hat{g}(q, a_\phi)$ by (2.12).
- **Phase 4: Reward questions by optimizer-aware influence score.** For each $(q, a_\phi) \in \mathcal{Q}_\phi$, compute its AdamW update direction $\hat{\Gamma}(q, a_\phi)$ from $\hat{g}(q, a_\phi)$, and assign reward $\hat{s}(q, a_\phi) = \text{cossim}(\hat{g}_{\text{dev}}, \hat{\Gamma}(q, a_\phi))$. For each invalid question, assign penalty ρ_{inv}.
- **Phase 5: Improve the generator.** Treat n sampled questions from the same document as a group, update the generator with per question rewards computed in Phase 4 and the DuGRPO advantage in (2.14).
- **Phase 6: Improve the solver.** Treat n sampled answers from the same question as a group, update the solver on curriculum $\mathcal{Q}_\phi$ using solver rollouts and scores obtained in Phase 3 and apply Dr.GRPO.

return *the trained solver* π_θ.

Dev-set-based influence score estimate. The ideal outer objective J averages over the full target distribution $\mathcal{P}$, but INFUSER only needs a local direction that tells the current solver what "improving on the target task" means. We estimate this direction from a *small fixed* development set

$\mathcal{D}_{\text{dev}} = \{(q_i, a_i^*)\}_i$ sampled from $\mathcal{P}$, replacing J with the empirical surrogate

$$\widehat{J}(\theta) \;=\; \frac{1}{|\mathcal{D}_{\text{dev}}|} \sum_{(q,a^*)\in\mathcal{D}_{\text{dev}}} \mathbb{E}_{a\sim\pi_\theta(\cdot|q)}[r(a, a^*; q)], \tag{2.9}$$

which is made fully computable by the rollout-based estimator in (2.10) below. At the beginning of each iteration, we roll out the current solver on $\mathcal{D}_{\text{dev}}$ and compute $\nabla_\theta \widehat{J}(\theta)$. This gradient is then held fixed as the reference direction in the influence score (2.7): a generated question is useful when its induced solver-update direction aligns with this dev-improving direction.

The dev set therefore acts as an anchor for credit assignment, not as solver training data or generator prompt context. The solver update is performed on generated curriculum questions, and the generator is not prompted with dev questions. Since this anchor defines what counts as useful for the solver, $\mathcal{D}_{\text{dev}}$ should reflect the target question style; we analyze its effect on the resulting curriculum in §3.2 and §3.3.

Training objectives for solver–generator co-evolution. So far, we have described the population quantities that define INFUSER. In implementation, four quantities are estimated from rollouts: the dev reference gradient $\widehat{g}_{\text{dev}}$, the per-question solver direction used to form $\widehat{\Gamma}(q, a_\phi)$, the actual solver update gradient, and the generator update gradient. The first three are solver-side estimates, all differentiated with respect to θ; the last is a generator-side estimate differentiated with respect to ϕ. They all use the same clipped rollout objective, differing only in the policy, input, sampled outputs, and advantage.

Let us take ψ to represent θ or ϕ, let π_ψ be a policy with input z, let $\{x_1, \ldots, x_n\}$ be a group of outputs sampled from the rollout policy $\pi_{\psi_{\text{old}}}(\cdot \mid z)$. We estimate the corresponding gradient by plugging the row-specific advantage $\widehat{A}_i$ into

$$\mathcal{J}_\psi(z) = \frac{1}{n}\sum_{i=1}^{n} \frac{1}{C}\sum_{t=1}^{|x_i|} \min\left\{\rho_{i,t}\cdot\widehat{A}_i,\; \text{clip}(\rho_{i,t},\, 1{-}\epsilon,\, 1{+}\epsilon)\cdot\widehat{A}_i\right\}, \tag{2.10}$$

where $\rho_{i,t} = \pi_\psi(x_{i,t} \mid z, x_{i,<t})/\pi_{\psi_{\text{old}}}(x_{i,t} \mid z, x_{i,<t})$ is the token-level importance sampling ratio, n is the group size, $\widehat{A}_i$ is the advantage, ϵ is the clipping hyperparameter, and C is a fixed maximum generation length. The factor $1/C$ replaces GRPO's per-response normalization $1/|x_i|$, removing the length bias identified by Liu et al. (2025e) in Dr.GRPO. Throughout training, we use the same group size $n = 8$ for both the solver and generator. We note that if $\widehat{A}_i$ are the unnormalized advantage, this target coincides with the Dr.GRPO target.

For any reference pair (q, b), let $\mathcal{J}_\theta(q, b)$ denote (2.10) instantiated with the solver policy, input question q, solver answers sampled from $\pi_\theta(\cdot \mid q)$, binary rewards $r(a^i, b; q)$, and the mean-centred solver advantage in Table 1. The first row of the table gives the dev reference direction

$$\widehat{g}_{\text{dev}} = \frac{1}{|\mathcal{D}_{\text{dev}}|} \sum_{(\tilde{q},\tilde{a}^*)\in\mathcal{D}_{\text{dev}}} \nabla_\theta \mathcal{J}_\theta(\tilde{q}, \tilde{a}^*) \approx \nabla_\theta \widehat{J}(\theta), \tag{2.11}$$

computed once per iteration. For each generated pair, the second row of Table 1 gives the finite-rollout gradient

$$\widehat{g}(q, a_\phi) = \nabla_\theta \mathcal{J}_\theta(q, a_\phi), \tag{2.12}$$

which estimates $g(q, a_\phi)$ in (2.6); applying the AdamW preconditioning from §D.2 yields $\widehat{\Gamma}(q, a_\phi)$. The empirical influence reward for the generator is then

$$\widehat{s}(q, a_\phi) = \text{cossim}\big(\widehat{g}_{\text{dev}},\, \widehat{\Gamma}(q, a_\phi)\big). \tag{2.13}$$

Table 1: Sample-based gradient estimators in INFUSER. Each row is obtained by instantiating (2.10) with the listed policy, input, sampled output group, and advantage.

Quantity	Policy	Input z	Output group x_i	Advantage $\widehat{A}_i$
Dev reference $\widehat{g}_{\text{dev}}$	Solver π_θ	Dev pair $(\widetilde{q}, \widetilde{a}^*)$	Solver answers $\widetilde{a}^i \sim \pi_\theta(\cdot \mid \widetilde{q})$	$\widetilde{r}_i - \frac{1}{n}\sum_j \widetilde{r}_j$, where $\widetilde{r}_i = r(\widetilde{a}^i, \widetilde{a}^*; \widetilde{q})$
Per-question direction $\widehat{\Gamma}(q, a_\phi)$	Solver π_θ	Generated pair (q, a_ϕ)	Solver answers $a^i \sim \pi_\theta(\cdot \mid q)$	$r_i - \frac{1}{n}\sum_j r_j$, where $r_i = r(a^i, a_\phi; q)$
Solver update	Solver π_θ	Retained generated pair (q, a_ϕ)	Same solver answers a^i	Same mean-centred solver advantage as above
Generator update	Generator π_ϕ	Document d	QA pairs $(q_i, a_{\phi,i}) \sim \pi_\phi(\cdot \mid d)$	DuGRPO-normalized influence reward, defined in (2.14)

The third row uses the same solver-side objective to update θ on retained generated questions, while the fourth row plugs the generator policy into (2.10) and uses $\widehat{s}(q, a_\phi)$ as the reward.

Dual-normalized generator advantage (DuGRPO). Using influence scores as generator rewards poses a distinct normalization challenge: unlike binary correctness rewards, these rewards are continuous, noisy, and estimated from finite solver rollouts. Directly reusing existing RLVR advantage normalizers creates two issues:

1. *GRPO-style noise amplification.* Normalizing each document group by its own σ_d forces even low-variance groups to have unit-scale advantages, amplifying rollout noise when the generated questions have nearly indistinguishable influence scores.
2. *Dr.GRPO-style high-variance domination.* Using the raw mean-centered advantage without normalization avoids the previous amplification, but lets high-variance document groups dominate the generator gradient.

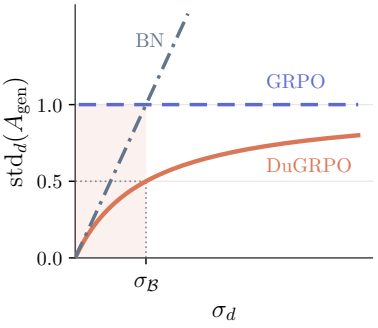

Figure 5: Within-group advantage std w.r.t. σ_d (fix $\sigma_{\mathcal{B}}$).

For a document d, let μ_d and σ_d denote the mean and standard deviation of the influence scores $\{s(q^k, a_\phi^k)\}_{k=1}^n$ generated from $\pi_\phi(\cdot \mid d)$. For a document batch $\mathcal{B}$, define $\sigma_{\mathcal{B}} := \text{mean}\{\sigma_{d'} : d' \in \mathcal{B}\}$. DuGRPO addresses both issues by keeping the within-group normalizer σ_d but adding a cross-group normalizer $\sigma_{\mathcal{B}}$ that can adapt to the overall advantage spread in the batch:

$$\widehat{A}_{\text{gen}}(q^k, a_\phi^k) := \frac{s(q^k, a_\phi^k) - \mu_d}{\sigma_d + \sigma_{\mathcal{B}} + \epsilon}, \quad k = 1, \ldots, n. \tag{2.14}$$

Its within-group standard deviation is $\text{std}_d(A_{\text{gen}}) = \sigma_d/(\sigma_d + \sigma_{\mathcal{B}} + \epsilon)$. As we show in Figure 5, DuGRPO elegantly damps the low-variance groups ($\sigma_d < \sigma_{\mathcal{B}}$ with no significant advantage) and roughly maintains the unit-spread benefit of GRPO when $\sigma_d > \sigma_{\mathcal{B}}$. Two ablation normalizers plotted in Figure 5 and will be compared in §3.3 are GRPO-style $\widehat{A}_{\text{GRPO}}$ and batch-normalized $\widehat{A}_{\text{BN}}$:

$$\widehat{A}_{\text{GRPO}}(q^k, a_\phi^k) := \frac{s(q^k, a_\phi^k) - \mu_d}{\sigma_d + \epsilon}, \qquad \widehat{A}_{\text{BN}}(q^k, a_\phi^k) := \frac{s(q^k, a_\phi^k) - \mu_d}{\sigma_{\mathcal{B}} + \epsilon}. \tag{2.15}$$

Other algorithm components. Two implementation details determine which rollouts contribute gradients. First, we remove only zero-variance groups: document groups with identical influence rewards yield no generator advantage, and question groups with identical correctness rewards yield no solver advantage. Invalid generated questions are excluded from solver rollouts and influence scoring; in the reported INFUSER runs, their generator-side penalty is set to $\rho_{\text{inv}} = 0$. This choice treats invalid questions as having zero influence because they neither help nor hurt the solver update, and it still discourages invalid generations: valid questions that are useful for training can receive positive influence rewards and therefore win in the generator update. After variance filtering, the solver trains on the retained generated questions using its standard correctness reward. Second, the generator update is applied before the solver update on the same rollout batch, so generator credit assignment is based on the current solver state and all dev directions and influence scores are recomputed at the next iteration. Both models use minibatch size $M = 32$, so a retained rollout batch can yield multiple optimizer steps. To control the resulting off-policy drift from the rollout policy $\pi_{\psi_{\text{old}}}$, we apply token-level Truncated Importance Sampling (Yao et al., 2025), clipping the current-policy-to-rollout-policy ratio at $\rho_{\max} = 2.0$ when evaluating (2.10).

3 Experiments

3.1 Training Setup and Benchmark Evaluation

Training configuration. For INFUSER, we use a document pool of size $|\mathcal{D}_{\text{doc}}| = 12{,}260$ chunks collected from textbooks in Astronomy, Biochemistry, Geography, and Physics. The dev set $\mathcal{D}_{\text{dev}}$ contains 800 randomly sampled questions from the SuperGPQA (M-A-P Team et al., 2025) science subset, comprising 3% of the full SuperGPQA set. We chose SuperGPQA science because it spans diverse scientific subfields and has been carefully curated for question quality. We show in §3.3 that little leakage occurs through this dev set for INFUSER training, so we still treat SuperGPQA as a valid evaluation benchmark. We train INFUSER for $T = 100$ iterations on $8\times$ H100 GPUs with document batch size $B = 128$, group size $n = 8$ for both generator and solver rollouts, AdamW with weight decay 0.01 and mini-batch size 32. We use solver learning rate 2×10^{-6} and generator learning rates 6×10^{-6} and 4×10^{-6} for Qwen3-4B-Base and Qwen3-8B-Base anchors, respectively. More details are in §G.

Evaluation protocol. We evaluate on general reasoning, math & physics, and two out-of-domain transfer suites, medical and coding; benchmarks, prompts, and sampling scheme are in §F. Throughout, Δj denotes the performance gap between a method and the base model on the same benchmark.

INFUSER outperforms self-evolution baselines across domains and scales. We compare **INFUSER** with the base model and four contemporaneous self-evolution methods: R-Zero (Huang et al., 2025), AZR (Zhao et al., 2025), R-Few (Yu et al., 2025b), and SPICE (Liu et al., 2025b) on Qwen3-4B-Base and Qwen3-8B-Base as anchors. Table 2 reports the per-benchmark and category-average accuracies for all methods. We observe three key trends: (i) **INFUSER yields the largest gains on aligned domains.** INFUSER's gains are strongest on the general reasoning and Math & physics benchmarks, with nearly 20% improvements for both anchors. These two fields are the most aligned with our document pool and dev set. (ii) **INFUSER unlocks cross-domain transfer.** Despite the domain gap, INFUSER still improves over the base model on the medical and coding benchmarks, with gains comparable to or exceeding the best baselines. The out-of-domain transfer is consistent with previous findings on RLVR (Liu et al., 2025c; Wang et al., 2025a; Wen et al., 2025). (iii) **INFUSER's gains scale to larger models.** INFUSER uniformly outperforms other methods

Table 2: Solver accuracy (%) on held-out benchmarks for Qwen3-4B-Base and Qwen3-8B-Base. Bolded entries mark the best score among the five training methods per row. Dashes indicate the benchmark was not reported by that method. The Base, INFUSER, R-Zero, and AZR columns are trained (where applicable) and evaluated by us under the unified harness in §F; daggered columns (R-Few†, SPICE†) are self-reported numbers taken from the original papers. INFUSER's scores are averaged over 3 seeded training runs.

	Qwen3-4B-Base						Qwen3-8B-Base					
Benchmark	Base	INFUSER	R-Zero	AZR	R-Few†	SPICE†	Base	INFUSER	R-Zero	AZR	R-Few†	SPICE†
General reasoning												
MMLU-Pro	52.98	**60.20**	55.80	57.53	56.20	58.10	59.91	**66.20**	61.82	62.32	63.20	65.00
GPQA-Diamond	31.41	36.80	34.44	37.17	**39.90**	39.40	36.87	45.48	42.73	44.14	**46.50**	39.40
SuperGPQA	25.88	**33.48**	28.40	28.31	29.40	30.20	30.62	**37.77**	32.06	32.63	33.50	35.70
BBEH	7.57	11.22	10.06	8.70	11.80	**12.30**	10.30	13.04	11.93	11.33	12.30	**14.90**
Category average	29.46	**35.43**	32.18	32.93	34.33	35.00	34.43	**40.62**	37.14	37.61	38.88	38.75
Rel. improv. over Base (%)	—	**+20.26**	+9.23	+11.78	+16.53	+18.81	—	**+17.98**	+7.87	+9.24	+12.92	+12.55
Math & physics reasoning												
MATH500	61.20	76.65	76.85	73.90	**78.00**	**78.00**	76.05	**82.77**	80.55	80.95	82.60	79.40
AIME2024	10.42	11.35	9.38	**13.54**	—	12.20	12.92	18.58	13.96	**19.48**	—	18.40
AIME2025	8.44	10.73	7.19	13.75	—	**19.10**	11.87	15.87	13.33	14.17	—	**18.20**
HMMT	2.49	2.94	2.65	**4.50**	—	—	2.96	**7.04**	3.86	6.01	—	—
OlympiadBench (Math)	35.31	42.38	**43.18**	**43.18**	42.80	42.70	40.36	**50.24**	45.10	47.92	46.40	42.50
OlympiadBench (Phys)	10.17	10.31	**11.44**	10.17	—	—	12.29	**14.41**	13.98	13.14	—	—
Category average	21.34	25.73	25.12	**26.51**	—	—	26.08	**31.49**	28.46	30.28	—	—
Rel. improv. over Base (%)	—	+20.57	+17.71	**+24.23**	—	—	—	**+20.74**	+9.13	+16.10	—	—
Medical												
MedQA	55.46	58.86	58.92	**59.62**	—	—	64.18	**65.78**	65.12	65.28	—	—
MedXpertQA	13.02	13.78	**14.57**	12.65	—	—	14.49	**15.25**	15.22	14.49	—	—
Category average	34.24	36.32	**36.75**	36.14	—	—	39.34	**40.52**	40.17	39.89	—	—
Rel. improv. over Base (%)	—	+6.07	**+7.33**	+5.55	—	—	—	**+3.00**	+2.11	+1.40	—	—
Coding												
HumanEval+	70.27	**74.90**	73.48	72.64	—	—	75.94	78.57	**79.19**	78.05	—	—
LiveCodeBench v1-5	20.68	**22.35**	21.82	22.33	—	—	25.23	28.01	25.91	**28.30**	—	—
Category average	45.47	**48.63**	47.65	47.49	—	—	50.59	**53.29**	52.55	53.18	—	—
Rel. improv. over Base (%)	—	**+6.95**	+4.79	+4.44	—	—	—	**+5.34**	+3.87	+5.12	—	—

on all four category averages at 8B. Its 4B-to-8B gain decay is minimal: math-and-physics holds ($+20.57\% \rightarrow +20.74\%$) and general-reasoning drops only ~ 2.3 points ($+20.26\% \rightarrow +17.98\%$). Baselines lose substantially more, e.g., R-Zero's math gain nearly halves ($+17.71\% \rightarrow +9.13\%$) and SPICE's general-reasoning gain drops ~ 6.3 points ($+18.81\% \rightarrow +12.55\%$).

Comparison with General-Reasoner. Figure 6a compares INFUSER with General-Reasoner (Ma et al., 2025) on Qwen3-8B-Base. Note that General-Reasoner is *not* a self-evolution method: it is standard RLVR over a fixed dataset of 230K closed-model-curated questions (details in §G). INFUSER instead co-evolves the generator with the solver from a 12K-chunk science-textbook pool, with no closed-source teacher, verifier, or judge inside the iterative training loop. The document-pool construction stage uses an external browsing assistant only to locate open-access textbook sources, as detailed in §I. Despite this much weaker data-side supervision, INFUSER is stronger on 5 of 6 math benchmarks, remains competitive on the general-reasoning benchmarks, and is more balanced across the out-of-domain benchmarks.

3.2 Generator Quality Analysis

To assess whether the co-evolving generator produces a useful curriculum, we evaluate the questions produced by INFUSER generator (Qwen3-8B-Base anchor) at checkpoints $\{0, 30, 60, 90\}$ with

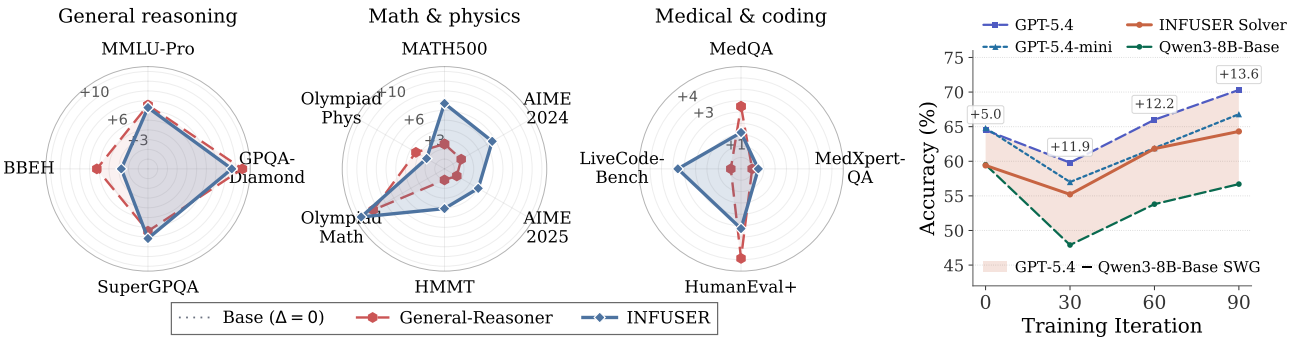

(a) General-Reasoner comparison.

(b) Generator quality.

Figure 6: **Left:** per-benchmark Δ over Qwen3-8B-Base for INFUSER and General-Reasoner. **Right:** solver accuracy on the questions produced by INFUSER's co-evolving generator in training; the annotation is the *strong-against-weak gap* (SWG) between GPT-5.4 and Qwen3-8B-Base.

four solvers: the Qwen3-8B-Base, the evolving INFUSER solver, GPT-5.4-mini, and GPT-5.4. We track both *per-solver accuracy* and the *strong-against-weak gap* (SWG), which is the accuracy gap between GPT-5.4 and Qwen3-8B-Base on the generator-produced questions, verified against the generator's own reference answers a_ϕ. A rising SWG indicates questions that grow harder for the base model yet remain well-posed (i.e., solvable by a strong solver), ruling out degenerate or ill-posed drift.

INFUSER produces a rising curriculum at the solver's learning frontier. Figure 6b reveals a two-phase dynamic. From iteration 0 to 30, both solvers' accuracy drops yet the SWG more than doubles from $+5.0$ to $+11.9$, indicating that the added difficulty reflects genuine reasoning challenge rather than ill-posed questions. From iteration 30 to 90, the generator transitions to a *hardness-vs-quality trade-off*: both solvers' accuracy rises, but GPT-5.4 grows significantly faster, widening the SWG to $+13.6$. The INFUSER solver stays 7–8 points above the base model and tracks GPT-5.4-mini from iteration 30 onward, indicating that INFUSER's co-evolving solver can indeed learn from such a rising curriculum.

A qualitative example. We further provide an example in Figure 7 to examine in detail what improves in the generated questions and highlight two attributes: *self-containedness* and *factual correctness of the ground-truth key*. More details can be found in the related discussion in §C.3.

Source document: lecture notes on membrane biophysics, ion permeability of lipid bilayers

$\cdots$ [$\approx$3700 characters skipped] $\cdots$

A calculation of the image force gives the following result for the work necessary to move a charge from water to the middle of a membrane,

$$\Delta G = \frac{q^2}{2a}\left(\frac{1}{\varepsilon_{\mathrm{h}}} - \frac{1}{\varepsilon_{\mathrm{w}}}\right) - \frac{q^2}{\varepsilon_{\mathrm{h}}\, l}\ln\left(\frac{2\varepsilon_{\mathrm{w}}}{\varepsilon_{\mathrm{w}} + \varepsilon_{\mathrm{h}}}\right) \qquad (14.2),$$

where l is the membrane thickness, a the ionic radius, and q the charge. If we envision the flux as a barrier-crossing process, the rate is proportional to $J \propto e^{-\Delta G/KT}$ (14.3).

$\cdots$ [$\approx$3000 characters skipped] $\cdots$

Base model question (ill-posed)

Q. Given the free energy difference equation (14.2) for an ion moving from water to the interior of a membrane, which of the following factors would NOT increase the ion's flux across the membrane according to the barrier-crossing rate equation (14.3)?
(A) Increasing the ion's effective radius
(B) Decreasing the dielectric constant of the membrane interior
(C) Reducing the thickness of the membrane
(D) Lowering the temperature
Ground truth: (A) ✗.

Checkpoint 90 question (well-posed)

Q. Given the free energy difference equation for moving an ion from water to the middle of a membrane, $\Delta G = \frac{q^2}{2a}\left(\frac{1}{\varepsilon_{\mathrm{h}}} - \frac{1}{\varepsilon_{\mathrm{w}}}\right) - \frac{q^2}{\varepsilon_{\mathrm{h}}\, l}\ln\left(\frac{2\varepsilon_{\mathrm{w}}}{\varepsilon_{\mathrm{w}}+\varepsilon_{\mathrm{h}}}\right)$, which of the following correctly describes the impact of increasing the membrane thickness l on the flux J of an ion, assuming the flux is proportional to $e^{-\Delta G/KT}$?
(A) Increasing l decreases ΔG and thus increases J
(B) Increasing l increases ΔG and thus decreases J
(C) Increasing l has no effect on ΔG and thus no effect on J
(D) Increasing l decreases ΔG but increases J only slightly
(E) Increasing l increases ΔG but decreases J only slightly
(F) Increasing l makes ΔG zero and thus J infinite
Ground truth: (B) ✓.

Figure 7: Qualitative comparison of questions produced by INFUSER's co-evolving generator from the same source document at checkpoint 0 and checkpoint 90.

3.3 Ablation Study

To better understand the role of each component in INFUSER, we compare against alternative training strategies that represent natural design choices. Unless stated otherwise, all experiments in this section use **Qwen3-8B-Base** as the anchor model, with $\mathcal{D}_{\mathrm{dev}}$ set to an 800-question subset of SuperGPQA Science. For each method, we perform a single seeded training run and report the best checkpoint selected by the validation protocol of §F.2 (validation accuracy on a small validation set, checked every 5 training iterations). The reported scores therefore differ slightly from those in Table 2, which are averaged over three seeds.

3.3.1 Ablation on generator

The generator is the component that turns $\mathcal{D}_{\mathrm{doc}}$ into a usable training curriculum. We ablate it along three axes: whether the generator is needed (*Dev-only*), whether it must co-evolve with the solver (*Fix-gen*), and whether it must be trained at all (*Strong-gen*). The comparison is summarized in Figure 8. All four runs share the same solver configuration (learning rate, batch size, number of iterations) as the INFUSER anchor on Qwen3-8B-Base.

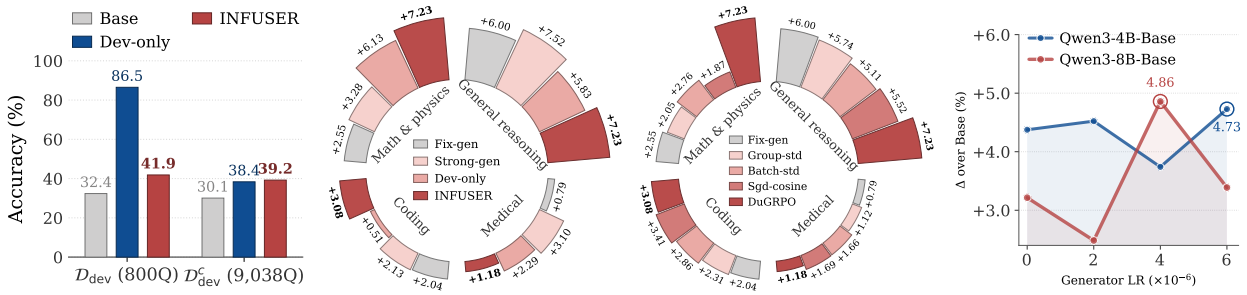

(a) Dev-set leakage. (b) Generator ablation. (c) Update-rule ablation. (d) Generator-LR sweep.

Figure 8: Generator ablations on Qwen3-8B-Base. **(a)** Dev-only memorizes $\mathcal{D}_{\text{dev}}$ while trailing INFUSER on the held-out complement $\mathcal{D}^{\text{c}}_{\text{dev}}$. **(b)** Δ over Base by benchmark category for four generator-source variants (Fix-gen, Strong-gen, Dev-only, INFUSER). **(c)** Two DuGRPO normalization variants and one influence-score variant without optimizer-awareness. **(d)** Mean accuracy over 14 benchmarks vs. generator learning rate on Qwen3-4B-Base and Qwen3-8B-Base. For each method, we report the best checkpoint chosen by the validation protocol of §F.2.

Direct dev-set training still generalizes, but trails INFUSER. To test whether the generator is needed at all, we introduce a **Dev-only** baseline that drops the generator and trains the solver directly on the 800-question $\mathcal{D}_{\text{dev}}$. This baseline is useful as a diagnostic, and it is not a pure failure: Figure 8b shows that it improves over the base model on all four category averages. However, it is not a viable training recipe: high-quality evaluation questions are scarce and expensive to produce (M-A-P Team et al., 2025; Rein et al., 2023), and using them as solver training data contaminates the signal used to measure progress. To diagnose whether such direct training generalises, we evaluate every method on two splits drawn from the same source distribution: $\mathcal{D}_{\text{dev}}$ itself, and the *held-out complement* $\mathcal{D}^{\text{c}}_{\text{dev}}$, defined as the $9{,}038$ remaining SuperGPQA Science questions after $\mathcal{D}_{\text{dev}}$ is removed. Figure 8a illustrates this. On $\mathcal{D}_{\text{dev}}$, Dev-only scores 86.5%, far above INFUSER's 41.9%. But on $\mathcal{D}^{\text{c}}_{\text{dev}}$, Dev-only collapses to 38.4% while INFUSER holds at 39.2%. In other words, Dev-only mostly memorises the 800-question training sample rather than learning $\mathcal{P}$, whereas INFUSER's nearly identical scores on the two splits indicate that the dev signal has been turned into a generalising curriculum. INFUSER also leads on the math, general reasoning and coding category averages in Figure 8b, demonstrating the value of using a generator to turn the dev signal into a renewable curriculum $\mathcal{Q}_\phi$.

INFUSER beats training with a larger frozen generator. A natural question is whether the generator needs to co-evolve with the solver at all. An initial document-conditioned generator might already provide enough useful questions, or a much stronger frozen generator might compensate for the lack of adaptation by producing higher-quality questions. We therefore test two fixed-generator baselines under the same solver updates as INFUSER: **Fix-gen** keeps the same 8B generator frozen at its initial checkpoint, while **Strong-gen** replaces it with a frozen Qwen3-32B thinking model.

At the same-size level, Fix-gen underperforms INFUSER on *all* four categories, and the gap is especially large on math ($+7.23$ vs. $+2.55$). Thus, a static same-size generator is not enough: the curriculum must track the solver's changing learning frontier. Scaling the frozen generator helps. Strong-gen wins on general reasoning and medical. However, INFUSER, with only an 8B generator, still wins on math and coding, and is within 0.3 points of Strong-gen on general reasoning.

Finding 3.1. Adaptation beats scale on reasoning, scale wins on knowledge. An 8B INFUSER generator outperforms a frozen 32B strong generator when used to train the solver on math and coding, and trails by only 0.3 points on general reasoning. The frozen 32B generator's broader prior helps mainly on the more knowledge-heavy domains, namely general reasoning and medical.

INFUSER benefits from both document knowledge and dev-set influence. The generator-source ablation in Figure 8b further reveals that the dev set and the document pool appear to play different roles. On math, the single-source **Dev-only** variant already delivers a large gain among the baselines ($+6.13$), substantially ahead of the two document-conditioned runs (Fix-gen $+2.55$, Strong-gen $+3.28$). This pattern reverses on general reasoning: both document-conditioned runs (Fix-gen $+6.00$, Strong-gen $+7.52$) outperform Dev-only ($+5.83$). This suggests that the dev-set signal directs the curriculum toward math-style logical reasoning, while the document pool supplies broader source material that transfers better to general reasoning.

Finding 3.2. INFUSER excels at combining knowledge and reasoning. The document-conditioned generator supplies diverse training content, while the influence signal from $\mathcal{D}_{\text{dev}}$ directs that content toward the desired reasoning patterns. The resulting joint gains are the largest we observe on math and remain competitive on general reasoning.

Together, §3.3.1 confirms the central INFUSER design: pair a document-conditioned generator with influence-guided supervision from $\mathcal{D}_{\text{dev}}$, so that the curriculum becomes increasingly targeted and high-quality as training progresses.

3.3.2 Optimizer-aware influence score and DuGRPO are essential

The generator update rule combines two ingredients: the DuGRPO advantage in (2.14), which normalizes the raw influence signal at both the within-group and batch levels, and the optimizer-aware influence score itself (defined in §2, (2.7)). We ablate each ingredient in isolation while holding the **Qwen3-8B-Base INFUSER configuration** and generator learning rate (4×10^{-6}) fixed. `group_std` (the standard GRPO advantage A_{GRPO}) and `batch_std` (A_{BN}), both defined in (2.15), keep only the within-group or only the batch term of the DuGRPO advantage, respectively. `sgd_cosine` keeps the full DuGRPO advantage but swaps the optimizer-aware influence score for a plain SGD-style cosine, dropping the AdamW preconditioner $\Gamma(q, a_\phi)$ in favor of the raw per-question gradient $g(q, a_\phi)$ from the SGD decomposition in (2.5). For reference we also overlay the *Fix-gen* baseline from the previous section, which freezes the generator entirely and therefore provides a lower bound for any generator-update rule in this configuration. The resulting comparison is shown in Figure 8c.

Replacing DuGRPO with either `group_std` or `batch_std` reduces performance on math and general reasoning, yielding performance close to the Fix-gen reference (Figure 8c). Swapping the optimizer-aware influence score for the plain `sgd_cosine` variant has the same effect: general reasoning and math regress toward Fix-gen, while coding and medical change by less than a point. In effect, neither alternative normalization nor the SGD-style influence score produces effective generator training, so the solver trains against a curriculum that is indistinguishable from a frozen generator. This matches the motivation in (2.14): DuGRPO's combined group and batch scaling, together with the optimizer-aware influence score, turns noisy influence signals into generator

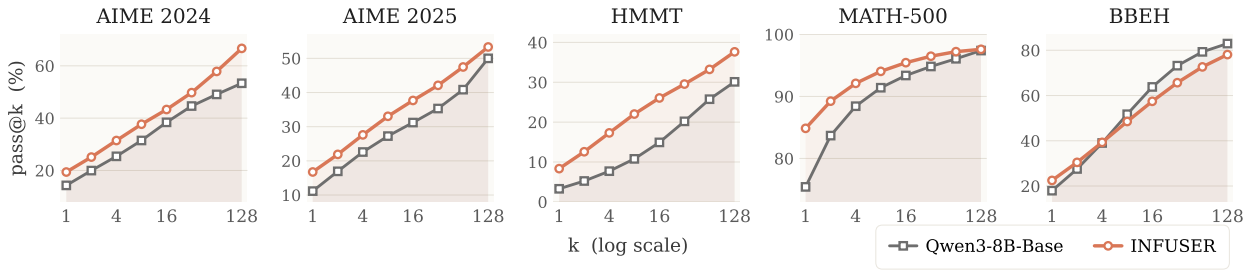

Figure 9: pass@k curves on four open-form math benchmarks plus BBEH for the Qwen3-8B-Base anchor, comparing the base model to **INFUSER**. We exclude pure multiple-choice tasks because pass@k on a small answer space is heavily inflated by random guessing.

updates that move beyond the frozen-generator baseline.

3.3.3 Generator learning rate requires per-anchor tuning

To justify the anchor-specific generator learning rates used in §3.1, we sweep the generator learning rate over $\{0, 2 \times 10^{-6}, 4 \times 10^{-6}, 6 \times 10^{-6}\}$ on both Qwen3-4B-Base and Qwen3-8B-Base, where 0 corresponds to the Fix-gen baseline and nonzero points report the best checkpoint per run selected by the validation protocol of §F.2. As shown in Figure 8d, the sweep peaks at 6×10^{-6} on Qwen3-4B-Base and at 4×10^{-6} on Qwen3-8B-Base, which are exactly the generator learning rates used for each anchor in §3.1. More broadly, the anchor-dependent and non-monotone shape of the sweep underscores that INFUSER is a dynamical two-player game: the generator learning rate sets the tempo at which the generator adapts to the solver, and the best operating point is a joint property of the two players rather than a universal step-size choice.

3.4 Pass@k study

Top-1 accuracy alone cannot distinguish whether a method merely sharpens its best sample or improves the support of its sampled reasoning distribution. To make pass@k meaningful, we therefore restrict attention to hard math and general-reasoning benchmarks that are not pure multiple choice. On pure MCQ tasks, a model can artificially improve pass@k by sampling many guesses over a small answer space, so the resulting curve reflects random-choice coverage rather than reasoning diversity. Figure 9 therefore plots the Qwen3-8B-Base anchor on four open-form math benchmarks plus BBEH, a general-reasoning benchmark whose answer space is broad enough to suppress random-guessing effects. INFUSER's curve stays above the base model for all $k \leq 128$ on AIME 2024, AIME 2025, HMMT, and MATH-500. By contrast, on the general-reasoning benchmark BBEH, the two curves cross at $k = 4$. This reflects a distinct reasoning pattern: on general reasoning, the model produces more consistent but less diverse outputs than on math.

4 Extension to Instruction-Finetuned Models

Our main experiments all start from pretrained base models (Qwen3-4B-Base and Qwen3-8B-Base). A natural question is whether INFUSER still yields gains when the anchor is already an *instruction-finetuned* (IF) model whose next-token distribution has been reshaped by supervised finetuning. The IF setting is also a stricter stress test: INFUSER must adapt the model to a document-grounded curriculum without destroying the formatting and instruction-following habits learned during SFT.

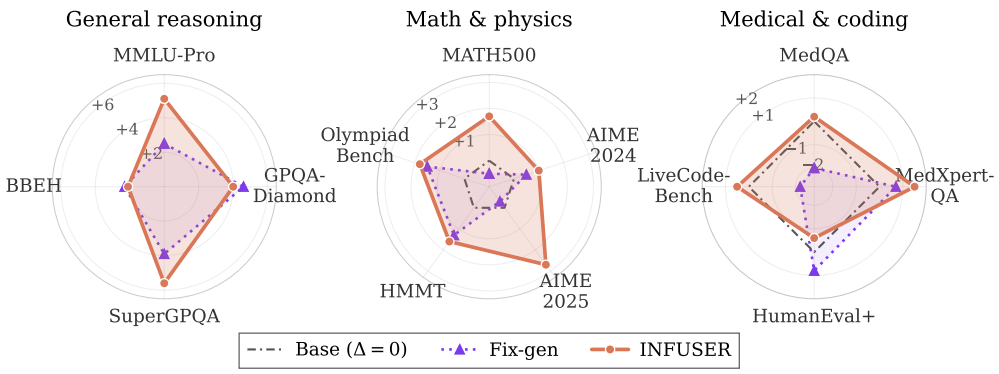

Figure 10: Per-benchmark Δ over the OLMo-3-7B-Instruct-SFT base for Fix-gen and INFUSER, grouped into general reasoning (left), math & physics (center), and medical & coding (right). The dash-dot ring at $\Delta = 0$ marks the base IF checkpoint. The full per-benchmark accuracy table is in Table 13.

We test this with **OLMo-3-7B-Instruct-SFT** (Team Olmo, 2025), chosen because OLMo-3 releases its training recipe and instruction-tuning mixture, which makes attribution and contamination auditing possible for an IF anchor. By contrast, instruction-tuned Qwen3 checkpoints have undergone private post-training with large-scale SFT, RL, and/or teacher distillation, making additional gains or regressions much harder to attribute. We compare the untrained IF **Base**, **Fix-gen** (solver-only DrGRPO with a frozen generator), and **INFUSER** under the same document pool, 800-question SuperGPQA Science development set, and evaluation protocol as the main experiments. Both trained runs use solver learning rate 2×10^{-6}; INFUSER uses generator learning rate 4×10^{-6}. Full setup, checkpoint-selection, anchor-choice, and contamination-audit details are deferred to Sections C.4 and J. The audit finds no near-duplicate overlap between either $\mathcal{D}_{\text{doc}}$ or $\mathcal{D}_{\text{dev}}$ and the released OLMo-3 SFT mixture under the protocol of §J.

Results. Figure 10 shows the per-benchmark gain of Fix-gen and INFUSER over the IF base. INFUSER leads on 10 of the 13 benchmarks and attains the highest overall average. We see substantial gains on MMLU-Pro ($\Delta = +5.1$) and SuperGPQA ($\Delta = +5.6$), and the same alignment pattern from the pretrained anchors reappears: gains are largest on general reasoning, the INFUSER polygon encloses Fix-gen on all five math axes, and out-of-domain medical/coding transfer is smaller. Fix-gen also improves general reasoning, but it sits inside INFUSER on math and dips below the base IF checkpoint on MedQA and LiveCodeBench. Thus, influence-guided generator updates continue to add value beyond solver-only DrGRPO even after the anchor has already been instruction-finetuned.

5 Extension: Augmenting Self-Evolution with RLVR

Our main experiments drive self-evolution entirely from unlabeled documents: every solver update is supervised by questions the generator synthesizes from $\mathcal{D}_{\text{doc}}$. A complementary source of solver signal is rule-verifiable RLVR, where the solver trains directly on externally answered problems scored by a programmatic checker. The two signals are usually studied in isolation. We ask whether a single **INFUSER** loop can combine them, training one solver jointly on document-grounded science self-evolution and verifiable math RLVR. The question is motivated by a concrete failure mode of the science-only setting as follows.

A seed instability in math coupled with response length collapse. In Figure 11, left, we show both the average category accuracy and the cross-seed sample standard deviation of that accuracy across three seeds for the INFUSER Qwen3-8B-Base anchor (under Science-only INFUSER group). Across three seeds, science-only INFUSER is stable on general reasoning, medical, and coding (cross-seed sample standard deviations of 0.96, 0.37, and 0.51 percentage points), but unstable on math & physics, where the cross-seed standard deviation is 2.80 percentage points. Plotting each checkpoint's evaluation-time response length against its math-and-physics accuracy (Figure 11, right), we find a strong log-linear correlation ($r = 0.997$). The solver's learned evaluation-time response length, i.e., how much reasoning it allocates per problem, almost entirely determines its math accuracy: seeds that yield in longer responses score higher, while the seed whose length collapses to ≈800 tokens scores lowest. Notably, the science-only INFUSER seed-123 running fails to incentivize the solver to sustain the thinking length that math problems require, and instead collapses to a suboptimal equilibrium with short responses and low math accuracy. We attribute this to that science-only setting providing little signal that anchors reasoning depth required by hard math problems.

	Math & phys.	General	Medical	Coding
Science-only INFUSER				
seed 456	33.31	41.66	40.52	53.67
seed 123	28.26	40.47	40.88	53.51
seed 42	32.89	39.75	40.15	52.71
Average	**31.49 ± 2.80**	40.62 ± 0.96	40.52 ± 0.37	53.29 ± 0.51
Math-RLVR & INFUSER				
seed 456	33.07	39.82	38.89	52.00
seed 123	32.31	38.94	39.14	52.18
seed 42	32.18	39.36	40.15	53.28
Average	**32.52 ± 0.48**	39.37 ± 0.44	39.39 ± 0.67	52.49 ± 0.69

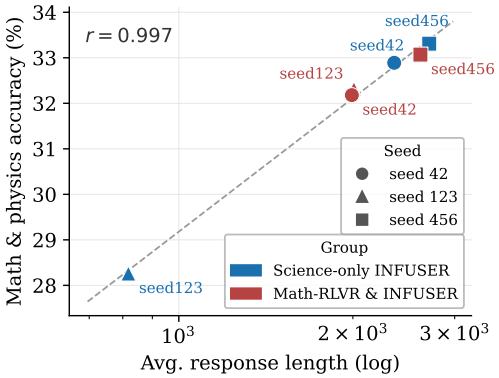

Figure 11: Hybrid science+RLVR on Qwen3-8B-Base, three seeds per setting. **Left:** per-seed category accuracy (averaged over the same benchmark grouping as Table 2); *Average* rows give mean ± sample std, with **red** marking the unstable science-only scores on math. **Right:** evaluation-time response length versus math-and-physics accuracy across all six seeds, with a log-linear fit ($r = 0.997$). Together, adding verifiable math RLVR (red) reduces the Science-only (blue) math variance by anchoring every seed to sufficient test-time compute. Full setup in §H.

RLVR-augmented training It is observed by previous RLVR work (Guo et al., 2025; Hu et al., 2025; Kimi Team et al., 2025) that RLVR involving math reasoning elicits a strong pattern on long CoT reasoning. Therefore, we naturally hypothesize that adding a verifiable math RLVR signal to the training loop will anchor reasoning depth across seeds, resolving the seed-dependent equilibrium ambiguity and stabilizing math performance. We test it by adding a verified math component to both the dev set that acts as influence anchor and the document pool that provides training curriculum, leaving the Qwen3-8B-Base INFUSER recipe otherwise unchanged. The 800-question dev set $\mathcal{D}_{\text{dev}}$ is split evenly between SuperGPQA Science MCQs and AIME free-form problems (we use AIME data before 2024 to avoid benchmark leakage), so the influence direction carries both science-MCQ and math signal. The document pool augments the 12,260 science document chunks with 10,000 externally Putnam/AIME-history rows where ground truth answers are already attached. These math rows supply directly verifiable RLVR targets. Curriculum

construction, verifier routing, and the full per-seed table are deferred to §H.

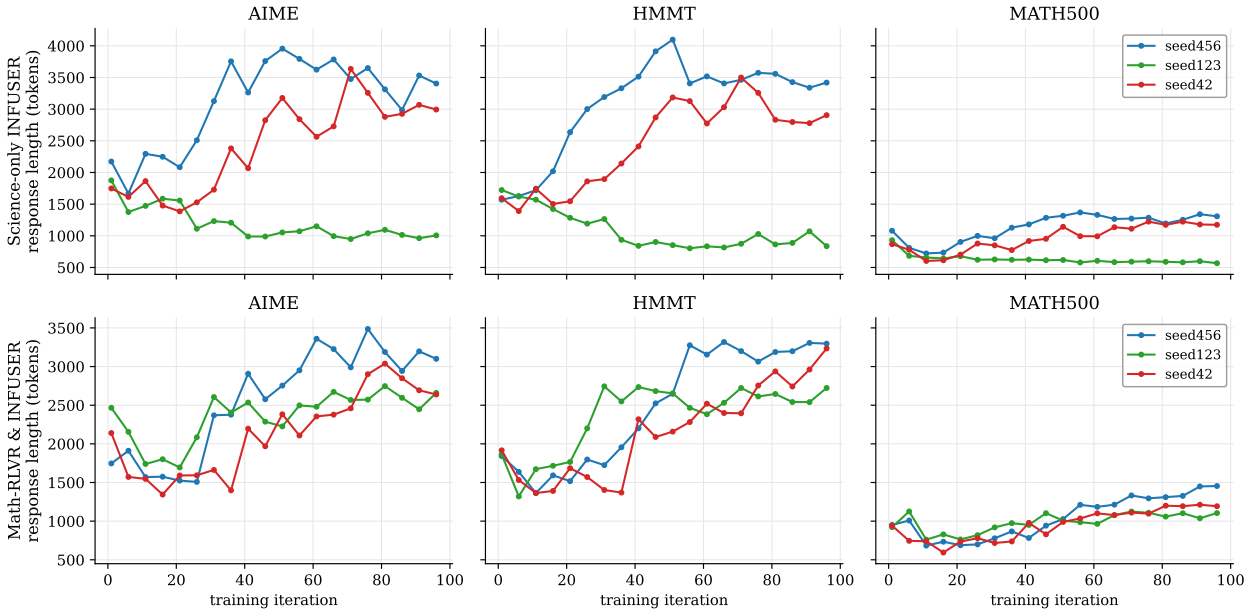

Figure 12: Response length on AIME, HMMT, and MATH500 over the training course. Top row: three Science-only INFUSER seeds, which diverge onto different length regimes, the source of the cross-seed math accuracy variance. Bottom row: three Math-RLVR & INFUSER seeds, which collapse onto a tightly clustered trajectory, confirming that verifiable math RLVR anchors reasoning depth across seeds.

RLVR-augmented INFUSER improves math via long CoT. Adding verifiable math RLVR significantly reduces the seed variance it was designed to target (Figure 11, left). The cross-seed standard deviation of the math-and-physics average falls from 2.80 to 0.48 percentage points, while the math-and-physics mean rises from 31.49 to 32.52. Figure 12 exposes the mechanism: the three science-only seeds (top row) diverge onto different response-length regimes on AIME, HMMT, and MATH500, whereas the three hybrid seeds (bottom row) collapse onto a single tightly clustered length trajectory in training, and we see the reasoning length steadily increase over training, a good sign of the emergence of a long-CoT regime. The alignment of length stabilization with accuracy stabilization confirms that well-designed verifiable RLVR augmentation can work well with the rising curriculum.

The stabilization is not free (Figure 11, left). General reasoning, medical, and coding each dip slightly below the science-only baseline (40.63 $\rightarrow$ 39.37, 40.52 $\rightarrow$ 39.39, and 53.30 $\rightarrow$ 52.49). This is a budget-allocation effect: the science pool is 12,260 of 22,260 training rows ($\approx$55%), so under a fixed solver-step budget ($T = 100$) the model sees only half as many science documents as the original INFUSER training, weakening precisely the science-related fields uniformly.

Finding 5.1. Hybrid INFUSER improves math reasoning under a fixed budget. A single INFUSER loop can jointly run document-grounded science self-evolution with math RLVR. The RLVR component strengthens the long CoT behavior that is crucial for math reasoning, while we only see a small decline on other fields under the fixed training budget.

6 Conclusion

We introduced **INFUSER**, a self-evolution framework that casts generator–solver co-training as a cooperative bilevel game and rewards the generator not by how *hard* its questions are, but by how *useful* they are to the current solver. The key ingredient is an optimizer-aware influence score (2.7) that, through a first-order approximation of the bilevel objective, measures whether training on a generated question moves the solver along a dev-anchored target direction. Optimizing this score with **DuGRPO**, a dual-normalized policy-gradient update tailored to the continuous and noisy influence reward, turns an unstructured document pool into an adaptive curriculum that tracks the solver's learning frontier rather than a fixed notion of difficulty.

Empirically, INFUSER outperforms strong self-evolution baselines on Qwen3-4B-Base and Qwen3-8B-Base, with the largest gains on the domains most aligned with its document pool and dev set, positive transfer to out-of-domain medical and coding benchmarks, and gains that persist as the anchor scales from 4B to 8B where baselines decay. Our analyses support the central design: an 8B co-evolving generator outperforms a frozen 32B one on math and coding (§3.3.1), the document pool and dev set play complementary roles (§3.3.1), and both the optimizer-aware influence score and DuGRPO are necessary for the generator to move beyond a frozen-generator baseline. The framework further extends to instruction-finetuned anchors (§4) and composes with verifiable RLVR to stabilize math reasoning depth (§5).

Limitations and future work. First, INFUSER relies on a small dev set to define the target direction, so its gains are strongest where this anchor and the document pool are well aligned; extending the influence signal to steer co-evolution toward out-of-domain targets remains open. Second, although INFUSER produces a rising curriculum (§3.2), the strong-solver evaluation and qualitative inspection (Figure 7) show that the correctness and quality of the generated questions are still not close to perfect, which leaves room for further improvement, e.g., by equipping the generator with a more sophisticated agent loop with external tools for auditing the question quality and fixing errors. Third, the hybrid results expose a fixed-budget trade-off in which strengthening one domain can slightly weaken others, suggesting adaptive allocation across signal sources as a natural next step.

More broadly, influence-guided self-evolution offers a path to convert abundant unstructured corpora into structured training signal without a curated training set or teacher model, and we believe coupling utility-based curriculum generation with larger document pools and longer training horizons is a promising direction for scaling reasoning.

References

Allen Institute for AI (2025). Dolci-Instruct-SFT: The instruction-tuning mixture for OLMo 3 7B Instruct SFT. https://huggingface.co/datasets/allenai/Dolci-Instruct-SFT. Hugging Face dataset card, accessed 2026-04-24; associated technical report arXiv:2512.13961. 40, 61

Andrychowicz, M., Denil, M., Gomez, S., Hoffman, M. W., Pfau, D., Schaul, T., Shillingford, B. and De Freitas, N. (2016). Learning to learn by gradient descent by gradient descent. *Advances in neural information processing systems*, **29**. 36

Bailey, L., Wen, K., Dong, K., Hashimoto, T. and Ma, T. (2026). Scaling self-play with self-guidance. *arXiv preprint arXiv:2604.20209*.
https://arxiv.org/abs/2604.20209 35

Başar, T. and Olsder, G. J. (1998). *Dynamic noncooperative game theory*. SIAM. 5

Broder, A. Z. (1997). On the resemblance and containment of documents. In *Proceedings of Compression and Complexity of Sequences 1997*. IEEE. 61

Cerebras Systems (2024). Data deduplication pipeline (Model Zoo, release 2.5.0). https://training-docs.cerebras.ai/rel-2.5.0/model-zoo/components/data-deduplication-pipeline. Accessed 2026-04-24. 61, 62

Chae, J. Y., Alam, M. T. and Rastogi, N. (2025). Towards understanding self-play for llm reasoning. *arXiv preprint arXiv:2510.27072*. 35

Chen, M., Tworek, J., Jun, H., Yuan, Q., Pinto, H. P. d. O., Kaplan, J., Edwards, H., Burda, Y., Joseph, N., Brockman, G., Ray, A., Puri, R., Krueger, G., Petrov, M., Khlaaf, H., Sastry, G., Mishkin, P., Chan, B., Gray, S., Ryder, N., Pavlov, M., Power, A., Kaiser, L., Bavarian, M., Winter, C., Tillet, P., Such, F. P., Cummings, D., Plappert, M., Chantzis, F., Barnes, E., Herbert-Voss, A., Guss, W. H., Nichol, A., Paino, A., Tezak, N., Tang, J., Babuschkin, I., Balaji, S., Jain, S., Saunders, W., Hesse, C., Carr, A. N., Leike, J., Achiam, J., Misra, V., Morikawa, E., Radford, A., Knight, M., Brundage, M., Murati, M., Mayer, K., Welinder, P., McGrew, B., Amodei, D., McCandlish, S., Sutskever, I. and Zaremba, W. (2021). Evaluating large language models trained on code. *arXiv preprint arXiv:2107.03374*.
https://arxiv.org/abs/2107.03374 45

Chen, X., Lu, J., Kim, M., Zhang, D., Tang, J., Piché, A., Gontier, N., Bengio, Y. and Kamalloo, E. (2025). Self-evolving curriculum for LLM reasoning. *arXiv preprint arXiv:2505.14970*. 35

Chen, Z., Deng, Y., Yuan, H., Ji, K. and Gu, Q. (2024). Self-play fine-tuning converts weak language models to strong language models. *arXiv preprint arXiv:2401.01335*. 35

Cui, G., Yuan, L., Wang, Z., Wang, H., Zhang, Y., Chen, J., Li, W., He, B., Fan, Y., Yu, T. et al. (2025). Process reinforcement through implicit rewards. *arXiv preprint arXiv:2502.01456*. 35

Dang, Q.-A. and Ngo, C. (2025). Reinforcement learning for reasoning in small llms: What works and what doesn't. *arXiv preprint arXiv:2503.16219*. 34

Dong, K. and Ma, T. (2025). STP: Self-play LLM theorem provers with iterative conjecturing and proving. *arXiv preprint arXiv:2502.00212*.
https://arxiv.org/abs/2502.00212 4, 35

Fan, Z., Chen, R., Hu, T., Peng, R., Huang, Z., Xu, H., Chen, Y., Wu, J., Zhao, J. and Liu, Z. (2026). OptimSyn: Influence-guided rubrics optimization for synthetic data generation. *arXiv preprint arXiv:2604.00536*. 4, 36

Finn, C., Abbeel, P. and Levine, S. (2017). Model-agnostic meta-learning for fast adaptation of deep networks. In *International Conference on Machine Learning (ICML)*. 7, 36, 43, 44

Guo, D., Yang, D., Zhang, H., Song, J., Wang, P., Zhu, Q., Xu, R., Zhang, R., Ma, S., Bi, X. et al. (2025). Deepseek-r1: Incentivizing reasoning capability in LLMs via reinforcement learning. *arXiv preprint arXiv:2501.12948*. 2, 3, 5, 20, 34

Hampel, F. R. (1974). The influence curve and its role in robust estimation. *Journal of the American Statistical Association*, **69** 383–393.
http://dx.doi.org/10.1080/01621459.1974.10482962 7

Harding Graesser, L., Cho, K. and Kiela, D. (2019). Emergent linguistic phenomena in multi-agent communication games. In *Proceedings of the 2019 conference on empirical methods in natural language processing and the 9th international joint conference on natural language processing (EMNLP-IJCNLP)*.
https://aclanthology.org/D19-1384/ 37

Harvard–MIT Mathematics Tournament (2026a). Problems and results archive. Official HMMT archive listing past tournament problem sets, including February 2025, November 2025, and February 2026. Accessed April 17, 2026.
https://www.hmmt.org/www/archive/problems 45

Harvard–MIT Mathematics Tournament (2026b). Testing information. Official description of HMMT round structure and difficulty. Accessed April 17, 2026.
https://www.hmmt.org/www/tournaments/testing 45

He, C., Luo, R., Bai, Y., Hu, S., Thai, Z. L., Shen, J., Hu, J., Han, X., Huang, Y., Zhang, Y., Liu, J., Qi, L., Liu, Z. and Sun, M. (2024). Olympiadbench: A challenging benchmark for promoting AGI with olympiad-level bilingual multimodal scientific problems.
https://arxiv.org/abs/2402.14008 45

He, J., Liu, J., Liu, C. Y., Yan, R., Wang, C., Cheng, P., Zhang, X., Zhang, F., Xu, J., Shen, W. et al. (2025). Skywork open reasoner 1 technical report. *arXiv preprint arXiv:2505.22312*. 35

Hendrycks, D., Burns, C., Kadavath, S., Arora, A., Basart, S., Tang, E., Song, D. and Steinhardt, J. (2021). Measuring mathematical problem solving with the MATH dataset.
https://arxiv.org/abs/2103.03874 44

Hospedales, T., Antoniou, A., Micaelli, P. and Storkey, A. (2021). Meta-learning in neural networks: A survey. *IEEE transactions on pattern analysis and machine intelligence*, **44** 5149–5169. 4, 36

Hu, J., Zhang, Y., Han, Q., Jiang, D., Zhang, X. and Shum, H.-Y. (2025). Open-reasoner-zero: An open source approach to scaling up reinforcement learning on the base model. *arXiv preprint arXiv:2503.24290*. 20, 34

Huang, C., Yu, W., Wang, X., Zhang, H., Li, Z., Li, R., Huang, J., Mi, H. and Yu, D. (2025). R-Zero: Self-evolving reasoning LLM from zero data. *arXiv preprint arXiv:2508.05004*.
https://arxiv.org/abs/2508.05004 2, 4, 12, 35, 53, 54

Huisman, M., Van Rijn, J. N. and Plaat, A. (2021). A survey of deep meta-learning. *Artificial Intelligence Review*, **54** 4483–4541. 36

Jain, N., Han, K., Gu, A., Li, W.-D., Yan, F., Zhang, T., Wang, S., Solar-Lezama, A., Sen, K. and Stoica, I. (2024). Livecodebench: Holistic and contamination free evaluation of large language models for code.
https://arxiv.org/abs/2403.07974 45

Jin, B., Zeng, H., Yue, Z., Yoon, J., Arik, S., Wang, D., Zamani, H. and Han, J. (2025). Search-r1: Training LLMs to reason and leverage search engines with reinforcement learning. *arXiv preprint arXiv:2503.09516*. 35

Jin, D., Pan, E., Oufattole, N., Weng, W.-H., Fang, H. and Szolovits, P. (2020). What disease does this patient have? a large-scale open domain question answering dataset from medical exams.
https://arxiv.org/abs/2009.13081 45

Karpathy, A. (2026). autoresearch: AI agents running research on single-GPU nanochat training automatically. https://github.com/karpathy/autoresearch. GitHub repository, accessed 2026-04-20. 43

Kazemi, M., Fatemi, B., Bansal, H., Palowitch, J., Anastasiou, C., Mehta, S. V., Jain, L. K., Aglietti, V., Jindal, D., Chen, P., Dikkala, N., Tyen, G., Liu, X., Shalit, U., Chiappa, S., Olszewska, K., Tay, Y., Tran, V. Q., Le, Q. V. and Firat, O. (2025). Big-bench extra hard. *arXiv preprint arXiv:2502.19187*.
https://arxiv.org/abs/2502.19187 45

Kimi Team, Du, A., Gao, B., Xing, B., Jiang, C., Chen, C., Li, C., Xiao, C., Du, C., Liao, C. et al. (2025). Kimi k1.5: Scaling reinforcement learning with LLMs. *arXiv preprint arXiv:2501.12599*. 2, 20, 34

Kingma, D. P. and Ba, J. (2015). Adam: A method for stochastic optimization. In *International Conference on Learning Representations (ICLR)*. 41

Koh, P. W. and Liang, P. (2017). Understanding black-box predictions via influence functions.
https://arxiv.org/abs/1703.04730 4, 7, 36

Lee, K., Ippolito, D., Nystrom, A., Zhang, C., Eck, D., Callison-Burch, C. and Carlini, N. (2022). Deduplicating training data makes language models better. In *Proceedings of the 60th Annual Meeting of the Association for Computational Linguistics (Volume 1: Long Papers)*. 61, 62

Li, X., Yu, Z. and Xiong, C. (2024). Montessori-instruct: Generate influential training data tailored for student learning. *arXiv preprint arXiv:2410.14208*. 4, 36

Li, Z., Zhou, F., Chen, F. and Li, H. (2017). Meta-sgd: Learning to learn quickly for few-shot learning. *arXiv preprint arXiv:1707.09835*. 36

Liao, A., Tomlin, N. and Klein, D. (2024). Efficacy of language model self-play in non-zero-sum games. *arXiv preprint arXiv:2406.18872*.
https://arxiv.org/abs/2406.18872 37

Liu, B., Guertler, L., Yu, S., Liu, Z., Qi, P., Balcells, D., Liu, M., Tan, C., Shi, W., Lin, M. et al. (2025a). Spiral: Self-play on zero-sum games incentivizes reasoning via multi-agent multi-turn reinforcement learning. *arXiv preprint arXiv:2506.24119*. 35

Liu, B., Jin, C., Kim, S., Yuan, W., Zhao, W., Kulikov, I., Li, X., Sukhbaatar, S., Lanchantin, J. and Weston, J. (2025b). SPICE: Self-play in corpus environments improves reasoning. *arXiv preprint arXiv:2510.24684*.
https://arxiv.org/abs/2510.24684 2, 4, 12, 35, 53

Liu, J., Xia, C. S., Wang, Y. and Zhang, L. (2023). Is your code generated by ChatGPT really correct? rigorous evaluation of large language models for code generation.
https://arxiv.org/abs/2305.01210 45

Liu, M., Diao, S., Lu, X., Hu, J., Dong, X., Choi, Y., Kautz, J. and Dong, Y. (2025c). ProRL: Prolonged reinforcement learning expands reasoning boundaries in large language models. *arXiv preprint arXiv:2505.24864*.
https://arxiv.org/abs/2505.24864 12

Liu, M., Jiang, L., Liang, Y., Du, S. S., Choi, Y., Althoff, T. and Jaques, N. (2025d). Chasing moving targets with online self-play reinforcement learning for safer language models. *arXiv preprint arXiv:2506.07468*. 35, 37

Liu, Z., Liu, C., Zheng, W., Yang, X., Yang, Z., Qiu, L. et al. (2025e). Understanding R1-zero-like training: A critical perspective. *arXiv preprint arXiv:2503.20783*. 2, 10, 35

Luo, M., Tan, S., Wong, J., Shi, X., Tang, W. Y., Roongta, M., Cai, C., Luo, J., Zhang, T., Li, L. E. et al. (2025). Deepscaler: Surpassing o1-preview with a 1.5 b model by scaling RL. *Notion Blog*, **3**. 35

M-A-P Team, Du, X., Yao, Y., Ma, K., Wang, B., Zheng, T., Zhu, K., Liu, M., Liang, Y., Jin, X., Wei, Z., Zheng, C., Deng, K., Gavin, S., Jia, S., Jiang, S., Liao, Y., Li, R., Li, Q., Li, S., Li, Y., Li, Y., Ma, D., Ni, Y., Que, H., Wang, Q., Wen, Z., Wu, S., Hsing, T., Xu, M., Yang, Z., Wang, Z. M., Zhou, J., Bai, Y., Bu, X., Cai, C., Chen, L., Chen, Y., Cheng, C., Cheng, T., Ding, K., Huang, S., Huang, Y., Li, Y., Li, Y., Li, Z., Liang, T., Lin, C., Lin, H., Ma, Y., Pang, T., Peng, Z., Peng, Z., Qi, Q., Qiu, S., Qu, X., Quan, S., Tan, Y., Wang, Z., Wang, C., Wang, H., Wang, Y., Wang, Y., Xu, J., Yang, K., Yuan, R., Yue, Y., Zhan, T., Zhang, C., Zhang, J., Zhang, X., Zhang, X., Zhang, Y., Zhao, Y., Zheng, X., Zhong, C., Gao, Y., Li, Z., Liu, D., Liu, Q., Liu, T., Ni, S., Peng, J., Qin, Y., Su, W., Wang, G., Wang, S., Yang, J., Yang, M., Cao, M., Yue, X., Zhang, Z., Zhou, W., Liu, J., Lin, Q., Huang, W. and Zhang, G. (2025). SuperGPQA: Scaling LLM evaluation across 285 graduate disciplines. *arXiv preprint arXiv:2502.14739*.
https://arxiv.org/abs/2502.14739 12, 16, 45, 57

Ma, X., Liu, Q., Jiang, D., Zhang, G., Ma, Z. and Chen, W. (2025). General-reasoner: Advancing LLM reasoning across all domains. *arXiv preprint arXiv:2505.14652*.
https://arxiv.org/abs/2505.14652 4, 13, 35, 53, 54

Mathematical Association of America (2024). 2024 american invitational mathematics examination (AIME). Official competition source; this paper evaluates on the 2024 AIME problem set. Accessed April 17, 2026.
https://maa.org/maa-invitational-competitions/ 45

Mathematical Association of America (2025). 2025 american invitational mathematics examination (AIME). Official competition source; this paper evaluates on the 2025 AIME problem set. Accessed April 17, 2026.
https://maa.org/maa-invitational-competitions/ 45

Mishra, N., Rohaninejad, M., Chen, X. and Abbeel, P. (2017). A simple neural attentive meta-learner. *arXiv preprint arXiv:1707.03141*. 36

Munkhdalai, T. and Yu, H. (2017). Meta networks. In *International conference on machine learning*. PMLR. 36

Oreshkin, B., Rodríguez López, P. and Lacoste, A. (2018). Tadam: Task dependent adaptive metric for improved few-shot learning. *Advances in neural information processing systems*, **31**. 36

Parashar, S., Gui, S., Li, X., Ling, H., Vemuri, S., Olson, B., Li, E., Zhang, Y., Caverlee, J., Kalathil, D. et al. (2025). Curriculum reinforcement learning from easy to hard tasks improves llm reasoning. *arXiv preprint arXiv:2506.06632*. 35

Qwen Team (2025). Qwen3 technical report. https://arxiv.org/abs/2505.09388 46, 58, 59

Ravi, S. and Larochelle, H. (2017). Optimization as a model for few-shot learning. In *International conference on learning representations*. 36

Rein, D., Hou, B. L., Stickland, A. C., Petty, J., Pang, R. Y., Dirani, J., Michael, J. and Bowman, S. R. (2023). GPQA: A graduate-level Google-proof Q&A benchmark. *arXiv preprint arXiv:2311.12022*. 16, 45

Rusu, A. A., Rao, D., Sygnowski, J., Vinyals, O., Pascanu, R., Osindero, S. and Hadsell, R. (2018). Meta-learning with latent embedding optimization. *arXiv preprint arXiv:1807.05960*. 36

Santoro, A., Bartunov, S., Botvinick, M., Wierstra, D. and Lillicrap, T. (2016). Meta-learning with memory-augmented neural networks. In *International conference on machine learning*. PMLR. 36

Sarkar, B., Xia, W., Liu, C. K. and Sadigh, D. (2025). Training language models for social deduction with multi-agent reinforcement learning. In *Proceedings of the 24th International Conference on Autonomous Agents and Multiagent Systems*. AAMAS '25, International Foundation for Autonomous Agents and Multiagent Systems. 37

Shao, Z., Wang, P., Zhu, Q., Xu, R., Song, J., Li, X., Zhang, M., Zhang, Y., Li, Y., Wu, Y. and Guo, D. (2024). DeepSeekMath: Pushing the limits of mathematical reasoning in open language models. *arXiv preprint arXiv:2402.03300*. 2, 3, 5, 6, 34

Snell, J., Swersky, K. and Zemel, R. (2017). Prototypical networks for few-shot learning. *Advances in neural information processing systems*, **30**. 36

Sun, Q., Liu, Y., Chua, T.-S. and Schiele, B. (2019). Meta-transfer learning for few-shot learning. In *Proceedings of the IEEE/CVF conference on computer vision and pattern recognition*. 36

Sung, F., Yang, Y., Zhang, L., Xiang, T., Torr, P. H. and Hospedales, T. M. (2018). Learning to compare: Relation network for few-shot learning. In *Proceedings of the IEEE conference on computer vision and pattern recognition*. 36

Team Olmo (2025). Olmo 3. *arXiv preprint arXiv:2512.13961*. https://arxiv.org/abs/2512.13961 19, 39

v. Mises, R. (1947). On the asymptotic distribution of differentiable statistical functions. *The Annals of Mathematical Statistics*, **18** 309–348. http://dx.doi.org/10.1214/aoms/1177730385 7

Vanschoren, J. (2018). Meta-learning: A survey. *arXiv preprint arXiv:1810.03548*. 4, 36

Vilalta, R. and Drissi, Y. (2002). A perspective view and survey of meta-learning. *Artificial intelligence review*, **18** 77–95. 4, 36

Vinyals, O., Blundell, C., Lillicrap, T., Wierstra, D. et al. (2016). Matching networks for one shot learning. *Advances in neural information processing systems*, **29**. 36

Wan, Z., Li, Y., Wen, X., Song, Y., Wang, H., Yang, L., Schmidt, M., Wang, J., Zhang, W., Hu, S. et al. (2025). Rema: Learning to meta-think for LLMs with multi-agent reinforcement learning. *arXiv preprint arXiv:2503.09501*.
https://arxiv.org/abs/2503.09501 37

Wang, T., Zhu, J.-Y., Torralba, A. and Efros, A. A. (2018). Dataset distillation. *arXiv preprint arXiv:1811.10959*. 36, 43, 44

Wang, Y., Ma, X., Zhang, G., Ni, Y., Chandra, A., Guo, S., Ren, W., Arulraj, A., He, X., Jiang, Z., Li, T., Ku, M., Wang, K., Zhuang, A., Fan, R., Yue, X. and Chen, W. (2024). Mmlu-pro: A more robust and challenging multi-task language understanding benchmark.
https://arxiv.org/abs/2406.01574 45

Wang, Y., Yang, Q., Zeng, Z., Ren, L., Liu, L., Peng, B., Cheng, H., He, X., Wang, K., Gao, J., Chen, W., Wang, S., Du, S. S. and Shen, Y. (2025a). Reinforcement learning for reasoning in large language models with one training example. *arXiv preprint arXiv:2504.20571*.
https://arxiv.org/abs/2504.20571 12, 34

Wang, Z., Cui, G., Li, Y.-J., Wan, K. and Zhao, W. (2025b). Dump: Automated distribution-level curriculum learning for RL-based LLM post-training. *arXiv preprint arXiv:2504.09710*. 35

Wang, Z., Wang, K., Wang, Q., Zhang, P., Li, L., Yang, Z., Jin, X., Yu, K., Nguyen, M. N., Liu, L. et al. (2025c). Ragen: Understanding self-evolution in LLM agents via multi-turn reinforcement learning. *arXiv preprint arXiv:2504.20073*. 35

Wen, X., Liu, Z., Zheng, S., Ye, S., Wu, Z., Wang, Y., Xu, Z., Liang, X., Li, J., Miao, Z., Bian, J. and Yang, M. (2025). Reinforcement learning with verifiable rewards implicitly incentivizes correct reasoning in base LLMs. *arXiv preprint arXiv:2506.14245*.
https://arxiv.org/abs/2506.14245 12, 35

Williams, R. J. (1992). Simple statistical gradient-following algorithms for connectionist reinforcement learning. *Machine learning*, **8** 229–256. 39

Wu, M., Qian, Q., Liu, W., Wang, X., Huang, Z., Liang, D., Miao, L., Dou, S., Lv, C., Wang, Z. et al. (2025). Progressive mastery: customized curriculum learning with guided prompting for mathematical reasoning. *arXiv preprint arXiv:2506.04065*. 35

Wu, Y., Sun, Z., Yuan, H., Ji, K., Yang, Y. and Gu, Q. (2024). Self-play preference optimization for language model alignment. *arXiv preprint arXiv:2405.00675*. 35

Xi, Z., Chen, W., Hong, B., Jin, S., Zheng, R., He, W., Ding, Y., Liu, S., Guo, X., Wang, J. et al. (2024). Training large language models for reasoning through reverse curriculum reinforcement learning. *arXiv preprint arXiv:2402.05808*. 35

Xia, M., Malladi, S., Garg, S., Bubeck, S. and Chen, D. (2024). LESS: Selecting influential data for targeted instruction tuning. *arXiv preprint arXiv:2402.04333*. 4, 8, 36, 42

Xie, T., Gao, Z., Ren, Q., Luo, H., Hong, Y., Dai, B., Zhou, J., Qiu, K., Wu, Z. and Luo, C. (2025). Logic-RL: Unleashing LLM reasoning with rule-based reinforcement learning. *arXiv preprint arXiv:2502.14768*. 34

Yao, F., Liu, L., Zhang, D., Dong, C., Shang, J. and Gao, J. (2025). Your efficient RL framework secretly brings you off-policy RL training. Notion page. First published August 5, 2025; last updated October 13, 2025. Accessed April 17, 2026.
https://fengyao.notion.site/off-policy-rl 12

Yu, Q., Zhang, Z., Zhu, R., Yuan, Y., Zuo, X., Yue, Y., Dai, W., Fan, T., Liu, G., Liu, L. et al. (2025a). Dapo: An open-source LLM reinforcement learning system at scale. *arXiv preprint arXiv:2503.14476*. 2, 35

Yu, R., Liu, S. and Wang, X. (2023). Dataset distillation: A comprehensive review. *IEEE transactions on pattern analysis and machine intelligence*, **46** 150–170. 36

Yu, W., Liang, Z., Huang, C., Panaganti, K., Fang, T., Mi, H. and Yu, D. (2025b). Guided self-evolving LLMs with minimal human supervision. *arXiv preprint arXiv:2512.02472*.
https://arxiv.org/abs/2512.02472 2, 12, 35, 53

Yuan, W., Pang, R. Y., Cho, K., Li, X., Sukhbaatar, S., Xu, J. and Weston, J. (2024). Self-rewarding language models. *arXiv preprint arXiv:2401.10020*. 35

Yue, Y., Chen, Z., Lu, R., Zhao, A., Wang, Z., Song, S. and Huang, G. (2025a). Does reinforcement learning really incentivize reasoning capacity in LLMs beyond the base model? *arXiv preprint arXiv:2504.13837*. 35

Yue, Y., Yuan, Y., Yu, Q., Zuo, X., Zhu, R., Xu, W., Chen, J., Wang, C., Fan, T., Du, Z. et al. (2025b). Vapo: Efficient and reliable reinforcement learning for advanced reasoning tasks. *arXiv preprint arXiv:2504.05118*. 35

Zelikman, E., Harik, G., Shao, Y., Jayasiri, V., Haber, N. and Goodman, N. D. (2024). Quiet-star: Language models can teach themselves to think before speaking. *arXiv preprint arXiv:2403.09629*. 35

Zelikman, E., Wu, Y., Mu, J. and Goodman, N. (2022). Star: Bootstrapping reasoning with reasoning. *Advances in Neural Information Processing Systems*, **35** 15476–15488. 4, 35

Zeng, W., Huang, Y., Liu, Q., Liu, W., He, K., Ma, Z. and He, J. (2025). Simplerl-zoo: Investigating and taming zero reinforcement learning for open base models in the wild. *arXiv preprint arXiv:2503.18892*. 3, 34

Zhang, K., Zuo, Y., He, B., Sun, Y., Liu, R., Jiang, C., Fan, Y., Tian, K., Jia, G., Li, P., Fu, Y., Lv, X., Zhang, Y., Zeng, S., Qu, S., Li, H., Wang, S., Wang, Y., Long, X., Liu, F., Xu, X., Ma, J., Zhu, X., Hua, E., Liu, Y., Li, Z., Chen, H., Qu, X., Li, Y., Chen, W., Yuan, Z., Gao, J., Li, D., Ma, Z., Cui, G., Liu, Z., Qi, B., Ding, N. and Zhou, B. (2025). A survey of reinforcement learning for large reasoning models. *arXiv preprint arXiv:2509.08827*.
https://arxiv.org/abs/2509.08827 2

Zhao, A., Wu, Y., Yue, Y., Wu, T., Xu, Q., Yue, Y., Lin, M., Wang, S., Wu, Q., Zheng, Z. and Huang, G. (2025). Absolute zero: Reinforced self-play reasoning with zero data. *arXiv preprint arXiv:2505.03335*.
https://arxiv.org/abs/2505.03335 2, 4, 12, 35, 53, 54

Zhao, B., Mopuri, K. R. and Bilen, H. (2020). Dataset condensation with gradient matching. *arXiv preprint arXiv:2006.05929*. 36

Zhao, Z., Dong, H., Saha, A., Xiong, C. and Sahoo, D. (2024). Automatic curriculum expert iteration for reliable LLM reasoning. *arXiv preprint arXiv:2410.07627*. 35

Zhu, E. (2024). datasketch: Python probabilistic data structures for processing and searching large datasets. https://github.com/ekzhu/datasketch. Open-source library; this work uses version 1.10.0. 62

Zhu, E., Jiang, D., Wang, Y., Li, X., Cheng, J., Gu, Y., Niu, Y., Zeng, A., Tang, J., Huang, M. and Wang, H. (2025). Data-efficient RLVR via off-policy influence guidance. *arXiv preprint arXiv:2510.26491*.
https://arxiv.org/abs/2510.26491 36

Zhu, E., Nargesian, F., Pu, K. Q. and Miller, R. J. (2016). LSH Ensemble: Internet-Scale domain search. *Proceedings of the VLDB Endowment*, **9** 1185–1196. 61

Zintgraf, L., Shiarli, K., Kurin, V., Hofmann, K. and Whiteson, S. (2019). Fast context adaptation via meta-learning. In *International conference on machine learning*. PMLR. 36

Zuo, Y., Qu, S., Li, Y., Chen, Z., Zhu, X., Hua, E., Zhang, K., Ding, N. and Zhou, B. (2025). Medxpertqa: Benchmarking expert-level medical reasoning and understanding.
https://arxiv.org/abs/2501.18362 45

Contents

A Setup and Notation

Tables 3 and 4 collect the notation used in §2. Table 3 covers the problem setup: models and data, the curriculum and rewards, and the population objectives together with the one-step influence score. Table 4 covers the algorithmic side: the rollout-based estimators, the RL update, and the training hyperparameters.

Table 3: Notation for the problem setup and influence score (§2).

Symbol	Meaning
Models, distributions, and data	
$\theta,\ \phi$	Solver and generator model parameters
$\pi_\theta,\ \pi_\phi$	Solver and generator policies parameterized by θ and ϕ
$\mathcal{P}$	Target distribution over verified question–answer pairs (q, a^*)
$\mathcal{D}_{\text{dev}}$	Development set: a finite sample $\{(q_i, a_i^*)\}_{i=1}^m$ from $\mathcal{P}$, used only to anchor the influence direction
$\mathcal{D}_{\text{doc}}$	Source document pool for question generation; not itself the target distribution
d	A document sampled from $\mathcal{D}_{\text{doc}}$
Questions, answers, curriculum, and reward	
$q,\ a^*$	A question and its true gold answer (on $\mathcal{P}$ or $\mathcal{D}_{\text{dev}}$)
$(q, a_\phi) \sim \pi_\phi(\cdot \mid d)$	Generated question q with its *generated golden answer* a_ϕ from document d
a_ϕ	Generated golden answer; a proxy for a^* inside $\mathcal{Q}_\phi$, possibly noisy or wrong
$a \sim \pi_\theta(\cdot \mid q)$	Solver answer sampled given q
$r(a, b; q) \in \{0, 1\}$	Correctness reward for solver answer a on q, scored against reference b ($b = a^*$ on $\mathcal{P}/\mathcal{D}_{\text{dev}}$, $b = a_\phi$ on $\mathcal{Q}_\phi$)
$\mathcal{Q}_\phi = \{(q_j, a_{\phi,j})\}$	Curriculum of question–answer pairs induced by π_ϕ
Objectives, solver update, and influence score	
$J(\theta)$	Solver's target performance, $\mathbb{E}_{(q,a^*)\sim\mathcal{P}}\mathbb{E}_{a\sim\pi_\theta(\cdot\mid q)}[r(a, a^*; q)]$
$J(\theta; \mathcal{Q}_\phi)$	Solver objective on the curriculum (reference a_ϕ); $J(\theta; q, a_\phi)$ is its single-question version, see (2.6)
$\widehat{J}(\theta)$	Empirical estimate of $J(\theta)$ on $\mathcal{D}_{\text{dev}}$, (2.9)
$\theta^*(\phi)$	Ideal best-response solver, $\operatorname{argmax}_\theta J(\theta; \mathcal{Q}_\phi)$
$\theta^+(\phi)$	One-step solver-update map, $\theta + \Delta\theta(\phi)$, (2.2)
$\Delta\theta(\phi),\ \mathrm{Opt}(\cdot)$	One-step parameter update $\mathrm{Opt}(\nabla_\theta J(\theta; \mathcal{Q}_\phi))$ and the optimizer update rule (AdamW)
$g(q, a_\phi)$	Per-question solver policy gradient $\nabla_\theta J(\theta; q, a_\phi)$
$\Gamma(q, a_\phi)$	AdamW-preconditioned per-question update direction induced by $g(q, a_\phi)$ (§D.2)
$\mathrm{cossim}(u, v)$	Cosine similarity $\langle u, v\rangle/(\|u\|\,\|v\|)$
$s(q, a_\phi)$	Optimizer-aware influence score $\mathrm{cossim}(\nabla_\theta J(\theta), \Gamma(q, a_\phi))$, (2.7)

Table 4: Notation for INFUSER's rollout estimators, RL update, and hyperparameters (§2).

Symbol	Meaning
Rollout estimators and RL update	
$\mathcal{J}_\psi(z)$	Clipped rollout objective for policy π_ψ on input z, (2.10); $\psi \in \{\theta, \phi\}$
$\pi_{\psi_{\text{old}}}$	Rollout (behavior) policy that generated a batch
$\rho_{i,t}$	Token-level importance ratio $\pi_\psi / \pi_{\psi_{\text{old}}}$ in (2.10)
$\widehat{A}_i$	Per-row advantage in (2.10); $\widehat{A}_{\text{sol}}$ is the mean-centered solver advantage
$\widehat{g}_{\text{dev}}$	Rollout estimate of $\nabla_\theta \widehat{J}(\theta)$, the dev reference direction, (2.11)
$\widehat{g}(q, a_\phi),\ \widehat{\Gamma}(q, a_\phi)$	Finite-rollout estimates of g and Γ
$\widehat{s}(q, a_\phi)$	Empirical influence reward $\text{cossim}(\widehat{g}_{\text{dev}}, \widehat{\Gamma}(q, a_\phi))$, (2.13)
$\mu_d,\ \sigma_d$	Mean and std of $\{s(q^k, a_\phi^k)\}_{k=1}^n$ for document d
$\mathcal{B},\ \sigma_{\mathcal{B}}$	Document batch and its cross-group normalizer $\text{mean}\{\sigma_{d'} : d' \in \mathcal{B}\}$
$\widehat{A}_{\text{gen}}$	DuGRPO generator advantage, (2.14)
$\widehat{A}_{\text{GRPO}},\ \widehat{A}_{\text{BN}}$	Group-only and batch-only ablation normalizers, (2.15)
Hyperparameters and constants	
n	Group size for solver and generator rollouts ($n = 8$)
B	Document batch size ($B = 128$)
M	Minibatch size for optimizer steps ($M = 32$)
T	Number of training iterations (answer loops)
$\eta_{\text{sol}},\ \eta_{\text{gen}}$	Solver and generator learning rates
ϵ	PPO-style clipping coefficient in (2.10)
C	Fixed maximum generation length (Dr.GRPO length normalizer)
$\rho_{\max}$	Truncated importance-sampling clip ($\rho_{\max} = 2.0$)

Remark (shared initialization). The generator and solver maintain *separate* model weights ϕ and θ, each with its own optimizer state. Both are initialized from the same pretrained checkpoint but diverge during training.

B Related Works

Reinforcement Learning for LLM Reasoning. Reinforcement learning has surged as a main-stream post-training method. DeepSeek-R1-Zero first showed that rule-based RL can elicit long-chain reasoning, self-reflection, and verification from a base model, while also exposing readability and language-mixing issues that motivated the later cold-start pipeline of DeepSeek-R1 (Guo et al., 2025). This line builds on DeepSeekMath, which introduced Group Relative Policy Optimization (GRPO) for efficient mathematical RL (Shao et al., 2024), and is related to Kimi k1.5, which scales long-context RL for strong long-CoT reasoning (Kimi Team et al., 2025). Subsequent works study the robustness and scalability of zero-style RLVR: SimpleRL-Zoo shows that its success depends on base-model capability, reward design, query difficulty, and training dynamics (Zeng et al., 2025); Open-Reasoner-Zero reproduces R1-Zero-like length and performance scaling with an open PPO/GAE recipe (Hu et al., 2025); Logic-RL validates rule-based RL on logical reasoning (Xie et al., 2025); and small-model or data-limited studies show that RLVR can still yield reasoning gains under constrained model size, data, or compute (Dang and Ngo, 2025; Wang et al., 2025a). Beyond math, General-Reasoner extends RLVR to broad domains using large-scale verifiable data and

generative verification (Ma et al., 2025), Search-R1 incorporates retrieval-augmented reasoning (Jin et al., 2025), and RAGEN studies multi-turn agentic RL with new stability and reward-shaping challenges (Wang et al., 2025c). In parallel, algorithmic refinements improve long-CoT RL training: DAPO introduces decoupled clipping and dynamic sampling (Yu et al., 2025a); Dr. GRPO identifies and corrects length-related GRPO bias (Liu et al., 2025e); VAPO develops value-based augmented PPO (Yue et al., 2025b); PRIME uses implicit process rewards (Cui et al., 2025); and open systems such as DeepScaleR and Skywork-OR1 further study RL recipes, entropy control, and length scaling for compact reasoning models (He et al., 2025; Luo et al., 2025). Finally, mechanism studies debate whether RLVR genuinely expands reasoning capacity or mainly reallocates probability mass over reasoning paths already present in the base model (Wen et al., 2025; Yue et al., 2025a). Together, these works establish zero-style RLVR as a promising paradigm for eliciting reasoning from base models, while leaving open questions about base-model prerequisites, verifier design, exploration, reward sparsity, length bias, and the source of reasoning improvement. In contrast, INFUSER does not rely on a curated pool of human-authored or frontier-model-filtered verifiable training problems; instead, it produces document-grounded training signals from unlabeled documents using the model itself, with only a small held-out target sample $\mathcal{D}_{\text{dev}}$ as external supervision to anchor the generator's reward.

Self-play and adaptive curriculum generation improve LLMs with RL by generating, filtering, or scheduling training problems according to the model's evolving capability rather than using a fixed human-curated dataset. Early self-improvement methods such as STaR iteratively generate and filter rationales for fine-tuning (Zelikman et al., 2022), while Quiet-STaR extends latent rationale generation to arbitrary text (Zelikman et al., 2024). For alignment, SPIN improves a model by contrasting its own responses with human demonstrations (Chen et al., 2024), SPPO casts preference optimization as a self-play game (Wu et al., 2024), and self-rewarding models use the model itself as a judge to generate rewards for iterative improvement (Yuan et al., 2024). More recent reasoning-oriented methods apply self-play directly to RL: R-Zero co-evolves a Challenger and Solver to generate tasks near the Solver's capability boundary (Huang et al., 2025); Absolute Zero removes external data by proposing and solving verifiable code-reasoning tasks with executor-based validation (Zhao et al., 2025); R-Few uses a few human examples to guide self-evolution and stabilize the curriculum (Yu et al., 2025b); SPICE mines corpus environments to construct document-grounded reasoning tasks (Liu et al., 2025b); and SGS scales conjecturer–prover self-play in Lean4 by adding a model-as-guide role that scores generated problems for target-relevance and naturalness to mitigate conjecturer reward hacking over long training horizons (Bailey et al., 2026). Related self-play frameworks study transferable reasoning through zero-sum games (Liu et al., 2025a) and online attacker–defender training for safety (Liu et al., 2025d). In parallel, adaptive curriculum methods make RL post-training more sample-efficient by constructing reverse curricula from correct demonstrations (Xi et al., 2024), automatically adjusting expert-iteration rewards (Zhao et al., 2024), scheduling problem distributions with learnability and exploration criteria (Wang et al., 2025b), formulating curriculum selection as a non-stationary bandit (Chen et al., 2025), progressing from easy to hard tasks (Parashar et al., 2025), or adapting difficulty and hints to model capability (Wu et al., 2025). Recent analyses further compare self-play with standard RLVR and SFT through update sparsity, entropy dynamics, and proposer reward design (Chae et al., 2025). The works most closely related to our setting are STP (Dong and Ma, 2025) and SPICE (Liu et al., 2025b), both of which generate questions adversarially. For example, in STP, a conjecturer is trained to generate conjectures that are barely provable by the current prover, thereby inducing an adaptive, self-generated curriculum. In contrast, we formulate generator learning as a cooperative bilevel curriculum game, and approximate the generator's outer-loop update using an influence-based first-order signal derived from held-out performance.

Influence-guided training data selection and synthesis. A separate line of work measures the utility of each training example by how much it improves a downstream objective. Influence functions (Koh and Liang, 2017) formalize this leave-one-out perturbation analysis, and gradient-alignment surrogates make it tractable at scale: LESS (Xia et al., 2024) approximates the AdamW-induced influence with low-rank gradient features and uses the resulting score as an offline filter over an existing instruction-tuning pool, and CROPI extends this selection paradigm to RLVR with an off-policy influence estimator built from pre-collected trajectories and sparse random projections, used to drive a multi-stage curriculum (Zhu et al., 2025). Recent works extend this signal from selection to generation. Montessori-Instruct (Li et al., 2024) measures the local data influence of synthesized instructions on a student model and trains a frozen teacher via DPO to favor high-influence outputs for instruction tuning. Concurrent work OptimSyn (Fan et al., 2026) couples an optimizer-aware influence score with a GRPO-trained rubric generator that synthesizes QA pairs conditioned on a seed document, closing the synthesis–training loop on a frozen target model. INFUSER shares the optimizer-aware per-question influence score with this line and shares with OptimSyn in particular the use of an RL-trained generator. We differ in that we (i) jointly co-evolve the solver and the generator from the same pretrained model, rather than improving training data for a frozen target student; (ii) operate directly on unlabeled documents with binary correctness rewards against the generator's reference answer, without rubric mediation or instruction-tuning supervision; and (iii) introduce DuGRPO to handle the variance of the continuous influence reward in a multi-document, multi-question batch.

Meta-Learning studies how knowledge accumulated across a distribution of tasks can improve adaptation to new tasks (Hospedales et al., 2021; Huisman et al., 2021; Vanschoren, 2018; Vilalta and Drissi, 2002; Wang et al., 2018). Existing methods are typically grouped into four families: model-based, optimization-based, metric-based, and data-based approaches (Hospedales et al., 2021; Huisman et al., 2021; Vanschoren, 2018). Model-based methods encode adaptation directly into the architecture through recurrent dynamics, external memory, or fast weights. Representative examples include memory-augmented neural networks (Santoro et al., 2016), Meta Networks (Munkhdalai and Yu, 2017), recurrent learned optimizers (Andrychowicz et al., 2016; Ravi and Larochelle, 2017), and attention-based architectures such as SNAIL (Mishra et al., 2017). Optimization-based methods instead learn parameters that can be adapted to a new task with only a few gradient steps (Finn et al., 2017). A canonical example is MAML, which learns an initialization optimized for rapid post-adaptation generalization (Finn et al., 2017). Later variants improve this paradigm through learned update directions (Li et al., 2017), low-dimensional adaptation (Zintgraf et al., 2019), and latent-space adaptation (Rusu et al., 2018). Metric-based methods learn an embedding space or similarity rule for few-shot prediction by comparing query examples with a small support set (Snell et al., 2017; Sung et al., 2018; Vinyals et al., 2016). Representative methods include Matching Networks (Vinyals et al., 2016), Prototypical Networks (Snell et al., 2017), and Relation Networks (Sung et al., 2018). Later extensions improve metric flexibility through task conditioning (Oreshkin et al., 2018) or by combining transfer learning with episodic adaptation (Sun et al., 2019). Data-based meta-learning meta-learns a small synthetic training set, rather than an initialization, optimizer, or metric, such that training on the synthetic data approximates training on the full dataset (Wang et al., 2018; Yu et al., 2023; Zhao et al., 2020). This line of work, often known as dataset distillation or dataset condensation, was initiated by Wang et al. (2018) and later improved through gradient matching (Zhao et al., 2020). Different from the previous three families, these methods meta-learn the training data itself and thus form a separate data-based paradigm (Yu et al., 2023). In contrast, our focus is on enabling the generator to adapt the curriculum to the solver's needs as the solver continuously improves, which can be viewed as a form of meta-learning with an evolving target task.

Multi-Agent RL for Language Models. Our work is also related to multi-agent reinforcement learning (MARL) for language models. Full-scale LLM training in MARL environments faces nontrivial challenges (Liu et al., 2025d; Wan et al., 2025). Existing language-model and multi-agent works address these challenges by using lighter models (Sarkar et al., 2025), simplifying communication-game environments (Harding Graesser et al., 2019), or studying self-play in text-game negotiation settings (Liao et al., 2024). In contrast, INFUSER jointly updates the solver and generator with carefully designed learning paces, which stabilize their interaction and improve performance.

C Omitted Details

C.1 Full Algorithm

Algorithm 2: Full INFUSER: Influence-Guided Self-Evolution

Input: Pretrained LLM (init. for π_θ, π_ϕ); doc pool $\mathcal{D}_{\text{doc}}$; dev set $\mathcal{D}_{\text{dev}}$; doc batch size B; group size n; answer-loop count T; minibatch size M; learning rates $\eta_{\text{sol}}, \eta_{\text{gen}}$; invalid question penalty ρ_{inv}; AdamW hyperparams.

Output: Trained solver π_θ and trained generator π_ϕ.

for $t \leftarrow 1$ **to** T **do**

  Phase 1. Dev Reference

    ▷ *Solver rollout on* $\mathcal{D}_{\text{dev}}$

    foreach $(\tilde{q}, \tilde{a}^*) \in \mathcal{D}_{\text{dev}}$ **do**

      Sample $\{\tilde{a}^i\}_{i=1}^n \sim \pi_\theta(\cdot \mid \tilde{q})$ and compute rewards $\{r(\tilde{a}^i, \tilde{a}^*; \tilde{q})\}_{i=1}^n$

      $\widehat{A}_{\text{sol}}(\tilde{q}, \tilde{a}^i) \leftarrow r(\tilde{a}^i, \tilde{a}^*; \tilde{q}) - \text{mean}\{r(\tilde{a}^j, \tilde{a}^*; \tilde{q})\}_{j=1}^n$ for $i = 1, \ldots, n$

    ▷ *Reference gradient on* $\mathcal{D}_{\text{dev}}$

    Compute $\widehat{g}_{\text{dev}} \leftarrow |\mathcal{D}_{\text{dev}}|^{-1} \sum_{(\tilde{q}, \tilde{a}^*) \in \mathcal{D}_{\text{dev}}} \nabla_\theta \mathcal{J}(\theta;\, \tilde{q}, \tilde{a}^*)$ using $\widehat{A}_{\text{sol}}$

  Phase 2. Batch rollout and parsing

    Sample document batch $\mathcal{B}_{\text{gen}} = \{d_b\}_{b=1}^B \sim \mathcal{D}_{\text{doc}}$

    ▷ *Generator rollout on document batch*

    foreach $d \in \mathcal{B}_{\text{gen}}$ **do**

      Generate $\{(q^i, a_\phi^i)\}_{i=1}^n \sim \pi_\phi(\cdot \mid d)$

    Parse generated outputs into valid question–answer pairs $\mathcal{Q}_\phi$ and malformed generations $\mathcal{I}_\phi$

    ▷ *Solver rollout on generated questions*

    foreach $(q, a_\phi) \in \mathcal{Q}_\phi$ **do**

      Sample $\{a^i\}_{i=1}^n \sim \pi_\theta(\cdot \mid q)$ and compute rewards $\{r(a^i, a_\phi; q)\}_{i=1}^n$

      $\widehat{A}_{\text{sol}}(q, a^i) \leftarrow r(a^i, a_\phi; q) - \text{mean}\{r(a^j, a_\phi; q)\}_{j=1}^n$ for $i = 1, \ldots, n$

      ▷ *Per question solver gradient*

      Compute $\widehat{g}(q, a_\phi) \leftarrow \nabla_\theta \mathcal{J}_\theta(q, a_\phi)$ using $\widehat{A}_{\text{sol}}$

  Phase 3. Influence Estimation

    foreach $(q, a_\phi) \in \mathcal{Q}_\phi$ **do**

      $\widehat{\Gamma}(q, a_\phi) \leftarrow$ AdamW-induced update direction from $\widehat{g}(q, a_\phi)$

      $\widehat{s}(q, a_\phi) \leftarrow \text{cossim}\big(\widehat{g}_{\text{dev}}, \widehat{\Gamma}(q, a_\phi)\big)$

  Phase 4. Generator Update

    Assign $\widehat{s}(x) \leftarrow \rho_{\text{inv}}$ for each invalid generation $x \in \mathcal{I}_\phi$

    foreach $d \in \mathcal{B}_{\text{gen}}$ **do**

      Compute DuGRPO advantage $\widehat{A}_{\text{gen}}(d, x_i) \leftarrow (\widehat{s}(x_i) - \text{mean}\{\widehat{s}(x_j)\}_{j=1}^n)/(\sigma_d + \sigma_{\mathcal{B}} + \epsilon)$ for each generated output x_i from d, where valid $x_i = (q^i, a_\phi^i)$ use influence rewards and invalid x_i use ρ_{inv}

    For each document in $\mathcal{B}_{\text{gen}}$, treat the n generated questions as a group; Filter out zero-variance documents in $\mathcal{B}_{\text{gen}}$; update ϕ by AdamW steps on (2.10) with $\widehat{A}_{\text{gen}}$, learning rate η_{gen} and minibatch size M

  Phase 5. Solver Update

    For each question in $\mathcal{Q}_\phi$, treat the n sampled answers as a group; Filter out zero-variance questions in $\mathcal{Q}_\phi$; update θ by AdamW steps on (2.10) with $\widehat{A}_{\text{sol}}$ (computed in Phase 2), learning rate η_{sol} and minibatch size M

return Trained solver π_θ and generator π_ϕ

Implementing Phase 3 under FSDP. The per-question direction $\widehat{\Gamma}(q, a_\phi)$ in Line 21 of Algorithm 2 is obtained by reusing the standard FSDP forward/backward path rather than per-sample autograd: each generated question is processed as its own mini-batch, and an in-place optimizer hook combines the resulting sharded gradient with the actor's live AdamW second-moment state to form $\widehat{\Gamma}(q, a_\phi)$ on the fly without materializing parameter-sized per-question tensors. The FSDP, microbatching, and memory-budget details are given in §D.3.

C.2 Policy-gradient view of the influence reward

Equation (2.8) has the standard policy-gradient form once the optimizer-aware influence score is treated as a sampled scalar reward. Treating d as the state, (q, a_ϕ) as the action, and $s(q, a_\phi)$ as the return, the REINFORCE policy-gradient estimator (Williams, 1992) is

$$\nabla_\phi \mathbb{E}_{d\sim\mathcal{D}_{\mathrm{doc}},\,(q,a_\phi)\sim\pi_\phi(\cdot|d)}\big[s(q,a_\phi)\big] = \mathbb{E}_{d\sim\mathcal{D}_{\mathrm{doc}},\,(q,a_\phi)\sim\pi_\phi(\cdot|d)}\big[s(q,a_\phi)\nabla_\phi \log \pi_\phi(q,a_\phi \mid d)\big].$$

This expression is only a policy-gradient view of why the influence score can serve as a generator reward. The implemented generator update uses the DuGRPO objective in §2.3.

C.3 Generator Question Quality Example

A qualitative example Beyond the aggregate gap, we examine *what* about the generator's questions improves over training. Figure 7 shows two questions produced by INFUSER's generator from the same source document, one at the beginning of training and one after 90 iterations. The comparison illustrates the quality improvement along two axes that the aggregate strong-minus-base gap does not distinguish. First, *self-containedness*: the base-model question refers to "equation (14.2)" and "equation (14.3)" without stating the self-energy expression or the barrier-crossing rate law, whereas the checkpoint 90 question restates the relevant equations inside the stem. Second, *factual correctness of the ground-truth key*: the base-model question marks increasing the ion radius as the answer even though it lowers ΔG and raises the flux, while the checkpoint 90 answer is consistent with the $-q^2/(\varepsilon_{\mathrm{h}}\, l)$ term. Together, these changes convert the generator's output from "ill-posed hard" into "well-posed with high quality," the regime that the aggregate strong-minus-base gap in Figure 6b is designed to detect.

C.4 Instruction-Finetuned Anchor Extension

This appendix gives the setup details omitted from the compact instruction-finetuned (IF) anchor experiment in §4.

Goal The main experiments start from pretrained base anchors (Qwen3-4B-Base and Qwen3-8B-Base). The IF extension asks whether INFUSER still improves a model whose next-token distribution has already been reshaped by supervised instruction tuning, and whether the learned generator continues to help beyond solver-only DrGRPO with a frozen generator.

Anchor, data, and variants We use OLMo-3-7B-Instruct-SFT (Team Olmo, 2025) as the IF anchor. The document pool $\mathcal{D}_{\mathrm{doc}}$ and the 800-question SuperGPQA Science development set $\mathcal{D}_{\mathrm{dev}}$ are identical to those used in §3.1. We compare three variants: **Base**, the OLMo-3-7B-Instruct-SFT checkpoint with no additional RL training; **Fix-gen**, a solver-only DrGRPO run with the generator frozen at its initial checkpoint; and **INFUSER**, which updates the generator using preconditioned cosine influence. Both training runs use solver learning rate 2×10^{-6}; INFUSER uses generator learning rate 4×10^{-6}. Unless noted otherwise, the runs inherit the main training configuration:

$T = 100$ iterations, document batch size $B = 128$, group size $n = 8$ for both generator and solver rollouts, AdamW with weight decay 0.01, and mini-batch size 32.

Evaluation and checkpoint selection All three columns are evaluated with the same benchmark suite, prompting, sampling, and answer-extraction pipeline as Table 2. The suite contains the same general-reasoning, math/physics, medical, and coding benchmarks used for the base-anchor experiments. The Fix-gen and INFUSER columns in Table 13 use the same best-checkpoint selection protocol as Table 2: every 5 training iterations we score the run on the held-fixed validation set described in §F.2 and report the iteration with the highest validation accuracy, which lands at checkpoint 85 for both runs.

Choice of IF anchor We choose OLMo-3-7B-Instruct-SFT instead of an instruction-finetuned Qwen3 checkpoint for attribution. Qwen3 instruct checkpoints have already undergone large-scale supervised finetuning followed by RL or teacher distillation, and their post-training corpus is not public. Consequently, additional gains or regressions from INFUSER would be hard to separate from unknown post-training data and objectives. OLMo-3 releases its training recipe and instruction-tuning mixture, which lets us audit whether $\mathcal{D}_{\text{doc}}$ or $\mathcal{D}_{\text{dev}}$ overlaps with the anchor's SFT data.

Contamination audit We audit the released OLMo-3 SFT mixture, `allenai/Dolci-Instruct-SFT` (Allen Institute for AI, 2025), using the near-duplicate protocol in §J. The audit builds word-13-gram MinHashLSH indexes at Jaccard threshold 0.8 and MinHashLSH-Ensemble containment indexes at threshold 0.8 over $\mathcal{D}_{\text{doc}}$ and $\mathcal{D}_{\text{dev}}$, then queries the released Dolci samples against both sets. The scan finds zero matches for either $\mathcal{D}_{\text{doc}}$ or $\mathcal{D}_{\text{dev}}$, so the IF-anchor gains in §4 cannot be explained by direct near-duplicate leakage into the OLMo-3 SFT mixture under this protocol.

Full results Table 13 reports the per-benchmark accuracies behind the radar plots in Figure 10. INFUSER leads on 10 of the 13 benchmarks and has the highest overall average (29.8 vs. 28.7 for Fix-gen and 27.7 for Base). Its largest category lift is on general reasoning ($+4.2$ over Base), followed by math/physics reasoning ($+1.8$). Medical gains are small but positive, while coding remains essentially tied with Base, consistent with neither the development set nor the document pool covering code.

D Derivation of the Influence Score

This appendix gives the detailed derivation of the per-question influence score $s(q, a_\phi)$ used by the generator in §2.2. We first formalise the first-order approximation of the outer objective and justify dropping the second-order remainder, then specialise to the AdamW optimiser and introduce the per-question decoupling surrogate.

D.1 Second-order remainder of the first-order approximation

Recall that the generator's objective is $J(\theta^+(\phi))$, where $\theta^+(\phi) = \theta + \Delta\theta(\phi)$ is the solver's parameters after one inner-loop update (2.2). By Taylor's theorem with the mean-value form of the remainder,

$$J(\theta^+) \;=\; J(\theta) \;+\; \big\langle \nabla_\theta J(\theta),\; \Delta\theta(\phi) \big\rangle \;+\; R_2, \qquad R_2 \;=\; \tfrac{1}{2}\, \Delta\theta(\phi)^\top H_J(\widetilde{\theta})\, \Delta\theta(\phi), \tag{D.1}$$

for some $\widetilde{\theta}$ on the line segment between θ and θ^+, where $H_J(\widetilde{\theta}) = \nabla^2_\theta J(\widetilde{\theta})$ is the Hessian of J at $\widetilde{\theta}$. The expression for R_2 is exact at $\widetilde{\theta}$ rather than a higher-order series remainder. Whenever H_J is locally bounded in operator norm on this segment,

$$|R_2| \;\le\; \tfrac{1}{2}\,\big\|H_J(\widetilde{\theta})\big\|_{\mathrm{op}}\,\|\Delta\theta(\phi)\|^2 \;=\; O\big(\|\Delta\theta(\phi)\|^2\big),$$

so $|R_2|$ is quadratic in the step size while the first-order term in (D.1) is linear.

In our setting, the single-step update $\|\Delta\theta(\phi)\|$ is controlled by AdamW's adaptive normalization combined with small learning rates. By construction, the bias-corrected ratio $\widehat{m}_t/(\sqrt{\widehat{v}_t}+\epsilon)$ is bounded coordinate-wise: in the standard regime $(1-\beta_1) > \sqrt{1-\beta_2}$, each coordinate satisfies $|\widehat{m}_t/\sqrt{\widehat{v}_t}| \le (1-\beta_1)/\sqrt{1-\beta_2}$ (Kingma and Ba, 2015, §2.1), so the gradient term of the AdamW step (D.2) obeys $\|\eta_s\,\widehat{m}_t/(\sqrt{\widehat{v}_t}+\epsilon)\|_\infty \lesssim \eta_s\,(1-\beta_1)/\sqrt{1-\beta_2}$. With η_s on the order of 10^{-6} (see §G), several orders of magnitude smaller than typical pre-training learning rates, and a constant prefactor $(1-\beta_1)/\sqrt{1-\beta_2} \approx 3.16$ at our standard $(\beta_1,\beta_2) = (0.9, 0.999)$, the first-order term is a local surrogate whose accuracy improves as $\|H_J\|_{\mathrm{op}}\|\Delta\theta(\phi)\|^2$ becomes small.

D.2 AdamW preconditioning and per-question decoupling

Starting from the first-order approximation (2.4), the generator's objective reduces to shaping the inner product $\langle\nabla_\theta J(\theta),\,\Delta\theta(\phi)\rangle$ through its choice of curriculum $\mathcal{Q}_\phi$. The structure of this inner product depends on how the optimiser maps the raw gradient to a parameter step. We specialise to AdamW here to keep the derivation concrete and directly aligned with our implementation.

AdamW update decomposition. Under our ascent convention for the solver objective J, the AdamW parameter update decomposes into a gradient-dependent term and a weight-decay term:

$$\Delta\theta(\phi) \;=\; \underbrace{\eta_s\,\frac{\widehat{m}_t}{\sqrt{\widehat{v}_t}+\epsilon}}_{\text{adaptive gradient step}} \;-\; \underbrace{\eta_s\,\lambda_t\,\theta}_{\text{weight decay}}\;, \tag{D.2}$$

where $\widehat{m}_t$ and $\widehat{v}_t$ are the bias-corrected first- and second-moment estimates that depend on $\nabla_\theta J(\theta;\,\mathcal{Q}_\phi)$, and λ_t is the weight-decay coefficient at step t. The weight-decay term $-\eta_s\lambda_t\theta$ is independent of $\mathcal{Q}_\phi$ and therefore contributes a constant to $\langle\nabla_\theta J(\theta),\,\Delta\theta(\phi)\rangle$ that does not affect the generator's optimisation over ϕ. Dropping it, the generator's objective reduces to maximising

$$\Big\langle\nabla_\theta J(\theta),\;\frac{\widehat{m}_t}{\sqrt{\widehat{v}_t}+\epsilon}\Big\rangle, \tag{D.3}$$

where the positive scalar η_s is absorbed into the argmax over ϕ. This parallels the SGD case in (2.5), where the per-question contribution takes the form $\langle\nabla_\theta J(\theta),\,g(q,a_\phi)\rangle$.

Batch coupling under AdamW. Let $g(q,a_\phi) = \nabla_\theta J(\theta;\,q,a_\phi)$ denote the solver-loss gradient induced by question q (and its generated golden answer a_ϕ). Let $\bar{g}_{\mathcal{Q}} = \frac{1}{|\mathcal{Q}|}\sum_{(q,a_\phi)\in\mathcal{Q}} g(q,a_\phi)$ denote the mean gradient over $\mathcal{Q}$, and let $\bar{g}^2_{\mathcal{Q}}$ denote its elementwise square, following the standard AdamW second-moment update. AdamW then uses

$$\widehat{m}_t = \frac{\beta_1 m_{t-1} + (1-\beta_1)\bar{g}_{\mathcal{Q}}}{1-\beta_1^t}, \qquad \widehat{v}_t = \frac{\beta_2 v_{t-1} + (1-\beta_2)\bar{g}^2_{\mathcal{Q}}}{1-\beta_2^t},$$

where m_{t-1}, v_{t-1} are the first- and second-moment states from previous solver update steps and β_1, β_2 are the corresponding decay rates. Under these exact AdamW semantics, a question's gradient $g(q, a_\phi)$ does not contribute to (D.3) in a purely additive way: it changes both the momentum term in the numerator and the adaptive normaliser in the denominator through $\bar{g}_{\mathcal{Q}}$, so its effective contribution depends on the other gradients in $\mathcal{Q}$. This coupling prevents any clean per-sample attribution of the batch update to individual questions.

Per-question decoupling surrogate. To recover a per-sample score, we borrow inspiration from Xia et al. (2024) and consider a surrogate objective in which each question q is evaluated as if it were the only question in the curriculum. We use the AdamW second-moment preconditioned direction associated with q alone (modulo the positive step size η_s):

$$\Gamma(q, a_\phi) \;=\; \frac{g(q, a_\phi)}{\sqrt{\big(\beta_2 v_{t-1} + (1-\beta_2)\, g(q, a_\phi)^2\big)/(1-\beta_2^t)} + \epsilon}. \tag{D.4}$$

We intentionally omit the first-moment numerator from this per-question score. The exact AdamW numerator would be

$$\widehat{m}_t(q, a_\phi) \coloneqq \frac{\beta_1 m_{t-1} + (1-\beta_1) g(q, a_\phi)}{1-\beta_1^t}.$$

The carried-over momentum state m_{t-1} is shared across all questions scored in the same iteration. Including this shared vector would mix optimizer history into the relative comparison among generated questions, whereas the goal of the influence score is to measure how each individual question's gradient aligns with the target direction. The second-moment term is retained because it provides the AdamW adaptive scaling used by the implemented similarity optimizer. In principle we could use $\langle \nabla_\theta J(\theta),\, \Gamma(q, a_\phi) \rangle$ directly as the influence score for question q. However, as noted by Xia et al. (2024), this raw inner product introduces a spurious correlation between sequence length and gradient norm: longer responses accumulate more tokens in the sum defining $g(q, a_\phi)$ and so systematically produce larger $\|\Gamma(q, a_\phi)\|$, biasing the score toward length rather than directional alignment with $\nabla_\theta J(\theta)$. We therefore replace the inner product in (D.3) with cosine similarity, recovering the main-text influence score (2.7).

D.3 Per-question gradient computation under FSDP

We now describe how the per-question direction $\Gamma(q, a_\phi)$ in (D.4) is computed at LLM scale. The implementation reuses the standard FSDP forward/backward path, so each iteration's influence-scoring phase costs roughly one solver-update epoch's worth of compute on the generated batch, with no extra resident memory beyond the actor's own gradient and optimizer shards.

Sequential per-question backward. For each generated pair $(q, a_\phi) \in \mathcal{B}_{\text{gen}}$, the solver processes the question's $n_{\text{sol}} = 8$ answer rollouts as a self-contained mini-batch and runs one Dr.GRPO forward/backward pass with the loss in (2.10) restricted to that question. After the backward pass, the parameter-gradient buffer of the FSDP-sharded actor holds exactly the per-question gradient $g(q, a_\phi)$ defined in §D.2, with each rank holding only its parameter shard. Questions are processed sequentially, and the same gradient buffer is zeroed and reused between questions so that no per-sample gradient tensor is ever materialized.

Microbatched gradient accumulation per question. Each per-question mini-batch is further split into micro-batches of size $b_\mu = 4$ rollouts (matching the solver-update micro-batch in §G), with the

loss scaled by $1/(\#\text{ micro-batches})$ on each backward pass so that the accumulated buffer at the end of the mini-batch equals $g(q, a_\phi)$. A question's n_{sol} rollouts are first dispatched evenly across the dp data-parallel ranks, so each rank backpropagates through n_{sol}/dp rollouts before the FSDP all-reduce assembles $g(q, a_\phi)$ across shards. Activation memory in this phase is therefore bounded by the same envelope as ordinary policy training.

AdamW preconditioning via an in-place optimizer hook. Once the buffer holds $g(q, a_\phi)$, the per-question direction $\Gamma(q, a_\phi)$ is built on the fly without ever materializing a parameter-sized Γ tensor. A lightweight "similarity optimizer" takes the place of the real AdamW step for this phase: for every sharded parameter it reads the live second-moment state v_{t-1} and decay rate β_2 from the actor's existing AdamW optimizer, forms $v_t(q, a_\phi) = \beta_2 v_{t-1} + (1-\beta_2)\, g(q, a_\phi)^2$ and the bias-corrected denominator $\sqrt{v_t(q, a_\phi)/(1-\beta_2^t)} + \epsilon$ in place, and accumulates the local scalars $\langle \Gamma(q, a_\phi),\, g_{\text{dev}} \rangle$ and $\|\Gamma(q, a_\phi)\|^2$ on each shard. A single 3-element `all_reduce` per mini-batch then yields the global numerator and denominator of the cosine similarity in (2.7); no parameter-sized tensor crosses ranks.

Memory and compute footprint. Beyond the resident actor weights, the additional FSDP-shard memory held during Phase 3 is (i) one shard of the parameter-gradient buffer, already sized for ordinary training, and (ii) one shard of the dev-gradient reference g_{dev} produced once per iteration when the solver computes $\nabla_\theta \widehat{J}(\theta)$ (§2.3). The AdamW second-moment shard v_{t-1} is the actor's existing optimizer state and is loaded onto GPU at the start of the phase when CPU-offload is enabled. Per-question compute is one forward and one backward pass on the question's n_{sol} rollouts, so the wall-clock cost of Phase 3 with $|\mathcal{B}_{\text{gen}}| = B \cdot n_{\text{gen}} = 128 \cdot 8 = 1024$ generated questions matches one solver-update epoch over the same $1024 \cdot n_{\text{sol}} = 8192$ rollouts. In our 8B-Base runs on a single 8×H100 node this places Phase 3 at the same order of magnitude as a single solver-update sweep, never the dominant cost in the iteration.

E Comparison with Alternative Formulations

Black-box outer-loop search. One natural approach to (2.3) is to perturb the generator, rerun the solver update, and keep the generator change only if the held-out objective improves. Systems such as `autoresearch` (Karpathy, 2026) instantiate this pattern for code- and hyperparameter-level experimentation. In our setting, however, such keep-or-discard retraining is too expensive for online curriculum adaptation, because each outer-loop proposal would require a separate inner-loop LLM RL run to estimate its effect on the held-out development objective.

Exact meta-gradient optimization. A second approach is exact bilevel differentiation. The objective in (2.3) can be mapped to MAML-style meta-learning (Finn et al., 2017): both update model parameters on support or training data, then evaluate the post-update model on held-out data. In MAML, tasks $\mathcal{T}_i \sim p(\mathcal{T})$ are sampled from a task distribution, and the meta-learner optimizes an initialization ϑ through

$$\min_{\vartheta} \sum_{\mathcal{T}_i \sim p(\mathcal{T})} \mathcal{L}^{\text{qry}}_{\mathcal{T}_i}(f_{\vartheta'_i}) \quad \text{s.t.} \quad \vartheta'_i = \vartheta - \alpha \nabla_\vartheta \mathcal{L}^{\text{sup}}_{\mathcal{T}_i}(f_\vartheta).$$

Our formulation differs in the object being optimized: MAML optimizes the shared initialization ϑ, whereas INFUSER optimizes generator parameters ϕ that control the training-data distribution. This also relates to dataset distillation (Wang et al., 2018), which optimizes training data through

the learner's update, but does so by directly optimizing a small synthetic dataset rather than a generator policy over curricula. In principle, we could differentiate $J(\theta^+(\phi))$ through (2.2); in practice, exact bilevel differentiation through LLM-scale RL updates is prohibitively expensive, motivating the first-order influence approximation in §2.2.

Table 5: Comparison with alternative formulations.

Formulation	Fits because	Limitation
MAML-style meta-learning (Finn et al., 2017)	Identical bilevel structure: inner-loop update, outer-loop evaluation on held-out data.	MAML optimises a shared *initialisation*; we optimise a data-generating *policy*. MAML requires backprop through the inner step (Hessian); we use a first-order approximation.
Dataset distillation (Wang et al., 2018)	Outer loop optimises synthetic training data to maximise post-update performance on real data.	Distillation optimises fixed data vectors; we optimise a *generative model* that produces an unbounded curriculum. Distillation typically assumes SGD; we handle AdamW with momentum preconditioning.
Zero-sum / adversarial (GAN-like)	Generator "challenges" the solver.	Objectives are aligned, not opposed. The generator is rewarded for *helping*, not fooling. No minimax structure.
Bilevel meta-learning (ours)	Both levels aligned toward objective J; generator shapes inner-loop update dynamics via influence-scored curriculum. Influence score $\approx$ first-order meta-gradient.	Requires first-order approximation; exact meta-gradient intractable for large LMs.

F Training and Evaluation Protocol

All held-out benchmark scores reported in §3.1 are produced by the same evaluation pipeline, which evaluates the trained solver in vLLM with a fixed set of sampling hyperparameters and a fixed pair of prompt templates (one for multiple-choice questions and one for free-form answers). This appendix specifies this configuration in detail.

F.1 Benchmarks

We evaluate INFUSER on four benchmark families: mathematical reasoning, general reasoning, medical reasoning, and coding. For clarity, we enumerate the exact benchmark sources used in Table 2.

Mathematical reasoning.

- **MATH500.** We use the standard 500-problem evaluation subset of the MATH benchmark introduced by Hendrycks et al. (2021).

- **AIME2024.** We evaluate on the 2024 edition of the American Invitational Mathematics Examination (AIME), following recent zero-data reasoning work that treats the official MAA exam problems as a held-out benchmark (Mathematical Association of America, 2024).
- **AIME2025.** We likewise evaluate on the 2025 edition of the American Invitational Mathematics Examination from the Mathematical Association of America (Mathematical Association of America, 2025).
- **HMMT.** We use a held-out benchmark assembled from official Harvard–MIT Mathematics Tournament problem archives. In our evaluated benchmark, the 93 questions are drawn from the February 2025, November 2025, and February 2026 HMMT tournaments, which are olympiad-style high-school mathematics contests with algebra, geometry, combinatorics, and team-style problem-solving rounds (Harvard–MIT Mathematics Tournament, 2026a,b).
- **OlympiadBench (Math).** We use the mathematics subset of OlympiadBench, an olympiad-level bilingual benchmark spanning advanced mathematics and physics (He et al., 2024).
- **OlympiadBench (Phys).** We use the physics subset of the same OlympiadBench benchmark (He et al., 2024).

General reasoning.

- **MMLU-Pro.** We use MMLU-Pro, a more robust and reasoning-focused successor to MMLU with harder questions and more answer choices (Wang et al., 2024).
- **GPQA-Diamond.** We use the Diamond split of GPQA, a graduate-level Google-proof question answering benchmark designed to resist superficial pattern matching (Rein et al., 2023).
- **SuperGPQA.** We use SuperGPQA, a graduate-level reasoning benchmark spanning 285 disciplines (M-A-P Team et al., 2025).
- **BBEH.** We use BIG-Bench Extra Hard (BBEH), a general reasoning benchmark designed to replace each BBH task with a substantially harder counterpart probing a similar reasoning skill (Kazemi et al., 2025).

Medical reasoning.

- **MedQA.** We use MedQA, a medical multiple-choice QA benchmark collected from professional medical exams, including the USMLE setting commonly used in LLM evaluation (Jin et al., 2020).
- **MedXpertQA.** We use the text-evaluation subset of MedXpertQA, an expert-level medical reasoning benchmark spanning specialties and body systems; the local benchmark file contains 2,450 text questions, matching the Text subset described in the benchmark paper (Zuo et al., 2025).

Coding.

- **HumanEval+.** We use HumanEval+, the EvalPlus extension of HumanEval with substantially expanded unit tests for more rigorous code evaluation (Chen et al., 2021; Liu et al., 2023).
- **LiveCodeBench.** We use LiveCodeBench, a contamination-resistant coding benchmark built from temporally fresh competitive-programming problems (Jain et al., 2024). In our implementation, we choose problems released between May 2023 and January 2025 according to the official dataset release notes.

Table 6: Per-source quotas of the 2000-question validation set $\mathcal{D}_{\text{val}}$, sampled with seed 42 from the listed benchmark sources.

Source	Count	Source	Count
AIME (2024, 2025)	60	MedXpertQA (text)	275
GPQA-Diamond	198	OlympiadBench (Math, Phys)	275
HMMT	93	BBEH (MCQ)	70
MMLU-Pro (test)	275	BBEH (open)	205
MATH-500	275	SuperGPQA (all)	274
		Total	2,000

F.2 Checkpoint Selection

Whenever a result is reported as the "best checkpoint" of a training run, the selection follows a fixed protocol. We save a checkpoint every 5 training iterations and score each saved checkpoint on a 2000-question validation set $\mathcal{D}_{\text{val}}$ that is held fixed across all methods, anchors, and ablations. $\mathcal{D}_{\text{val}}$ is distinct from the dev set $\mathcal{D}_{\text{dev}}$ that supplies the influence anchor and is not used in the per-iteration generator update. We then keep the checkpoint with the highest validation accuracy and evaluate *only that checkpoint* on the held-out benchmarks in §3.1 and §3.3. The same every-5-iterations schedule and the same $\mathcal{D}_{\text{val}}$ are used for the rerun R-Zero and AZR baselines.

Composition of $\mathcal{D}_{\text{val}}$. $\mathcal{D}_{\text{val}}$ is a stratified sample (random seed 42) drawn from a broader benchmark pool, with the per-source quotas in Table 6. The quotas are chosen to give roughly balanced signal across the math, general-reasoning, and medical benchmark families that we report on in Table 2. HumanEval+, LiveCodeBench, and MedQA are deliberately excluded from $\mathcal{D}_{\text{val}}$, so the entire coding category and one of the two medical benchmarks remain fully out of sample for checkpoint selection. Because the quotas are sampled from the benchmark sources themselves, individual $\mathcal{D}_{\text{val}}$ questions can overlap with the corresponding held-out evaluation set; we treat this as a known limitation, partially mitigated by the small size of $\mathcal{D}_{\text{val}}$ relative to the full evaluation suite and by holding the same $\mathcal{D}_{\text{val}}$ fixed across all methods, anchors, and ablations so any selection bias applies uniformly.

F.3 Sampling Hyperparameters

For every benchmark and every trained model we sample from the solver with temperature 0.7, top-p 0.8, top-k 20, prompt length 4096, and response length 8192. These settings follow the official Qwen3 non-thinking-mode recommendations (Qwen Team, 2025) for the sampling parameters supported by our evaluation pipeline. The only exceptions are the two coding benchmarks (HumanEval+ and LiveCodeBench), where we extend the response length to 16384 to accommodate longer code generations.

The number of samples drawn per question, n, depends on the benchmark. For most benchmarks we decode $n = 1$ response per question; for benchmarks with smaller question sets or higher variance we decode multiple responses and report the average accuracy:

Benchmark	n samples/question
AIME2024, AIME2025, HMMT	32
HumanEval+	8
GPQA-Diamond	5
MATH500	4
LiveCodeBench	2
all other benchmarks	1

F.4 Prompt Templates

Each question is rendered into a chat conversation with a system turn and a user turn, and the resulting messages are tokenized via the model's chat template before being sent to vLLM. We use one of two templates, chosen based on the benchmark's answer type.

Multiple-choice questions (MCQ). This template is used for INFUSER training and for MCQ-type benchmarks such as MMLU-Pro, GPQA-Diamond, SuperGPQA, BBEH, MedQA, and MedXpertQA. The system turn fixes the output contract, and the user turn wraps the question with step-by-step instructions and requires the final letter to be enclosed in `\boxed{}`:

MCQ Prompt Template

System

```
You are a knowledgeable assistant that solves multiple choice
questions step by step. Always show your reasoning and put your
final answer letter in \boxed{}.
```

User

```
Solve the following multiple choice question step by step.

{question}

Think through this problem carefully. Show your reasoning
process, then provide your final answer.

IMPORTANT: Your final answer MUST be enclosed in \boxed{}
using ONLY the letter of the correct choice (A, B, C, D, etc.).

Example format for your final answer:
\boxed{<correct choice letter>}

Now solve the problem:
```

At scoring time the first `\boxed{...}` span in the response is parsed and compared against the gold letter; all MCQ benchmarks in Table 2 are graded by exact match on the extracted letter.

Free-form questions. This template is used for MATH500, AIME2024, AIME2025, HMMT, OlympiadBench (Math and Phys), HumanEval, and LiveCodeBench. The template mirrors the MCQ variant but asks for the final answer itself (number, expression, or code) inside `\boxed{...}`:

Free-Form Prompt Template

System

```
You are a knowledgeable assistant that solves questions step
by step. Always show your reasoning and put your final answer
in \boxed{}.
```

User

```
Solve the following question step by step.

{question}

Think through this problem carefully. Show your reasoning
process, then provide your final answer.

IMPORTANT: Your final answer MUST be enclosed in
\boxed{<answer>}

Now solve the problem:
```

For math benchmarks, the extracted `\boxed{...}` span is passed through a programmatic equivalence checker, with an optional GPT-4o-class LLM judge as a tie-breaker for MATH500. For HumanEval and LiveCodeBench, the extracted span is treated as the candidate program and executed against the benchmark's unit tests in a sandboxed subprocess.

Generator prompt used during training. The main training runs use document-conditioned question generation (`question_source_mode=document`, the default setting in the training config). For each sampled document, the pipeline checks an explicit per-document `prompt_type` tag; untagged documents use the default MCQ prompt. Thus science documents typically use the MCQ prompt below, while math documents marked as `free_form` use the analogous free-form prompt whose JSON schema has no `choices` field and instead sets `benchmark_type=qa_open` and `data_source=math`. In both cases, the full document text is inserted into the `{text}` slot and the mixed parser dispatches the generated question to the corresponding solver/verifier path.

Generator Prompt Template (Document-Conditioned)

The generator prompt is shown as the following two chat turns.

System

```
You are an expert educator creating challenging multiple-choice questions.
   Always output valid JSON with the exact structure requested.
```

User

```
Your task is to create CHALLENGING exam questions from a document by
   identifying complex relationships and multi-step reasoning paths.

## Document
[BEGINNING OF THE DOCUMENT]
{text}
[END OF THE DOCUMENT]

## Instructions

### Step 1: Complex Information Extraction for MCQ Design

**PRIORITY: Focus on information that enables multiple plausible
   interpretations and requires synthesis.**

Scan the text and identify information that naturally creates opportunities
    for sophisticated multiple-choice questions:

**Ideal MCQ content requires:**
* **Synthesis opportunities**: Relationships between 3+ concepts spanning
   different sections, implicit conclusions requiring combination of
   multiple facts, systems where changing one parameter affects others
* **Multi-step reasoning paths**: Processes with intermediate steps (each
   step = potential distractor), calculations with sequential dependencies,
    procedures requiring decision points about when/how to apply methods
* **Rich comparison spaces**: Comparative analyses revealing subtle
   distinctions ("however," "but," "except," "unlike"), trade-offs between
   approaches, overlapping categories or edge cases, prerequisites or
   conditional relationships
* **Application complexity**: Principles applied to novel scenarios, cause-
   and-effect chains with intermediate stages, mechanisms where partial
   understanding yields plausible-but-incomplete explanations
* **Domain-specific depth**: Multi-variable calculations (unit conversions,
    stoichiometry, equilibrium perturbations), classification problems with
    boundary conditions, experimental design with multiple controlling
   factors, predictions integrating multiple scientific laws

**AVOID** (these create poor MCQ questions):
* Single, directly stated facts that allow simple lookup
* Simple definitions that stands alone
* Values or numbers mentioned in isolation
* Information that requires no synthesis
* Lists without relationships between items
* Trivial categorizations
```

```
* Information where all wrong answers would be obviously implausible

### Step 2: Difficulty Enhancement Process

**EXPLICITLY STATE YOUR HARDENING PROCESS** Before generating the question,
    describe your strategy to make it harder:
1. What simple version would you avoid?
2. What complexity layers will you add?
3. Are there any seamless traps for common misconceptions to exploit for
   distractors?
4. How can you leverage subtle, non-obvious interactions between different
   content elements to create more engaging and intellectually demanding
   questions?
5. What common shortcuts will you block?
6. How will you ensure multi-step reasoning is required?

### Step 3: Advanced Question Generation

Generate ONE high-quality MCQ question that:
* Requires applying multiple concepts from different parts of the document
* Tests understanding of relationships, not just recall of facts
* Forces reasoning through multiple steps to reach the answer
* May require comparing or contrasting different scenarios
* Could involve "what if" scenarios based on principles in the text
* Tests ability to apply concepts to slightly modified situations

**CRITICAL - Self-Contained Requirements**:
* Questions must be 100% self-contained and standalone
* NEVER use: "according to the document", "in the document", "as mentioned",
    "the passage states", "based on the analysis", etc.
* Write as if for a formal exam with no reference material
* Include all necessary context within the question itself, but don't
   reveal any intermediate reasoning steps or key insights that would make
   the question easy
* Define any specialized terms if needed for clarity

### Step 4: Difficulty-Driven Design

**TARGET: Generate HARD/EXTRA HARD questions by design**
* HARD: Synthesize 4+ concepts; multi-step problem solving; pattern
   recognition
* EXTRA HARD: Complex system analysis; counter-intuitive applications; edge
    cases

Design questions that CANNOT be answered by:
* Looking up a single fact
* Finding one sentence with the answer
* Simple keyword matching

### Step 5: Knowledge Integration Requirements

Document the reasoning path that shows why this is a difficult question:
* List 3+ distinct pieces of information needed from different parts
```

```
* Show the logical connections required between these pieces
* Explain why simple lookup won't work
* Include intermediate reasoning steps

### Step 6: Multiple Choice Design Guidelines

Create between 4 and 8 answer choices following these STRICT rules:

**Length Balance**: All options must be approximately equal length (+/-20%)
**Unit Consistency**: All numerical answers must use identical units and
   formatting
**Tone Neutrality**: Avoid overly certain language ("definitely", "always",
    "never") unless justified
**Plausibility**: All distractors must be genuinely plausible based on
   partial understanding
**More choices increase difficulty**: Use 6-8 choices for complex questions

**Distractor Design**:
* Common calculation errors from the multi-step process
* Results from applying only partial reasoning
* Mixing up related concepts from the document
* Reasonable approximations that miss key factors

### Step 7: Self-Testing Filter (AFTER MCQ Creation)

**SOLVE YOUR OWN MCQ AS A STUDENT WOULD** Now test the complete multiple
   choice question:
1. What's the quickest path a student might try with these options?
2. Can you eliminate 2+ options without full understanding? If yes,
   redesign distractors
3. Does seeing the options make the answer obvious? If yes, improve
   distractors
4. Count the reasoning steps required even with options visible - if less
   than 3, REJECT
5. Time estimate: Would this MCQ take <30 seconds? If yes, make it harder
6. Could a student guess correctly by pattern matching the options? If yes,
    rebalance

### Step 8: Final Complexity Verification

Before finalizing, verify your question is NOT Easy by checking:
* Can it be answered by finding one sentence? If yes, redesign
* Does it require connecting multiple document sections? If no, add
   complexity
* Would someone need to understand relationships, not just facts? If no,
   refocus
* Are all MCQ options balanced and using consistent formatting? If no,
   revise
* Did your self-test of the MCQ take more than 1 minute? If no, increase
   difficulty

## Output Format
```

```
You MUST output ONLY a valid JSON object with this exact structure:

{{
    "question_text": "Your complete, self-contained question here?",
    "choices": [
        "First choice text (without letter prefix)",
        "Second choice text (without letter prefix)",
        "Third choice text (without letter prefix)",
        "Fourth choice text (without letter prefix)",
        "Fifth choice text (optional)",
        "Sixth choice text (optional)",
        "Seventh choice text (optional)",
        "Eighth choice text (optional)"
    ],
    "ground_truth": "The exact text of the correct choice (must match one
   of the choices exactly)",
    "difficulty": "hard",
    "answer_quote": [
        "Relevant quote 1 from the document showing key information",
        "Relevant quote 2 from the document showing different piece needed",

        "Relevant quote 3 (include multiple quotes showing different pieces
    needed)"
    ],
    "hardening_process": "Your explicit strategy for making this question
   difficult (from Step 2)",
    "knowledge_and_reasoning_steps": "Detailed reasoning path showing why
   this is Hard/Extra Hard difficulty",
    "self_test_solution": "Your step-by-step solution of the MCQ showing
   the difficulty (from Step 7)"
}}

Field descriptions:
- "question_text": A challenging, self-contained question requiring
    synthesis. Return empty string if document lacks sufficient complexity.
- "choices": Array of 4-8 answer options without letter prefixes
- "ground_truth": The exact text of the correct choice (MUST match one of
    the choices exactly)
- "difficulty": Target difficulty level (hard or extra_hard)
- "answer_quote": Multiple verbatim quotes from the document showing the
    different pieces needed (not just one quote)
- "hardening_process": Your explicit strategy for making this question
    difficult (from Step 2)
- "knowledge_and_reasoning_steps": Detailed reasoning path showing why this
     is Hard/Extra Hard difficulty
- "self_test_solution": Your step-by-step solution of the MCQ showing the
    difficulty (from Step 7)

CRITICAL RULES:
1. Your final answer must contain exactly one JSON object matching the
    requested schema. Put this JSON object last.
2. The "choices" array must have at least 4 items and at most 8 items
3. Do NOT include letter prefixes (A), B), etc.) in the choices
```

```
4. "ground_truth" must be the exact text of one of the choices
5. The question must be answerable, with the key component or solution step
    within the document content
6. If the document lacks sufficient complexity, return empty strings for
   all fields

Schema illustration only (do not copy this content):
{{"question_text": "<new self-contained question derived from the document
   >", "choices": ["<choice 1>", "<choice 2>", "<choice 3>", "<choice 4>"],
    "ground_truth": "<exact text of one choice>", "difficulty": "hard", "
   answer_quote": ["<document quote 1>", "<document quote 2>", "<document
   quote 3>"], "hardening_process": "<difficulty strategy>", "
   knowledge_and_reasoning_steps": "<reasoning path>", "self_test_solution
   ": "<step-by-step solution>"}}.
```

Free-form math route. This is the case for the math RLVR and INFUSER hybrid runs in §5, which use the same training pipeline but with `prompt_type=free_form` for all math RLVR questions. For `prompt_type=free_form` math documents, the user prompt keeps the same document-conditioned structure but asks for one machine-verifiable math question. Its JSON object replaces the MCQ `choices` field with an answer type, marks the example as open-ended math QA, requires `ground_truth` to be a single concise mathematical answer without units, prose, lists, or surrounding `\boxed{}`, and routes the resulting question through the math verifier path.

G Training configurations for compared methods

We compare **INFUSER** with the base model and four contemporaneous self-evolution methods: R-Zero (Huang et al., 2025), AZR (Zhao et al., 2025), R-Few (Yu et al., 2025b), and SPICE (Liu et al., 2025b) on Qwen3-4B-Base and Qwen3-8B-Base as anchors. We report INFUSER as the mean over three random seeds, selecting the best checkpoint within each run by accuracy on a small validation set evaluated every 5 training iterations (§F.2). For R-Zero and AZR, we rerun their released training code under the original settings: 5 R-Zero iterations and 500 AZR training steps. R-Few and SPICE are self-reported because public training code is unavailable, and should be read with caution. Results are summarized in Table 2.

Table 7 compares the training configuration of **INFUSER** side-by-side with the three open-source baselines we rerun in §3.1: the two self-evolution methods R-Zero (Huang et al., 2025) and Absolute Zero Reasoner (AZR) (Zhao et al., 2025), together with General-Reasoner (GR) (Ma et al., 2025), a Zero-style RLVR baseline that we include for completeness even though it relies on frontier-model curation rather than self-evolution. We follow the row layout of Liu et al. (2025b, Table 5) so the configuration contrast is explicit. The mapping between role names is INFUSER's *generator* ↔ R-Zero *challenger* ↔ AZR *proposer*, and INFUSER's *solver* ↔ R-Zero *reasoner* ↔ AZR *solver* ↔ GR *actor*; GR trains a single solver-only actor on a fixed curated question pool and has no generator role.

INFUSER values are taken from our Qwen3 training runs (LR rows list the Qwen3-4B-Base and Qwen3-8B-Base settings); R-Zero and AZR values are reproduced from the configurations released with their training code, cross-checked against Liu et al. (2025b, Table 5) where they re-ran both baselines; GR values are the settings of our Qwen3-8B-Base rerun, which mirrors the Qwen3-14B-Base column of Ma et al. (2025, Table 9) on a single 8×H100 node.

Table 7: Training configurations for INFUSER and the three open-source baselines we rerun. The *Generator* role corresponds to the Challenger in R-Zero and to the Proposer in AZR; the *Solver* role corresponds to the Reasoner in R-Zero, to the Solver in AZR, and to the single-actor in GR (which has no generator). Slash-separated entries are role-specific or model-scale-specific as noted below.

Configuration	INFUSER	R-Zero	AZR	GR
Data Source				
Corpus documents	12,260	–	–	–
Dev set size ($\lvert\mathcal{D}_{\text{dev}}\rvert$)	800	–	–	100[g]
Question source	Doc-grounded	Self-generated	Self-generated	WebInstruct-verified[g]
External grounding	✓	×	Python executor	1.5B verifier model[g]
Training Details				
Generator training	✓	✓	✓	×
Generator sampling (n)	8	4	1	–
Solver training	✓	✓	✓	✓
Solver sampling (n)	8	5	1[a]	8
Temperature	0.7	1.0	1.0	0.7
Algorithm	Dr.GRPO / DuGRPO	GRPO	REINFORCE++	GRPO
Optimizer	AdamW	AdamW	AdamW	AdamW
Generator learning rate	$6/4 \times 10^{-6}$[b]	1×10^{-6}	1×10^{-6}[c]	–
Solver learning rate	2×10^{-6}	1×10^{-6}	1×10^{-6}[c]	5×10^{-7}
LR schedule	Constant (no warmup)	Constant (no warmup)	Constant (no warmup)	Constant (no warmup)
Mini-batch size	32	16 / 128[d]	384[c]	256
Rollout correction	Token-level TIS ($\rho_{\max}$=2.0)	None	None	None
Reward Design				
Generator reward	Influence (precond. cosine)	$1-2\lvert p-0.5\rvert$	$1-p$ if $0<p<1$, else 0	–
Solver reward	Binary correctness	Binary (vs. pseudo-label)	Binary (vs. executor)	Binary (vs. verifier model)[g]
Invalid penalty	0.0	-1 (Challenger)	-0.5 / -1*	0
Performance				
Training iterations	100	5†	500 (steps)	3 epochs (=669 steps)
Batch size	128 docs	8,000 generated questions[e]	64 tasks	1,024 questions
GPUs	8× H100 80 GB	4 / 8 GPUs[d]	2/4× 80 GB GPUs[f]	8× H100 80 GB

[a] AZR uses a single training rollout per task but estimates learnability from ~ 8 Monte-Carlo Solver attempts (Zhao et al., 2025, §4). [b] Generator learning rate values are 6×10^{-6} for Qwen3-4B-Base and 4×10^{-6} for Qwen3-8B-Base. [c] AZR trains a single shared actor policy for proposal and solution; its training script sets actor learning rate 1×10^{-6} and its runtime sets PPO mini-batch size to $64 \times 3 \times 2 = 384$. [d] R-Zero slash-separated values are Challenger / Reasoner values; its Challenger PPO uses batch size 16 on 4 GPUs, while Reasoner PPO uses batch size 128 on 8 GPUs. [e] R-Zero generates 1,000 candidate questions on each of 8 parallel generator workers before self-consistency filtering and Reasoner training. [f] AZR GPU counts are for Qwen3-4B-Base / Qwen3-8B-Base runs, respectively. † R-Zero is reported to degrade after ~ 5 iterations (Huang et al., 2025); we report its best checkpoint within those 5 iterations. * AZR applies -0.5 to an incorrect but well-formatted solver response and -1 to a malformed response. [g] GR trains on TIGER-Lab/WebInstruct-verified (Ma et al., 2025): ∼230K questions filtered from ∼5M web instructions by a frontier model, with a separately trained 1.5B generative verifier (TIGER-Lab/general-verifier) that supplies the binary solver reward; the validation slice is the first 100 rows of the WebInstruct-verified test split.

H Pilot Extension: Combining INFUSER with Rule-Verifiable Math RLVR

This appendix gives the construction and full per-seed results for the hybrid science+RLVR pilot summarized in §5. The pilot starts from the science-document INFUSER setting used in the main experiments and adds a verifiable mathematics component to both the influence anchor and the solver-training curriculum, asking whether one training loop can combine document-grounded science self-evolution with direct verifiable math RLVR. The motivating seed instability, the test-time-compute mechanism ($r = 0.997$ between evaluation-time response length and math accuracy),

and the headline results are presented in §5 together with Figures 11 to 13.

Data mixture. The mixed run follows the Qwen3-8B-Base INFUSER recipe: solver learning rate 2×10^{-6}, generator learning rate 4×10^{-6}, Dr.GRPO solver updates, DuGRPO generator updates, and preconditioned-cosine influence scoring. The dev anchor $\mathcal{D}_{\text{dev}}$ has 800 questions, split evenly between sampled SuperGPQA Science MCQs and AIME-history free-form questions. Science rows use the existing MCQ scoring path. The AIME dev-anchor rows have empty choice lists and `data_source=aime`, which sends them to the AIME integer verifier. This dev anchor should be distinguished from the training pool: Putnam enters through the training-side math pool, not through the 800-row dev anchor.

The training pool combines the original $12{,}260$ science textbook chunks with $10{,}000$ math rows drawn from Putnam and AIME-history. The math pool is constructed from 121 unique Putnam problems and 918 unique AIME-history problems, then filled to $10{,}000$ rows by round-robin repetition and shuffled with seed 42. The realized training mixture contains $1{,}210$ Putnam rows and $8{,}790$ AIME-history rows. At the data level, the resulting curriculum juxtaposes document-grounded science sources with verifiable mathematics: the science side still requires the generator to synthesize training questions from documents, while the Putnam/AIME-history side provides externally answered problems that can directly support RLVR.

Training recipe. The run uses the same five-phase INFUSER loop as Algorithm 1: compute a dev-set reference gradient on the mixed science/AIME anchor, build a training batch from the science and math pool, estimate influence scores for the resulting solver updates, update the generator with DuGRPO, and update the solver with Dr.GRPO. Unlabeled science chunks use the default document-conditioned MCQ generation path, so science supervision still depends on the generator's ability to convert documents into useful QA pairs. The math side supplies externally answered Putnam/AIME-history problems for the RLVR component: AIME rows use integer answer checking, while Putnam rows use the math-verification path for free-form mathematical answers. The mixed dev anchor supplies the influence-scoring direction, with science MCQ signal and AIME free-form signal both present in the dev gradients. We also add a small mid-EOS shaping penalty of -0.5 to discourage responses that emit `<|endoftext|>` before a boxed answer. This penalty is additive; it is not a length cap.

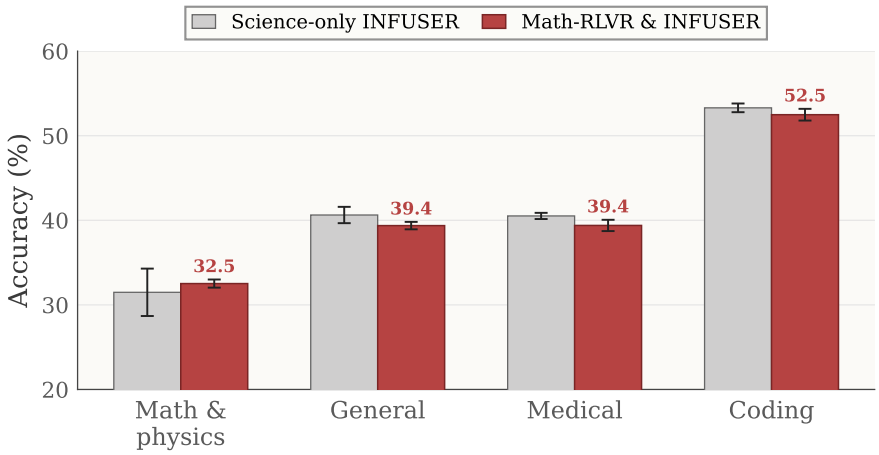

Figure 13: Category-average profile for the pilot mixed science+RLVR runs on Qwen3-8B-Base, visualizing the per-seed averages reported in Figure 11. Bars show the mean over three seeds for each setting; error bars show one cross-seed standard deviation. Verifiable math RLVR tightens the math-and-physics error bar (the channel it targets) while the non-math categories dip slightly under the reduced science document budget.

Full results. The per-seed category averages tabulated in the left panel of the main-text Figure 11, and re-plotted as a profile in Figure 13, use the same six-benchmark math grouping as Table 2 (MATH500, AIME2024, AIME2025, HMMT, OlympiadBench Math, and OlympiadBench Phys). The three Science-only INFUSER seeds correspond to the preconditioned-cosine checkpoints seed456/ckpt95, seed123/ckpt55, and seed42/ckpt95 that underlie the Qwen3-8B anchor in the main comparison; the three Math-RLVR & INFUSER seeds reuse the same seeds. Averaged over the three seeds, the mixed setting raises AIME2024 from 18.58% to 21.25% and the math-and-physics category average from 31.49% to 32.52%. More importantly, the cross-seed sample standard deviation of the math-and-physics average drops from 2.80 to 0.48 percentage points (and on AIME2024 from 2.94 to 0.27), confirming that verifiable math RLVR resolves the seed-dependent equilibrium ambiguity diagnosed in §5. The other categories decline modestly: general reasoning falls from 40.63% to 39.37%, medical from 40.52% to 39.39%, and coding from 53.30% to 52.49%. This tradeoff has a direct explanation rooted in the fixed total training budget. The math pool contributes $10{,}000$ of $22{,}260$ total training rows, roughly 45% of the curriculum. Under the same total number of solver training steps, the solver therefore sees approximately half as many science documents per training loop compared to the science-only setting. Reduced exposure to science documents weakens the curriculum signal that drives general reasoning and out-of-domain transfer, exactly the gains that science self-evolution delivers in the main experiments. The decline is therefore not a sign of interference between the two objectives, but a predictable consequence of the current budget allocation.

Response length. The bottom row of Figure 12 confirms the mechanism. Across all three hybrid seeds, response length on AIME, HMMT, and MATH500 collapses to a tightly clustered trajectory from early in training. The verifiable math RLVR signal imposes a hard constraint on reasoning depth: the solver must produce correct mathematical answers to earn reward, which prevents the collapse to short thinking that destabilizes science-only seeds. The alignment between length stabilization and accuracy stabilization supports the interpretation that reasoning-depth equilibrium is the primary mechanism through which seed variance manifests in science-only math performance.

Takeaway. Figures 11 and 13 confirm the feasibility of running INFUSER with a mixed anchor: one training loop can jointly handle document-grounded science self-evolution and verifiable math RLVR. The current $\approx 45\%$ math budget allocation stabilizes math performance at the cost of weakened science-document signal. This is a budget allocation problem rather than a fundamental incompatibility; tuning the ratio between math and science rows is the natural lever for future work aiming to obtain uniform gains across both dimensions.

I Document Pool Construction Pipeline

We describe the pipeline that builds the document pool $\mathcal{D}_{\text{doc}}$ used by **INFUSER**. The pipeline is fully automated and consists of five stages:

(i) The development set is parsed into a finite set of subdomains that the document pool must cover.

(ii) For each subdomain, an external LLM searches the open web and downloads open-access textbooks that target it.

(iii) Each downloaded PDF is converted to Markdown with a layout-aware tool.

(iv) The Markdown is split into token-bounded chunks with a structural-aware splitter.

(v) An LLM judge filters out non-essential content.

The corpus statistics that result from this pipeline (final size $|\mathcal{D}_{\text{doc}}| = 12{,}260$ chunks, broken down by discipline) are reported in §J.

Taxonomy extraction from the development set. Source selection is conditioned on the domain and the subdomain of each entry in the development set $\mathcal{D}_{\text{dev}}$. Here, the domain refers to the broad area of study (e.g. Physics), and the subdomain refers to a finer specialization within it (e.g. Quantum Mechanics under Physics), so that every $(\text{domain}, \text{subdomain})$ pair probed by the dev set receives dedicated textbook coverage in the pool. We distinguish two cases according to whether $\mathcal{D}_{\text{dev}}$ already provides a multi-level taxonomy.

- **Built-in taxonomy.** For development sets that already carry a multi-level taxonomy, we use it directly. SuperGPQA (M-A-P Team et al., 2025), our running example, annotates every question with three nested labels: a top-level `discipline` (e.g. Science), a `field` (e.g. Physics, Mathematics), and a fine-grained `subfield` (e.g. Quantum Mechanics, Ordinary Differential Equations) drawn from 285 subfields in total. We map `field` to the domain and `subfield` to the subdomain in our $(\text{domain}, \text{subdomain})$ representation, and pass both levels to the textbook search stage so that the search is guided by the broad area and refined by the specialization.
- **LLM-assigned taxonomy.** For general-purpose development sets that lack a built-in taxonomy (e.g. MedQA), we use an external LLM to assign each dev question both a domain and a subdomain label, and merge the resulting labels into a finite set of $(\text{domain}, \text{subdomain})$ pairs. Because labelling occurs entirely on the development side of the pipeline, the same external LLM can be reused for the downstream textbook search step described below.

Both cases produce the same intermediate object: a finite set $\mathcal{C} = \{(d_1, c_1), \ldots, (d_K, c_K)\}$ of $(\text{domain}, \text{subdomain})$ pairs that the document pool $\mathcal{D}_{\text{doc}}$ must cover. Individual dev questions are not used downstream of this step: only the pair set $\mathcal{C}$ is passed to the textbook search stage.

Open-access textbook search per (domain, subdomain) pair. For each $(d, c) \in \mathcal{C}$, the same external LLM acts as a web-research agent: it issues queries conditioned only on the pair (d, c) to find open-access textbooks targeting that specialization within the broad domain, validates the returned URLs by attempting a download, and stores the downloaded PDFs in a local source directory. The agent is equipped with web search, URL crawling, link extraction, and file-download tools. Crucially, the agent never sees individual dev questions; the search prompt receives only the $(\text{domain}, \text{subdomain})$ pair. This keeps any question-level signal out of the source-selection step and is sufficient to retrieve textbooks that cover the specialization. In our runs, the external LLM is the latest version of ChatGPT served through its web interface; any sufficiently capable conversational LLM with browsing tools is a drop-in replacement. Two operational constraints govern the resulting source set. *(a) Open access.* Only open-access resources are admitted; materials behind paywalls or other access restrictions are excluded. *(b) Source-level deduplication.* Before any download, the agent consults a curated registry that records every previously downloaded resource and admits a candidate only if its canonicalised identifier is not already present. As a result, the same textbook is never ingested twice across runs or across pairs.

Source registry. The agent maintains a curated registry that stores, for each admitted resource, a stable identifier, title, author, discipline, category (e.g. `textbook`, `reference`, `tutorial`), source and download URLs, the original filename, a short description, and the download date. This registry is the single source of truth for the raw-source side of the pipeline; downstream stages operate exclusively on the files it points to, so the chunker and the LLM judge are deterministic functions of the registry contents.

PDF to Markdown conversion. Every PDF in the registry is converted to Markdown with `marker-pdf`[1], a layout-aware converter that handles multi-column layouts, equations, tables, and figure captions, and performs OCR-style cleaning when the underlying PDF lacks an extractable text layer. The output is per-source Markdown that preserves the document's heading hierarchy. Preserving headings is critical: the chunker described next uses them as primary split points.

Header-aware chunking with multi-level fallback. We split each Markdown document into token-bounded chunks using a header-aware splitter,[2] with a guaranteed token budget per output chunk. Token counts are estimated with the Qwen3-32B tokenizer (Qwen Team, 2025); the chunker enforces a maximum of $T_{\max}$ tokens per chunk and discards stray fragments below $T_{\min}$. We set $T_{\min} = 200$ and $T_{\max} = 2048$. When a header section already fits within $T_{\max}$, it is emitted as a single chunk. When a section is oversized, the chunker applies the following four-level fallback in order, stopping as soon as every resulting fragment fits within $T_{\max}$: (1) paragraph split, (2) sentence split, (3) comma / semicolon split, (4) adaptive character split (chunk-size annealed until the fragments fit). This ordering preserves the natural prose structure as long as possible and falls through to lower-level splits only when the higher levels still produce oversized fragments. Every emitted chunk is therefore guaranteed to satisfy $T_{\min} \leq \text{tokens} \leq T_{\max}$.

LLM-driven content filtering. We apply LLM-driven filtering at two granularities. First, *before* chunking, an optional structure pass runs over the converted Markdown to identify the "first chapter" and "end marker" boundaries, so that front matter (table of contents, prefaces, lists of

[1] https://github.com/VikParuchuri/marker, accessed via the `marker_single` CLI.
[2] We use `MarkdownHeaderTextSplitter` from the `langchain-text-splitters` library.

contributors) and back matter (bibliography, indexes, appendix exercise keys) are excluded from the chunk pool wholesale. Second, *after* chunking, an LLM judge scores each remaining chunk for teaching value and drops chunks that fail the bar. The judge is a Qwen3-8B model (Qwen Team, 2025) served via vLLM and queried with a fixed rubric that asks the judge to return a binary `keep` decision plus a one-line reason. A chunk is kept only when it has at least a few complete sentences that explain a concept, method, result, or definition, and a reader could learn something non-trivial from it without seeing the surrounding pages. A chunk is discarded if any of the following hold: (i) it is mostly index-like or glossary-like (terms followed by page numbers, cross-references, or markdown page-anchor links); (ii) it is mostly tables, character tables, or matrices of symbols and numbers without surrounding explanation; (iii) it lacks professional-level content or is subjective navigation/structural text such as a preface, foreword, acknowledgements, bare structural headings, or labels like "Index", "References", "Table of Contents"; (iv) it is garbled OCR or broken fragments; (v) it consists mainly of pointers to other material ("see Figure 2", "see Chapter 5") without explaining the underlying ideas; or (vi) it is an answer key, solution manual, or list of short answers to review/practice questions, even if some entries carry brief explanations. A borderline rule biases the judge toward `keep=false` when a chunk mixes noise with only a tiny amount of real content, so the resulting pool is conservatively filtered toward self-contained teaching material. The judge is run with high parallelism per source document. The exact prompt template, including both keep/discard criteria and the two calibration examples used in production, is shown below; the chunk text is inserted into the `${content}` slot.

LLM Judge Prompt for Chunk-Quality Filtering

The LLM judge is queried with a single user turn containing the rubric, two calibration examples, and the chunk to evaluate.

User

```
You are evaluating a text chunk to decide if it should be kept as training
   material for knowledge distillation.

Goal: keep only chunks that contain self-contained, explanatory,
   professional-level content. If you are unsure, choose keep=false.

KEEP (keep=true) only if:
- The chunk has at least a few complete sentences that explain a concept,
   method, result, or definition.
- A reader could learn something non-trivial from this chunk without seeing
    surrounding pages.

DISCARD (keep=false) if ANY of the following are true:
1) The chunk is mostly index-like or glossary-like: terms followed by page
   numbers, cross-references, or markdown links like [282](#page-289-13).
   Example patterns:
   - 'molecular vibrations, 101-103; wave functions, 14-26; ...'
   - 'radial artery, **[890](#page-897-3)**, **[918](#page-925-17)** radial
    collateral ligament, ...'
   Even if the chunk is very long, if it is mostly terms + page numbers/
   links, discard it.
```

```
2) The chunk is mostly a table, character table, or matrix of symbols/
   numbers (including markdown tables with many '|' characters) and there
   is no surrounding explanation of what the table means.
3) The chunk lacks professional-level knowledge or contains subjective
   content (e.g. preface, foreword, acknowledgements, structural headings
   like 'Chapter 3 - Results', or navigation text like 'Index', 'References
   ', 'Table of Contents').
4) The chunk is obviously garbled OCR, or mainly broken fragments that are
   hard to interpret.
5) The chunk is mainly pointers to other material (e.g. 'see Figure 2', '
   see Chapter 5') without explaining the underlying ideas.
6) The chunk is an answer key, solution manual, or list of short answers to
    review/practice questions (e.g. '[1] B [2] D [3] C ...' or '[1] The
   kidneys. [2] X-rays.'). Even if some answers contain brief explanations,
    answer keys are not self-contained teaching material.

Borderline rule: if the chunk is a mix of noise and a tiny amount of real
   content, choose keep=false.

Examples (for calibration only):
Example KEEP:
Chunk: 'Gradient descent updates parameters by moving opposite to the
   gradient. Given learning rate eta, the update is theta_{t+1} = theta_t -
    eta * grad L(theta_t). This iteratively reduces the loss under mild
   smoothness assumptions.'
Output: {"keep": true, "reason": "Self-contained explanation of gradient
   descent and its update rule."}

Example DISCARD (index-like):
Chunk: 'Wave equation, 16; wave functions, 14-26; molecular orbitals, 117;
   selection rules, 414-415; semiconductors, 231-234; silicon, 231, 241,
   250.'
Output: {"keep": false, "reason": "Index-style terms with page numbers, no
   explanatory sentences."}

Now evaluate the following chunk.

Chunk:
${content}

MUST TO RETURN ONLY JSON WITH FORMAT:
{"keep": true|false, "reason": "short explanation (max 20 words)"}
```

Output format and final pool composition. Each source produces a single JSON file containing the surviving chunks, with one record per chunk and metadata indicating the source identifier and the header path of the chunk inside the original document. Concatenating across all sources in the registry yields the document pool $\mathcal{D}_{\text{doc}}$ with $|\mathcal{D}_{\text{doc}}| = 12{,}260$ chunks. The discipline-level composition (Biochemistry, Physics, Astronomy, Geography) and the average chunk length in characters and tokens are reported alongside the deduplication analysis in §J; we do not duplicate those numbers here.

Reproducibility. The pipeline is deterministic up to the LLM agents' sampling randomness and is reproducible from the registry: re-running the chunker and the LLM judge on the registered sources reproduces the same chunk pool up to floating-point and sampling variation. The registry, chunker, and judge configuration are released alongside the codebase.

J Deduplication check against the OLMo-3 SFT corpus

This appendix documents the near-duplicate check summarized in §4.

Motivation. Since the IF anchor in §4 is OLMo-3-7B-Instruct-SFT, a natural concern is that the benchmark signal on INFUSER could be inflated by data contamination: if our document pool $\mathcal{D}_{\text{doc}}$ or our development set $\mathcal{D}_{\text{dev}}$ overlaps with the OLMo-3 supervised-finetune mixture, the anchor has already seen the raw content from which INFUSER curates its curricula, and any observed lift could reflect memorization rather than influence-guided self-improvement. We therefore run a lexical near-duplicate check of both $\mathcal{D}_{\text{doc}}$ and $\mathcal{D}_{\text{dev}}$ against the publicly released OLMo-3 SFT data.

Corpora. The reference side comprises two components. $\mathcal{D}_{\text{doc}}$ is the document pool used in our training runs: a collection of $12{,}260$ PDF-derived chunks (Biochemistry 58%, Physics 24%, Astronomy 14%, Geography 5%; average length ~ 5k characters, ~ 1.3k tokens per chunk). $\mathcal{D}_{\text{dev}}$ is the 800-question SuperGPQA Science development subset used by INFUSER to drive the influence score. For indexing, we serialize each question by concatenating the question text, choice list, and reference answer into a single string.

The instruction-tuning side is the $2{,}152{,}112$-sample mixture `allenai/Dolci-Instruct-SFT` (Allen Institute for AI, 2025), released alongside OLMo-3-7B-Instruct-SFT. Each Dolci record carries an ordered `messages` list with four possible roles (`user`, `assistant`, `system`, `environment`). We concatenate the `user` and `assistant` contents per record, since these are the two roles in which textbook-derived content would plausibly appear (quoted in a prompt or reproduced in an answer). The `system` role is dominated by function-calling boilerplate and the `environment` role by tool-call JSON output; neither carries prose excerpted from a science textbook or a science exam.

Standard we follow. We follow the reference intra-corpus deduplication pipeline documented by Cerebras Systems (2024), which in turn reproduces the word-n-gram *MinHashLSH* approach of Lee et al. (2022) built on the probabilistic resemblance framework of Broder (1997). In this regime, each text blob is normalized under Unicode NFC, casefolded, stripped of ASCII punctuation, and collapsed to single whitespace; the resulting token stream is shingled into word 13-grams. A 128-permutation MinHash signature is computed per blob and inserted into a MinHashLSH index with Jaccard threshold 0.8. Following Cerebras Systems (2024), records shorter than 200 characters after normalization are excluded from indexing.

Containment pass. Because the document chunks in $\mathcal{D}_{\text{doc}}$ are typically much longer than a single SFT sample, symmetric Jaccard is not the only regime that matters: an SFT sample could copy a short passage fully contained in a much longer chunk, in which case the symmetric similarity would fall well below the 0.8 floor even when every shingle of the sample appears in the chunk. To handle this length-asymmetric case, we additionally build a *MinHashLSH Ensemble* (Zhu et al., 2016) over the same 128-permutation signatures, with a containment threshold of 0.8 and 32 partitions. The same construction is applied to $\mathcal{D}_{\text{dev}}$, so both the symmetric and asymmetric regimes are probed on each side. For every candidate pair returned by either index we verify the estimated Jaccard (and, for ensemble candidates, the MinHash-derived containment $|\widehat{A \cap B}|/|A|$

with $|\widehat{A \cap B}| = \hat{J} \cdot (|A| + |B|)/(1 + \hat{J})$) against the thresholds before recording a match. All signatures and indexes are computed with the `datasketch` Python library (Zhu, 2024), and scanning is parallelized across the 15 parquet shards of the Dolci train split.

Results. Across the full 2,152,111 non-trivial SFT samples (after dropping 76,337 below the length floor, 3.5%), the combined Jaccard-LSH + LSH-Ensemble scan returns **zero matches** against $\mathcal{D}_{\text{doc}}$ and **zero matches** against $\mathcal{D}_{\text{dev}}$ at the standard thresholds. No SFT sample has estimated Jaccard similarity ≥ 0.8 with any chunk or dev-question serialization, and no SFT sample has estimated containment ≥ 0.8 in any chunk or dev-question serialization. We therefore conclude that neither the document pool $\mathcal{D}_{\text{doc}}$ nor the dev set $\mathcal{D}_{\text{dev}}$ leaks into the OLMo-3 SFT mixture at the near-duplicate thresholds recommended by Cerebras Systems (2024) and Lee et al. (2022), so the benchmark lifts attributed to INFUSER in §4 cannot be explained by anchor-level memorization of our training corpus.

Caveats. Word 13-grams with a Jaccard threshold of 0.8 catch verbatim near-copies robustly but are deliberately insensitive to paraphrases, summaries, and fact-level reformulations. A secondary scan with word 5-grams at Jaccard threshold 0.5 and containment threshold 0.8 surfaces only two $\mathcal{D}_{\text{doc}}$ chunks (both from the same analytical-chemistry textbook) that share $\sim$ 20–30% of their shingles with two `OpenThoughts3+ Science` prompts. Manual inspection shows that the matched shingles are stock phrasing shared by exercises from the same textbook family (standard voltammetry setup, calibration language), not direct reuse of our chunk text; we therefore do not treat them as contamination. The looser scan finds no such near-misses for $\mathcal{D}_{\text{dev}}$. Finally, $\mathcal{D}_{\text{doc}}$ and $\mathcal{D}_{\text{dev}}$ cover the sciences only, while the Dolci mixture spans many non-science domains (coding, general instruction-following, tool use, multilingual). The *a priori* overlap probability with those domains is low, which is consistent with the null result.

K Raw Data Behind Main-Text Figures

The main text presents several results graphically. This appendix collects the raw per-benchmark accuracies behind those figures so that readers can audit individual numbers, recompute deltas, or quote specific benchmark scores.

Headline-benchmark scores. Table 8 reports the per-method accuracy on the four headline benchmarks plotted in Figure 1 (left). The values are pulled from the same report database as Table 2, so this table is the Qwen3-8B-Base subset of the main table on those four benchmarks, listed here for convenience.

Dev-set leakage test. Table 9 reports the dev-subset and held-out-complement accuracies underlying Figure 8a. The held-out complement row is derived by subtracting the 800-question dev counts from the full SuperGPQA Science pool.

Generator ablations (source and update). Table 10 consolidates the per-benchmark accuracies behind the two Qwen3-8B-Base ablations in §3.3. The first four trained columns, *INFUSER*, *Fix-gen*, *Strong-gen*, and *Dev-only*, correspond to the generator-source ablation in Figure 8b. The remaining three columns, `group_std`, `batch_std`, and `sgd_cosine`, correspond to the generator-update ablation in Figure 8c and isolate the within-group normalizer, the batch normalizer, and the SGD-style (non-preconditioned) similarity variant; INFUSER itself is the DuGRPO anchor for that ablation, so it appears once in the shared INFUSER column.

Table 8: Per-benchmark accuracy (%) for the four headline benchmarks plotted in Figure 1 (left) on the Qwen3-8B-Base anchor. Values are pulled from the same report database as Table 2, so this table is the Qwen3-8B-Base subset of the main table on these four benchmarks. R-Few† and SPICE† columns are self-reported (see §F). Bold entries mark the best score per row.

Benchmark	Base	R-Zero	AZR	R-Few†	SPICE†	INFUSER
MATH500	76.05	80.55	80.95	82.60	79.40	**82.77**
OlympiadBench (Math)	40.36	45.10	47.92	46.40	42.50	**50.24**
MMLU-Pro	59.91	61.82	62.32	63.20	65.00	**66.20**
SuperGPQA	30.62	32.06	32.63	33.50	35.70	**37.77**

Table 9: Dev-dataset leakage test on Qwen3-8B-Base. We score the base model, INFUSER, and the Dev-only baseline on the 800-question training dev subset ($\mathcal{D}_{\text{dev}}$) and on the 9,038-question SuperGPQA Science held-out complement (SuperGPQA Science with $\mathcal{D}_{\text{dev}}$ removed). Δ is the absolute improvement over the base model. The held-out complement row is derived automatically from the report's dev-subset and full-pool scores.

		INFUSER		Dev-only	
Dataset	Base	Acc.	Δ	Acc.	Δ
$\mathcal{D}_{\text{dev}}$ (800-question training subset)	32.37	41.85	+9.48	86.50	**+54.13**
SuperGPQA Science held-out (9,038 questions, $\mathcal{D}_{\text{dev}}$ removed)	30.06	39.22	+9.16	38.35	+8.29

Generator learning-rate sweep. Table 11 lists per-benchmark accuracies for the four generator learning rates plotted in Figure 8d on both the Qwen3-4B-Base and Qwen3-8B-Base anchors. G_{lr}=0 is the Fix-gen baseline.

Generator question quality. Table 12 reports the per-checkpoint accuracies of the four solvers tracked across the co-evolving generator's questions in Figure 6b.

Instruction-finetuned anchor extension. Table 13 reports the per-benchmark accuracy behind the three radar plots in §4.

Table 10: Per-benchmark solver accuracy (%) on Qwen3-8B-Base for the consolidated ablation behind Figure 8b (generator source: INFUSER, Fix-gen, Strong-gen, Dev-only) and Figure 8c (generator update: DuGRPO and its three normalization / similarity variants `group_std`, `batch_std`, `sgd_cosine`). INFUSER is the DuGRPO anchor and appears in both ablations. The INFUSER column is the seeded reference run that feeds Table 2; the corresponding cell in Table 11 (Qwen3-8B-Base, $G_{\text{lr}}{=}4{\times}10^{-6}$) uses a separate seedless sweep run with its own best checkpoint, so the two cells need not match. Bold entries mark the best score per row across the seven trained columns (i.e. excluding Base).

Benchmark	Base	INFUSER	Fix-gen	Strong-gen	Dev-only	`group_std`	`batch_std`	`sgd_cosine`
General reasoning								
MMLU-Pro	59.91	67.81	65.48	**68.46**	62.55	66.31	65.69	66.01
GPQA-Diamond	36.87	**47.47**	45.56	45.86	44.55	43.43	42.83	43.84
SuperGPQA	30.62	38.86	37.87	**41.01**	40.36	38.04	36.97	37.80
BBEH	10.30	12.51	12.79	12.46	**13.57**	12.91	12.66	12.15
Category average	34.43	41.66	40.43	**41.95**	40.26	40.17	39.54	39.95
Math & physics reasoning								
MATH500	76.05	**84.25**	78.70	82.35	83.05	80.10	80.05	80.00
AIME2024	12.92	19.06	15.31	14.90	**21.77**	15.00	15.21	12.60
AIME2025	11.87	**18.02**	14.06	13.33	17.60	12.40	13.13	11.98
HMMT	2.96	**9.64**	3.93	5.68	7.90	3.97	4.50	4.03
OlympiadBench (Math)	40.36	**54.45**	44.96	46.74	48.96	43.32	46.59	45.10
OlympiadBench (Phys)	12.29	14.41	**14.83**	13.14	13.98	13.98	13.56	13.98
Category average	26.08	**33.31**	28.63	29.36	32.21	28.13	28.84	27.95
Medical								
MedQA	64.18	66.46	65.04	67.40	**67.95**	65.99	65.67	66.06
MedXpertQA	14.49	14.57	15.22	**17.47**	15.31	14.94	16.33	16.00
Category average	39.34	40.52	40.13	**42.44**	41.63	40.46	41.00	41.03
Coding								
HumanEval+	75.94	78.86	77.52	76.68	75.61	78.12	78.89	**79.65**
LiveCodeBench v1-5	25.23	28.47	27.73	**28.75**	26.59	27.67	28.01	28.35
Category average	50.59	53.67	52.63	52.72	51.10	52.90	53.45	**54.00**

Table 11: Per-benchmark solver accuracy (%) for the generator learning-rate sweep on Qwen3-4B-Base and Qwen3-8B-Base (raw numbers behind Figure 8d). The G_{lr}=0 column is the Fix-gen baseline that freezes the generator at its initial checkpoint; nonzero columns use the best checkpoint per run, selected by the validation protocol of §F.2. Bold entries mark the best G_{lr} setting per row within each anchor.

Benchmark	Base	G_{lr}=0	G_{lr}=2×10^{-6}	G_{lr}=4×10^{-6}	G_{lr}=6×10^{-6}
Qwen3-4B-Base					
General reasoning					
MMLU-Pro	52.98	59.46	59.39	59.78	**60.68**
GPQA-Diamond	31.41	38.59	37.07	**39.39**	35.35
SuperGPQA	25.88	33.00	33.12	32.07	**33.90**
BBEH	5.18	10.55	9.21	9.30	**12.11**
Category average	28.86	35.40	34.70	35.14	**35.51**
Math & physics reasoning					
MATH500	61.20	76.25	76.75	74.85	**77.90**
AIME2024	10.42	10.62	**14.48**	9.27	11.87
AIME2025	8.44	8.85	10.42	9.79	**11.56**
HMMT	2.49	2.86	**3.36**	2.96	3.19
OlympiadBench (Math)	35.31	**42.43**	41.54	37.98	42.14
OlympiadBench (Phys)	10.17	**12.71**	11.86	11.86	8.90
Category average	21.34	25.62	**26.40**	24.45	25.93
Medical					
MedQA	55.46	58.37	56.95	58.68	**59.47**
MedXpertQA	13.02	**13.88**	13.18	13.18	13.80
Category average	34.24	36.13	35.07	35.93	**36.64**
Coding					
HumanEval+	70.27	74.54	**76.22**	74.47	75.23
LiveCodeBench v1-5	20.68	22.05	22.67	21.70	**23.01**
Category average	45.47	48.30	**49.45**	48.09	49.12
14-benchmark mean	28.78	33.15	33.30	32.52	**33.51**
Qwen3-8B-Base					
General reasoning					
MMLU-Pro	59.91	65.48	65.03	64.54	**66.00**
GPQA-Diamond	36.87	45.56	44.34	**45.76**	43.77
SuperGPQA	30.62	37.87	**37.92**	36.33	36.69
BBEH	10.30	**12.79**	11.97	12.35	12.14
Category average	34.43	**40.43**	39.82	39.75	39.65
Math & physics reasoning					
MATH500	76.05	78.70	80.55	**85.25**	81.03
AIME2024	12.92	15.31	12.92	**21.25**	17.05
AIME2025	11.87	14.06	11.25	**17.19**	14.27
HMMT	2.96	3.93	4.07	**8.17**	5.49
OlympiadBench (Math)	40.36	44.96	41.99	**51.48**	46.24
OlympiadBench (Phys)	12.29	**14.83**	11.86	13.98	12.01
Category average	26.08	28.63	27.11	**32.89**	29.35
Medical					
MedQA	64.18	65.04	63.79	65.12	**66.01**
MedXpertQA	14.49	15.22	**16.37**	15.18	15.33
Category average	39.34	40.13	40.08	40.15	**40.67**
Coding					
HumanEval+	75.94	77.52	**80.11**	77.97	78.43
LiveCodeBench v1-5	25.23	**27.73**	26.59	27.44	26.97
Category average	50.59	52.63	**53.35**	52.71	52.70
14-benchmark mean	33.86	37.07	36.34	**38.71**	37.25

Table 12: Per-checkpoint solver accuracy (%) on the questions produced by INFUSER's co-evolving generator at training iterations $\{0, 30, 60, 90\}$ on the Qwen3-8B-Base anchor (raw numbers behind Figure 6b). "Qwen3-8B-Base" is the fixed reference base solver, "INFUSER Solver" is the evolving co-trained solver's own training-time accuracy on its current questions, and "GPT-5.4-mini" / "GPT-5.4" are strong-solver references.

Solver	Iter. 0	Iter. 30	Iter. 60	Iter. 90
Qwen3-8B-Base	59.50	47.90	53.80	56.70
INFUSER Solver	59.40	55.22	61.82	64.31
GPT-5.4-mini	64.80	57.00	61.90	66.80
GPT-5.4	64.50	59.80	66.00	70.30

Table 13: Solver accuracy (%) on held-out benchmarks for OLMo-3-7B-Instruct-SFT as an instruction-finetuned anchor. Bolded entries mark the best score among the three variants per row; all three columns are produced by the same evaluation pipeline as Table 2. Fix-gen is the frozen-generator ablation from §3.3; INFUSER uses preconditioned-cosine influence with solver lr 2×10^{-6} and generator lr 4×10^{-6}.

Benchmark	Base	Fix-gen	INFUSER
General reasoning			
MMLU-Pro	49.0	51.5	**54.1**
GPQA-Diamond	31.6	**36.2**	35.6
SuperGPQA	22.8	26.7	**28.4**
BBEH	8.1	**10.4**	10.2
Category average	27.9	31.2	**32.1**
Math & physics reasoning			
MATH500	68.9	68.4	**70.6**
AIME2024	5.8	6.3	**6.8**
AIME2025	7.1	6.8	**9.8**
HMMT	3.2	4.5	**4.8**
OlympiadBench (Math+Phys)	25.5	27.0	**27.3**
Category average	22.1	22.6	**23.9**
Medical			
MedQA	45.1	43.1	**45.3**
MedXpertQA	12.7	13.4	**14.2**
Category average	28.9	28.3	**29.8**
Coding			
HumanEval+	67.2	**68.0**	66.6
LiveCodeBench	12.8	10.6	**13.3**
Category average	**40.0**	39.3	39.9
Overall average	27.7	28.7	**29.8**